THE PAI-1-VITRONECTIN-VIMENTIN TERNARY COMPLEX: MECHANISM OF

EXTRACELLULAR ASSEMBLY AND ROLE IN TRANSPLANT VASCULOPATHY

by

HON SING LEONG

B.Sc., The University of Alberta, 1999
M.Sc., The University of British Columbia, 2002

A THESIS SUBMITTED IN PARTIAL FULFILLMENT OF
THE REQUIREMENTS FOR THE DEGREE OF

DOCTOR OF PHILOSOPHY

in

THE FACULTY OF GRADUATE STUDIES

(Pathology and Laboratory Medicine)

THE UNIVERSITY OF BRITISH COLUMBIA

(Vancouver)

April 2008

© Hon Sing Leong, 2008

ABSTRACT

The active state of plasminogen activator inhibitor type-1 (PAI-1) is prolonged when it forms a complex with vitronectin (VN), a major serum protein. Active PAI-1 in the PAI-1:VN complex serves many functions related to fibrinolysis and cell migration but key to these effects is its extracellular distribution. PAI-1:VN complexes can bind to exposed vimentin (VIM) on activated platelet and platelet microparticles, resulting in the assembly of PAI-1:VN:VIM ternary complexes. However, the manner in which the vimentin cytoskeleton is presented extracellularly is not well understood.

I hypothesized that PAI-1:VN:VIM ternary complex assembly occurs on cell surfaces when microparticle release leads to exposure of vimentin cytoskeleton which can lead to either assembly of the ternary complex or become involved in an autoimmune response specific for vimentin.

To follow the intracellular and extracellular fate of PAI-1, I constructed an expression vector encoding PAI-1-dsRed, a fluorescent form of PAI-1, which would permit live cell tracking of PAI-1 in megakaryocytes and endothelial cells. Secondly, to study how vimentin is expressed on platelets and platelet microparticles, flow cytometry was used to isolate vimentin positive platelets or PMP's and atomic force microscopy was performed to image platelets or PMP's at nanoscale resolution. From these studies, I propose a model of vimentin expression in which the junction of microparticle release results in the exposure of cytoskeletal vimentin on both the cell and the microparticle. This exposed vimentin could potentially induce VN multimerization on the same cell surface leading to incorporation of multiple PAI-1:VN complexes.

Finally, I investigated how anti-vimentin antibodies can induce platelet:leukocyte conjugate formation. To achieve this, in vitro tests were performed to determine the binding site of anti-vimentin antibodies (AVA's) and how they induce blood cell activation. Overall, my results suggest that vimentin exposure in our model of microparticle release can lead to ternary complex assembly if suitable quantities of PAI-1 are released during platelet activation. In the setting of transplant vasculopathy with high titres of AVA's, vimentin-positive granulocytes can bind these autoantibodies, which then leads to platelet activation and the formation of platelet:leukocyte conjugates.

TABLE OF CONTENTS

CHAPTER IV: DISTRIBUTION OF PAI-1:VITRONECTIN:VIMENTIN TERNARY COMPLEXES ON ACTIVATED PLATELETS AND PLATELET MICROPARTICLES BY ATOMIC FORCE MICROSCOPY

CHAPTER V: VIMENTIN AUTO-ANTIBODIES INDUCE PLATELET ACTIVATION AND FORMATION OF PLATELET-LEUKOCYTE CONJUGATES VIA PLATELET-ACTIVATING FACTOR

LIST OF TABLES

LIST OF FIGURES

LIST OF ABBREVIATIONS

AFM   atomic force microscopy

AMI   acute myocardial infarction

AVA's   anti-vimentin antibodies

DMEM   Dulbecco's modified eagle's media

dsRed   red fluorescent protein analogous to GFP (green fluorescent protein)

Eahy926   name of endothelial hybridoma cell line

ECM   extracellular matrix

FACS   fluorescence activated cell sorting

FBS   fetal bovine serum

FITC   fluorescein isothiocyanate

FS   forward scatter

GFP   green fluorescent protein

HUVEC   human umbilical vein endothelial cells

IF   intermediate filaments

kDa   kilo Dalton

MEG-01   megakaryocyte cell line

PAI-1   plasminogen activator inhibitor type-1

PAI-1-dsRed plasminogen activator inhibitor type-1 fused with the dsRed fluorescent protein

PMP   platelet microparticle

PPP   platelet-poor plasma

PRP   platelet-rich plasma

RPMI-1640   culture media named after its site of origin: Roswell Park Memorial Institute

RT-PCR	reverse transcriptase polymerase chain reaction
SN	supernatant
SS	side scatter
TMAFM	tapping mode atomic force microscopy
TNF-α	tumor necrosis factor- alpha
tPA	tissue-type plasminogen activator
uPA	urokinase-type plasminogen activator
uPAR	urokinase-type plasminogen activator receptor
TVD	transplant vascular disease
VN	vitronectin
VIM	vimentin
vWF	von Willebrand's Factor
WPB	Weibel-Palade body

ACKNOWLEDGEMENTS

"Education is an admirable thing, but it is well to remember from time to time that nothing that is worth knowing can be taught." – Oscar Wilde (1854-1900)

I don't really know what Oscar Wilde meant when he penned that, but I interpret the axiom like this: the epiphany after a great trial of intellectual pursuit, a pursuit brought to a finale by a shackling realization. That there is more to come, with a darkness hugging the ocean horizon of scientific marathon. This is how I feel after doing a PhD.

I dedicate this thesis to my family: Phak Foo Leong (dad), Yut Yoong Leong (mom), Hon Fei Leong (brother), See Yuen Leong-Ng (sister), Johnny Ng (brother-in-law) and my beautiful and patient wife, Eva. I did not get through a single day without thinking of all you as I flailed in the trenches and did my time as a trainee. I hope that I make you all proud forever.

I thank God for giving me the mental makeup to survive the past 8 years and in helping me in some key moments that finally led to the completion of this PhD training.

I acknowledge my supervisors, Dr. Thomas Podor and Professor Rose for the completion of this thesis. My first supervisor, Dr. Podor has suffered greatly medically for the past seven years, but his incredible spirit and drive have permitted me to understand and contribute to the field in what we believe are important and salient issues regarding vimentin and vitronectin interactions. As indebted I am to Dr. Podor, I have learned a great deal about research independently. Dr. Podor has been much more than a supervisor; he has been a true mentor, scientist, and friend. I have gained a tremendous amount of experience and expertise, all because of his efforts to stay alongside my research with little regard for his own health. He is truly an inspiration to my future work and I hope to continue to be as dedicated to the pursuit of science as he has in the past five years, in spite of his medical conditions. I pray that his health returns because the field of PAI-1 and vitronectin will surely require his energy and knowledge for many years to come.

I also wish to acknowledge Professor Marlene Rose, who is a kindred spirit in the field of vimentin alongside Dr. Podor. They both met in Vienna, Austria in 2004 in which a spirited conversation about each other's interests in this intermediate filament resulted in a most fruitful collaboration that spanned the Atlantic Ocean. This international collaboration resulted in the development of the second half of my PhD studies, the role of vimentin in allograft rejection and its manner of expression in plasma that frequently leads to autoimmune responses in solid organ transplant patients. This collaboration proved to be the saving grace for my PhD project as the slight turn in focus became a bountiful exchange that builds on our knowledge of vimentin. I wish to conclude by saying any successes found in this thesis is intimately linked to the foresight and tenacity of Dr. Podor and the graciousness and formidable insight provided by Professor

Rose. I only hope to be even mentioned in the same breath as my mentors, luminaries in their own right.

I want to acknowledge the great friends I have made during these past 8 years in Vancouver (in random order). Bobby Yanagawa, who was the first person to make me realize how good we have it in science and in Vancouver; the first person to suggest Toastmasters to me, a person whose example has showed me how to pursue science. Caroline Cheung for her continual presence and encouragement, for her shoulder as I cried and for her laughter as I succeeded. Caroline is one person whose scientific demeanor and commentary will be well preserved in my mind and as I reflect on Vancouver and iCAPTURE. Melissa Westoby for her friendship and her lightheartedness and strength in the laboratory and outside of it. Hubert Walinski for demonstrating to me how senior graduate students can behave and how to properly navigate the shallow waters of iCAPTURE and Vancouver's citizenry. To Alan Quan, who may possibly be the greatest friend a poor pathetic graduate student can ever have, whose energy, thoughtfulness and attitude was always a refreshing break from all the dreary work and pain that this PhD has wrought upon me. Alan will always be in my plans as I move forward in science and industry. Ryon Bateman, a rock and the only big brother I have ever had. It's rare when you meet someone that sees the potential in you and decides to help unlock it. Whether or not he regrets doing this, we shared some memorable moments in science and under his wing, I realized sooner what it was like to be a real "imager" and a real scientist. He taught me some great one-liners and axioms as well as some great times in the lab and at the dinner table. Jerry Wong for being the science little brother that I mentored on an irregular basis. You made me realize that some good scientists DO go into medicine and that there is still some hope in this world for clinician scientists. Anna Meredith for her tireless pursuit of relevance and excellence in scientific endeavors and her caring ways in the lab. Beth Whalen for your time, talks, and technical help. Finally, Mahesh Balakrishnan, my brother from England/Bangalore, a man whose standing will surely be realized in this world and in India (a world onto itself). Truly an amazing man with equally amazing principles and a fervour for excellence that is grounded by spirituality and legacy.

Thank you all.

CO-AUTHORSHIP STATEMENT

Chapter II: I identified, designed, performed all experiments for this manuscript and I analyzed all data for this manuscript. I prepared 95% of the manuscript, with my supervisor Dr. Thomas Podor contributing the remaining 5%.

Chapter III: I identified, designed, performed all experiments for this manuscript and I analyzed all data for this manuscript. I prepared 100% of the manuscript.

Chapter IV: I identified, designed 60% of the experiments for this manuscript, I performed 95% of the experiments while Dr. Mahesh Balakrishnan contributed recombinant vimentin and the collection of human blood. I prepared 60% of the manuscript while Professor Marlene Rose contributed to the other 40%.

CHAPTER I. INTRODUCTION

The overall objective of this thesis is to understand the extracellular fates of a ternary complex composed of PAI-1, vitronectin and vimentin. These proteins both individually and together serve a broad scope of cellular functions related to cell motility and extracellular matrix metabolism, but the primary benefit of this ternary complex is to localize PAI-1 activity to sites of thrombus formation, specifically to sites of activated platelets and platelet microparticles.

1.1. Plasminogen activator inhibitor type-1 (PAI-1)

1.1.1. *Overview* – As its name implies, PAI-1 is a major inhibitor of plasminogen activators, such as tissue-type plasminogen activator (tPA) and urokinase plasminogen activator inhibitor (uPA) [1]. Inhibition occurs when PAI-1 forms a covalent bond with the PA via its reactive center loop, resulting in the formation of a PAI-1-PA complex, either tPA or uPA [1-3]. The premier feature of PAI-1 is its reactive centre loop (RCL) which dictates its activity and forms covalent bonds with serine proteases such as PA's [1-3] and form an acyl-enzyme complex in a positional conformation such that the catalytic sites on the PA's are blocked (Figure 1.1). Inhibition of t-PA prevents the conversion of plasminogen to its active form, plasmin, a protease with broad substrate specificity such as fibrin [4], fibronectin, thrombospondin, and von Willebrand Factor [5]. Inhibition of t-PA can prevent fibrinolysis as well as reduce certain facets of extracellular matrix metabolism (ECMM) [6, 7]. Similarly, inhibition of u-PA also results in decreased cell adhesion and cell motility [8] and its effects are highly relevant in angiogenesis and tissue remodeling [9].

1.1.2. *Biochemical properties* – PAI-1 is a 50 kDa protein belonging to the serine protease inhibitor (serpin) family that possesses a RCL that dictates its activity and inhibitory
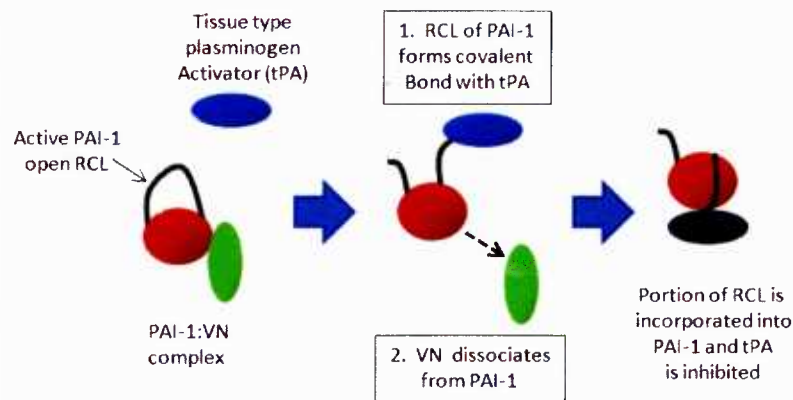
Figure 1.1. **Summary of PAI-1's interactions with vitronectin (VN) and tissue-type plasminogen activator (tPA).** PAI-1 contains a reactive centre loop (RCL) that when free, can bind to tPA via formation of a covalent bond (1). This interaction will cause dissociation of VN from PAI-1 (2) [10]. The inhibition of tPA occurs when the RCL is reinserted into PAI-1 molecule while the tPA is transferred to the other side of PAI-1, sterically hindering the active sites of tPA.

ability. For instance, during tPA inhibition, the RCL and P1 site on PAI-1 will interact with tPA

and form an intermediate Michaelis complex. This is followed by a cleavage in the P1-P1' bond

on PAI-1 and the formation of a covalent acyl PAI-1-tPA complex [1-3]. This will also result in

the insertion of the once-free RCL back into the body of the PAI-1 molecule. Once the RCL is

completely re-inserted, tPA becomes catalytically inactive in the final PAI-1-tPA complex.

However, when the RCL slowly re-inserts into the PAI-1 molecule, PAI-1 can dissociate from

the enzyme-inhibitor complex, leaving behind an inactive tPA molecule that may or may not

contain a part of the RCL [11].

The position of the RCL dictates PAI-1 activity; active PAI-1 has a free and exposed

RCL, but when the RCL is re-inserted into the PAI-1 molecule, it becomes the inactive or latent

conformation of PAI-1 that is unable to bind and inhibit tPA. Because of the RCL's propensity

to re-insert back into the PAI-1 molecule, the half-life of active PAI-1 is ~1-2 hours [12]. Latent

PAI-1 can be converted back to active PAI-1 by chemical denaturation and subsequent refolding

of purified latent PAI-1 [13, 14]. PAI-1 can also form complexes with vitronectin (VN) and α_1-

acid glycoprotein which stabilize the active conformation of PAI-1 [15]. In particular, the binding interaction between PAI-1 and vitronectin (VN) allows it to follow similar localization fates as vitronectin, thus broadening its participation and effects in various environments.

1.1.3. *Synthesis and cellular fates* – PAI-1 is synthesized by a wide range of cell types such as megakaryocytes, endothelial cells, adipocytes, smooth muscle cells and fibroblasts – all of mesenchymal origin [16, 17] as well as some epithelial cell types [18]. Post-synthesis, the intracellular fate of PAI-1 has only been described in megakaryocytes, platelets, endothelial cells and to a lesser extent, epithelial cells [19-21]. In terms of intracellular compartmentalization, PAI-1 is processed into storage granules such as α-granules in platelets and megakaryocytes. Stimulation by thrombin, collagen or calcium ionophore lead to immediate exocytosis of α-granules and release of PAI-1 [19]. A large percentage of PAI-1 stored within α-granules is of the latent and inactive conformation, perhaps indicative of the length of time spent in storage, which is beyond the half-life of active PAI-1 [22]. Endothelial cells are thought to synthesize the majority of circulating levels of active and latent PAI-1 in plasma [21] and variations in these PAI-1 plasma levels have been correlated with a variety of diseases such as obesity, thromboembolic disease and atherosclerosis [23-26]. However, the manner in which PAI-1 is intracellularly compartmentalized and stored within endothelial cells is unclear and controversial; one report points to the Golgi as the main storage organelle [27], whereas another report describes a loose cytoplasmic storage within endothelial cells while others report compartmentalization into storage granules [28], albeit in immortalized cell lines. Reports also demonstrate a mechanism of constitutive secretion into the lumen, however, it is unclear whether this secretion is mediated by exocytosis or passive release [29, 30].

1.1.4. *PAI-1 in disease* – Because of the inhibitory nature of PAI-1 on plasminogen activators (tPA and uPA), it is often implicated in the pathogenesis of a variety of diseases ranging from cancer metastasis to thrombosis as underscored by their pivotal roles in hemostasis and ECM metabolism, respectively. High plasma concentrations of PAI-1 which have been observed in individuals with insulin resistance and obesity can also lead to impaired fibrinolysis and an increased risk for cardiovascular disease [31]. Specifically, the long-term elevation of PAI-1 in plasma or intramurally (within a thrombus or vessel) can induce fibrosis of vessels or atherosclerotic lesion development and may even induce thrombotic disorders [32-34]. It is also believed that high plasma levels of PAI-1or an intracoronary thrombus with high PAI-1 content may counter the effects of thrombolytic therapy during its administration to patients undergoing an acute myocardial infarction [35, 36].

1.2. Vitronectin (VN)

1.2.1. *Overview* - Vitronectin is a major plasma glycoprotein predominantly synthesized by the liver but is also synthesized at low levels by other tissues such as adipose, brain,heart, and skeletal muscle [37]. In plasma it exists at concentrations of 3-5 μM [38] and is also found in abundance within the extracellular matrix (ECM) [39, 40]. Apart from its ability to stabilize PAI-1 [41], VN also interacts with heparin [42, 43], collagen [39], urokinase plasminogen activator receptor (uPAR) [44], components of the complement system [45] and thrombin/anti-thrombin III complexes [46]. Because of this wide range of biochemical interactions, VN plays an important mediating role in hemostasis, the innate immune system, angiogenesis and wound repair by either acting as a ligand parter for other proteins and determining the distribution or

substrates for these VN-ligand complexes. Key to the majority of these interactions is the presence of the somatomedin B domain and an Arg-Gly-Asp (RGD) sequence [47].

1.2.2. *Biochemical properties and interactions* - Vitronectin exists in two major conformations: monomeric and multimeric VN [48]. Monomeric VN is found in two conformations, a 75 kDa form and a 65+10 kDa two-chain form. The 65+10 kDa form is formed by proteolytic cleavage of the 75 kDa form, but remains intact post-proteolytic cleavage [49]. The majority of plasma VN exists in the monomeric form, whereas <2% of VN circulates as multimeric VN by virtue of several disulfide bridge linkages. These high molecular weight multimers of vitronectin [50] are highly active forms of VN [51] that are more readily available to bind to ligand partners such as PAI-1, which maintains PAI-1 activity. Because of its multi-ligand partner (adhesive) properties, multimeric VN can potentiate the inhibition of fibrinolysis by associating with PAI-1 and mediating its binding to fibrin clots and vimentin [52, 53].

By using sequence homology, the VN molecule can be defined by three major domains: the N-terminus which contains the somatomedian B domain; the central domain containing several hemopexin-like repeats; and the C-terminal domain. Within the N-terminus domain, the somatomedin B domain (aa 1-44) harbors functional groups that are largely responsible for its binding interactions with PAI-1 [54]. Because of this interaction, VN participates in pericellular proteolysis of ECM through its localization and binding to PAI-1 and subsequent inhibition of plasmin formation. Immediately upstream of this is the RGD sequence (aa 45-47), a key element in mediating cell motility and cell adhesion on ECM and adjacent cells via its binding interactions with various integrin receptors. Pericellular distribution and supply of VN can also regulate the extent of cell spreading and motility [55]. Adjacent to the RGD motif is the heparin binding site, as well as a domain responsible for anti-thrombin III binding (aa 53-64) [56], and

two collagen binding sites [40] that mediate vitronectin's binding to matrix. Because of this region, VN may act as a pro-coagulant because of its ability to neutralize and clear heparin out of the circulation [40]. When this occurs, less heparin becomes available to anti-thrombin, resulting in higher thrombin levels and higher incidences of coagulation and fibrin formation [40].

Beyond the N-terminus and within the central domain lie stretches of acidic and basic elements that, by ionic interaction, are likely involved in maintaining the 3-D structure of the VN molecule. This vast stretch of VN (aa 132-459) contains 6 hemopexin-like repeating domains that contain several cysteines that participate and are [57] central to disulfide bridge formation, VN molecular structure and VN multimerization. Other than these structural contributions, a biological role for hemopexin-like repeats on VN remains unclear; although some reports describe binding interactions with *S. pyogenes* to the extent where vitronectin "coats" the majority of the bacterial surface, hence suggesting an opsonization function for plasma VN[58].

The C-terminus end of VN contains a binding site for plasminogen (aa 332-348), and a second heparin binding site (aa 348-379) [59]. A second binding site for PAI-1 has also been determined at aa 348-370 [60], which enables VN to form both 1:1 or 1:2 stoichiometric ratio complexes with PAI-1[61].

1.2.3. *Synthesis and cellular fates* – Initially classified as "serum spreading factor", VN is synthesized by a variety of cell types, but is predominantly synthesized within the liver and secreted into the bloodstream to plasma concentrations of 200-400 µg/mL (3-5µM). VN is primarily synthesized by hepatocytes [37] but extra-hepatic synthesis of VN is known to occur in brain, fibroblasts, adipose tissue, heart and skeletal muscle albeit at a 25- to 100-fold lower amount compared to liver [37]. *In vitro* VN synthesis also occurs in macrophages, monocytes and human umbilical vascular endothelial cells (HUVEC). VN is a major constituent of ECM,

which exists predominantly in its multimeric form and bound to matrix and glycosaminoglycans (heparin) [62]. Tissue injury and wound healing is characteristically marked by VN accumulation, within necrotic cells [63] or in the provisional matrix, subsequently promoting fibrosis via its interactions with PAI-1 [64-67].

A vitronectin knockout mouse has been developed [68] for studies on the role of vitronectin in hemodynamics and thrombus formation. It has also been used for studies on wound healing and myocardial infarction. When compared to wildtype models, the vitronectin - /- mice generate highly unstable thrombi that dissolve quickly [69] and demonstrate markedly reduced wound healing as a result of decreased cell migration [70].

1.2.4. *VN in disease* – VN is part of a group of proteins called acute phase response proteins [71] whose plasma concentrations vary in response to the extent of inflammation. An acute phase response that follows a typical inflammatory response can result in local vasodilation, platelet aggregation, neutrophil chemotaxis, and the release of lysosomal enzymes, histamines, kinins and oxygen radicals [71]. Systemic events can result in fever, hormonal changes and even alterations in metabolism. For example, studies in rats and humans demonstrate substantial changes in these levels during the acute phase response following tissue injury [37, 72]. One such example of tissue injury is acute myocardial infarction (AMI), in which a thrombotic occlusion within a major coronary artery halts fresh blood perfusion of myocardium served downstream of the occlusion. This condition also triggers an acute phase response [71] with a concomitant increase in VN plasma levels [73]. In the event of an AMI, it is conceivable that increased acute phase reactant proteins such as VN act as heparin-binding proteins, serving to non-specifically bind heparin in circulation [74] which may decrease the anticoagulant effect of heparin because of its deposition into ECM and clearance from plasma –

a distribution which presents less heparin to anti-thrombin III. Abnormal plasma levels of VN are also present in patients with rheumatic disease [75]. In detail, increased VN present in synovial fluid and inflamed joints may promote cell motility and accelerate wound healing. Higher rates of VN synthesis in differentiating neuroblastic tumors have also been reported, implicating its roles in cell motility and adhesion on matrix [76].

1.3. Vimentin

1.3.1. *Overview* – Vimentin is a cytoskeletal protein that forms intermediate filaments (IF), a major component of a cell's cytoskeleton. Intermediate filaments composed of vimentin provide a substantial amount of structural rigidity within a cell and structurally supports the organelles and nucleus of a cell [77-79]. Moreover, intermediate filament networks are cortically distributed underneath the cell membrane to provide much needed mechanical support during cell-to-cell and cell-to-ECM interactions. IFs are so called because their diameter (8-12 nm) is intermediate between thin actin microfilaments (7 nm) and thick microtubules (25 nm) [77-79].

There are various classes of IFs with classification being based on sequence similarities. Prime examples of type I and II intermediate filament proteins are keratins; vimentin and desmin are examples of type III IF proteins; and neuronal proteins are examples of type IV IF proteins. Vimentin IFs are found in cells of a mesenchymal lineage: endothelium, fibroblasts, smooth muscle cells, erythrocytes, leukocytes, platelets, etc. [77-79]. Conversely, cardiac and skeletal muscle synthesize desmin IF's in which the main function is to specifically stabilize and organize sarcomeres by associating with the Z-disk of sarcomeres and connecting them with the Z-disks of other neighboring sarcomeres [80]. Vimentin IF networks resemble a radial

8

distribution alongside the shape of the cell, with IF's terminating at nuclear membranes and desmosomes at cell membranes as well wrapping around organelles and the nucleus to provide spatial distribution [77].

1.3.2. *Biochemical properties and interactions* –Assembly of type III IF's can incorporate either vimentin or desmin, often occurring in immature myoblasts but not in fully differentiated cell types [81, 82]. Tetramers of vimentin are the basic subunit for IF assembly and these will form long chains, two of which will associate with each other to form an α-helical dimer chain, resulting in a complete vimentin IF with a diameter of 8-12 nm [78]. Intermediate filament protein monomers have a common structural component, called the coiled-coil region (300-330 aa long) and the diversity of IF's lies within the diversity of sequence and length of the N-terminus and C-terminus. The coiled-coil region is largely responsible as a longitudinal spacer and/or a lateral packing module, hence providing rigidity and structural integrity. The amino-terminal has been shown to be essential for proper assembly of filaments [83-85] and is also highly susceptible to proteolytic attack usually leading to posttranslational modification. N-terminal structural modifications of vimentin IF's may possibly dictate its intracellular distribution and molecular organization in various physiological and pathological conditions [86]. Extracellularly, exposed vimentin IF's in activated or apoptosed cells may also undergo citrullination, a process that alters the biochemistry of vimentin in which arginine residues are deiminized and converted into citrulline [87, 88]. This deiminization of vimentin has been found to take place within the synovial fluid within joints, largely mediated by macrophages and monocytes in disease contexts such as rheumatoid arthritis [87, 88].

Apart from proteolytic modifications of vimentin, there are a number of important proteins that associate with vimentin, one group being proteins such as kinesin and dynein that

bind to vimentin and traverse along microtubules to help vimentin IF's generate their radial

network throughout the cell [89, 90]. Another set of proteins also associate with vimentin but

with each interaction providing a different function: VN has been shown to multimerize when

monomers first interact with exposed vimentin in the extracellular space [53]. This

multimerization of vitronectin is not well understood but the binding site on vimentin responsible

for this multimerization is found within the first 133 aa of the vimentin N-terminus and likely

upstream of the thrombin cleavage site (94 aa) on vimentin [53]. The observation of VN

multimerization as induced by exposed vimentin IF has many implications, particularly in

explaining how VN multimers are established within ECM and its origins.

The Fc receptors of heavy chain immunoglobulins have also been described with the

ability to bind to vimentin IF's, an interaction that proposes immune-targeted clearance of

activated and dead cells exposing vimentin to plasma [91, 92]. The first reports of this binding

interaction were observed on endothelial cells and implicated complement-mediated lysis as the

primary means of clearing dead endothelial cells [91, 92], a proposed mechanism preceding the

now accepted pathways of apoptosis as a means of clearing cells.

1.3.3. *Vimentin as the cell surface receptor for PAI-1*– PAI-1:VN complexes account

for 95% of active PAI-1 in plasma, at a normal concentration of 20 ng/mL [93]. The magnitude

and percentage of circulating active PAI-1 can vary significantly, particularly during

coagulation, tissue injury and wound healing. PAI-1:VN complexes have been observed in

abundance on fibrin fibils in clots and activated platelets with strong, high affinity binding

interactions in which $K_d \gg 10^{-7}$ [52, 53]. Other reports have also demonstrated low affinity

binding interactions with PAI-1, ligands such as the Aα chain of fibrinogen (16210568), alpha$_1$-

acid glycoprotein (16156651), but of a low affinity binding interaction ($\ll 10^{-5}$). PAI-1 binding

interactions with vitronectin, more likely to occur given its plasma concentration, mediates the

localization of PAI-1 to fibrin and activated platelets by interaction with γA/γ'fibrinogen

monomers within fibrin fibrils [52] and exposed vimentin cytoskeleton on the surface of

activated platelets and platelet microparticles [53]. More specifically, the N-terminus head of

vimentin interacts with vitronectin that results in multimerization of vitronectin on the vimentin

filament, with pre-existing PAI-1:VN complexes in plasma ready to be incorporated into the

multimerized VN via VN homotypic interactions (Figure 1.2) [94].
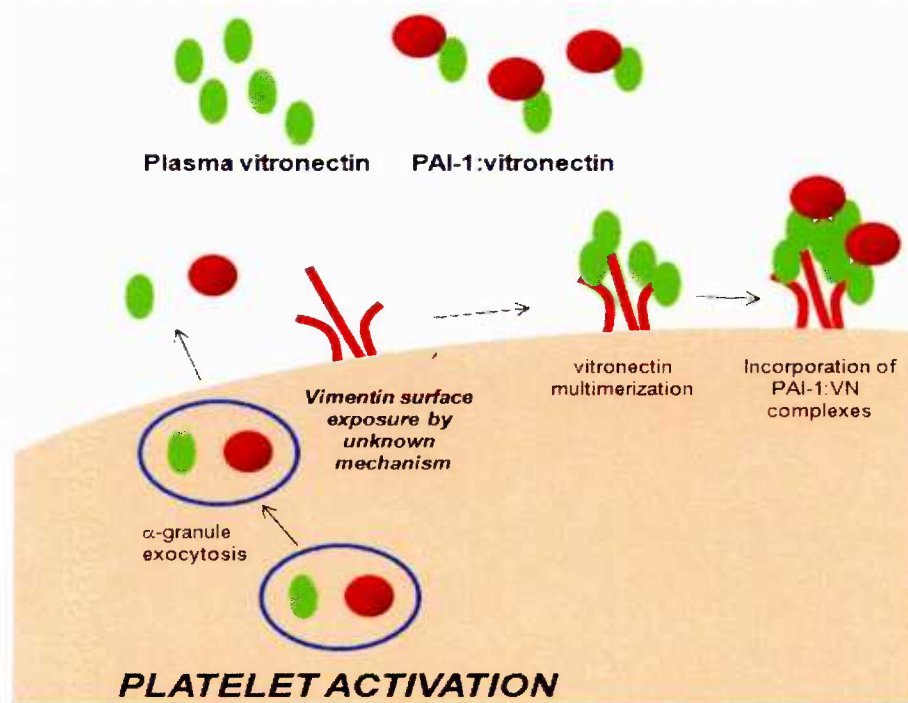
Figure 1.2. Summary of PAI-1-vitronectin-vimentin ternary complex formation. Upon platelet activation, platelet stores of VN and PAI-1 are released into plasma and is accompanied by the exposure of vimentin IF's via an unknown mechanism. This exposed vimentin is susceptible to vitronectin multimerization which provides a form of vitronectin amenable to homotypic interactions with pre-existing PAI-1:VN complexes in plasma. PAI-1:VN complexes become bound to this multimerized VN and the PAI-1-VN-VIM ternary complex is formed.

Extracellular presentation of PAI-1 occurs when it forms a ternary complex with

vitronectin and vimentin cytoskeleton that is exposed on the surface of an activated cell but this

mechanism of cell surface expression occurs without the requirement for a transmembrane

11

protein receptor. However, it does provide a mechanism as to how active PAI-1 in complex with vitronectin can be bound to cell surfaces, i.e., platelets and platelet microparticles. Moreover, because VN has self-association properties to form VN multimers, PAI-1-VN complexes can bind to the growing VN aggregate, due to VN-VN homotypic interactions, thus incorporating both circulating plasmaVN, pre-exiting PAI-1:VN plasma complexes and PAI-1:VN complexes exocytosed during platelet activation [94]. Thus, physical exposure of platelet vimentin cytoskeleton results in the PAI-1 localized on cell surfaces within thrombi, formation of ternary complexes that require multimerized VN.

1.3.4. *Vimentin in disease* – Vimentin was initially used as a histological marker of tumor malignancy and the extent of cancer progression in breast carcinomas and melanomas. Morphologically, tumor growth and its cytoskeleton assembly can outpace cell surface adaptability, leading to the exposure of internal structure to the extracellular environment, thus evoking the description of cancer as "tumors: wounds that do not heal" [95]. Because IF protein composition is a defined characteristic for all cell types, IF type I-VI composition can reveal the extent of tumor cell differentiation and previous cell-type identities of the cancer cell mass [96]. In terms of actual function, the abundance of vimentin IFs as observed in tumor cells both *in vitro* and *in vivo* may yield augmented motility and invasiveness of tumor cells [97] with a fibrillary pattern of distribution. Although not yet shown or determined, it is reasonable to speculate that if vimentin is exposed on the surface of tumor cells, it may mediate binding of multimerized vitronectin, thus providing an added element of cell adhesion, particularly at sites of cell damage or cell activation. Nonetheless, the hypothesis that over-expression of vimentin in some tumor cells confers a selective advantage remains to be elucidated.

Auto-antibodies specific for vimentin are a common diagnostic feature of diseases such as systemic lupus erythematosus (SLE) [98], rheumatoid arthritis (RA) [99] and transplant vasculopathy [100]. The pathogenesis of SLE is not well defined but it is hypothesized that impaired clearance of apoptosed cells may be the source of vimentin that leads to anti-vimentin antibody (AVA) production [101]. It is suspected that IF-nuclear complexes from incompletely apoptosed cells are responsible [98, 102]. To date, a pathogenic role for AVA has not been described in SLE patients. Patients with rheumatoid arthritis also develop anti-vimentin antibodies, but these are specific for citrinullated vimentin, its deiminated form. This citrinullated autoantigen may be generated from chronic destruction of synovial tissue, the soft connective tissue between joints. Inflammation of synovial tissue is often accompanied by mesenchymal fibroblast and chondrocyte proliferation, leading to vimentin release in the upwelling of synovial fluid within the cavity [103]. It is within this fluid-filled cavity that macrophages can release proteolytic enzymes that modify and citrullinate vimentin, which may possibly be processed by the immune system to generate an AVA response [87]. Again, no pathological function of autoantibodies specific for citrullinated vimentin has been determined.

1.4. Organ Transplant Vasculopathy

1.4.1. *Introduction* - Once commonplace, acute organ rejection has now been limited to <10% of all transplant recipients [104] due to the introduction of "immuno-suppresant" drugs. For example, Cyclosporin™ inhibits the synthesis of proliferative cytokines in immune cells, such as IL-2, that would have resulted in the proliferation of more lymphocytes that would induce a prolonged allo-immune response against the graft [105, 106]. However, despite a low incidence of acute rejection and an immunosuppressant regiment, these highly vascularized

grafts often succumb to another form of rejection, known as chronic rejection, and this occurs at 3-10 years post-transplantation [107]. Chronic rejection of heart and kidney grafts is characterized by obliterative arteriosclerosis as a result of chronic inflammation, medial necrosis and intimal thickening of all the vessels of the graft [108, 109].

1.4.2. *Chronic organ rejection and MHC-mismatches* - Chronic rejection, also known as transplant vasculopathy (TV) disease, is a multi-factorial disease that is distinct from conventional lipid-induced atherosclerotic lesions [108, 109]. Conventional atherosclerosis is morphologically distinct, as lesions are eccentric in their cross-sectional morphology and contain lipid-rich, necrotic cores. Furthermore, these lesions are only found in some of the larger arteries of the heart. On the contrary, TVD lesions are concentric in cross-section, and all vessels of the heart are uniformly narrowed, including the microvasculature and veins [108, 109]. Although there is a noticeable lack of a lipid-rich core in the early to middle stages of the disease, lipid-lowering agents have demonstrated pleiotropic and anti-inflammatory effects, contributing to enhanced management of TVD [110-112]. However, considering that only the vasculature of the graft is affected whereas other vessels in the body are not, the suppressed host immune system is implicated in the chronic development of atheromatous lesions in all graft vasculature.

Key to most immune responses are the MHC Class I (presents virally produced proteins and self antigens) and II (presents phagocytosed/endocytosed antigens that undergo proteolytic processing) complexes which function to present foreign or self-antigen on the cell surface that will subsequently generate a cellular and humoral immune response [113, 114]. MHC complexes are synthesized and found on the surface of every nucleated cell, but not all MHC complexes are identical; in fact, there are two major classes of human MHC molecules in which there are up to 100 different MHC molecules. Each person contains an exclusive set of 6 MHC

Class I complexes and 6 MHC Class II complexes and in the event of an organ or tissue transplant, efforts towards identifying the set of MHC molecules of a graft and finding a near-compatible host is critical in order to minimize the amount of MHC mismatch [113, 114]. Although organs are allocated to patients as to minimize MHC mismatches between the host and donor, there will usually be a minor mismatch and the host will develop an allo-immune response against the graft [113]. Despite immunosuppression, a dampened immune response will nevertheless target the organ; in which two major immune outcomes will result: maturation of T-cells (cell-mediated immunity) and antibodies (humoral immunity) against the foreign MHC molecules [115-117] and in some cases, the damaged graft itself (non-MHC antibodies).

1.4.3. *Antibody-mediated rejection and non-MHC autoantibodies* - Chronic rejection is the result of long term damage caused by low levels of activated graft-specific lymphocytes due to immunosuppression and antibody-mediated targeting of the graft. These antibodies can be grouped into: MHC and non-MHC antibodies wherein MHC antibodies are specific for non-host MHC molecules. Some prime examples of non-MHC antibodies are structural proteins such as myosin, collagen and vimentin [100, 118, 119]. Both MHC and non-MHC antibodies exert their effects on the graft by inducing complement-mediated lysis as seen by the abundance of complement split products deposited within the graft vasculature [120]. This antibody-mediated complement lysis of endothelium results in inflamed vasculature and dysfunction, thus promoting atherogenic mechanisms and further immune cell deposition into the graft vasculature [121].

Many studies have identified the intermediate filament vimentin as an important autoantigen after allotransplantation [122] leading to the formation of non-MHC antibodies specific for vimentin. Significant levels of these non-MHC anti-vimentin antibody titres after

heart transplantation are associated with the development of graft vasculopathy [123], and these patients also have self-restricted vimentin-specific CD8+-T-cells [124]. Recipients of renal allografts suffering from chronic rejection also have significant titres of anti-vimentin antibodies [125]. Moreover, renal allografts placed in recipients with previously high titers of anti-vimentin antibodies have a higher predisposition to suffer from steroid-resistant acute rejection [125].

The source of vimentin autoantigen is unclear in the context of transplant vasculopathy, but is suspected to originate from the cleavage of vimentin fragments off the surface of apoptosing endothelial cells [126], leukocytes [127], and activated platelets [53], all of which exist during the pathogenesis of TVD [126, 127]. As apoptotic cells and antigens released from these cells are processed by host dendritic cells and presented to self-MHC restricted recipient T-cells [126, 127], an antibody response may be mounted due to the high inflammatory state of the patient and associated coactivated T-cell population [128]. Moreover, long ischemic times increase apoptosis in the graft, which is associated with increased levels of caspase-3 [129], that cleave vimentin in the cytoskeleton early in apoptosis [130].

The potentially pathogenic contribution of anti-vimentin antibodies cannot be ignored. Moderate to high levels of anti-vimentin antibody titres (AVA) in patients with cardiac grafts demonstrate a strong correlation with the incidence of coronary artery disease [123]. However, the mechanisms of its pathogenic effects on the graft and hemostasis remain unknown.

1.5. References for Chapter I

1. Shore JD, Day DE, Francis-Chmura AM, Verhamme I, Kvassman J, Lawrence DA, Ginsburg D. A fluorescent probe study of plasminogen activator inhibitor-1. Evidence for reactive center loop insertion and its role in the inhibitory mechanism. *J Biol Chem* 1995; **270**:5395-8.

2. Kjoller L, Martensen PM, Sottrup-Jensen L, Justesen J, Rodenburg KW, Andreasen PA. Conformational changes of the reactive-centre loop and beta-strand 5A accompany temperature-dependent inhibitor-substrate transition of plasminogen-activator inhibitor 1. *Eur J Biochem* 1996; **241**:38-46.

3. Kvassman JO, Verhamme I, Shore JD. Inhibitory mechanism of serpins: loop insertion forces acylation of plasminogen activator by plasminogen activator inhibitor-1. *Biochemistry* 1998; **37**:15491-502.

4. Thelwell C, Longstaff C. The regulation by fibrinogen and fibrin of tissue plasminogen activator kinetics and inhibition by plasminogen activator inhibitor 1. *J Thromb Haemost* 2007; **5**:804-11.

5. Bonnefoy A, Legrand C. Proteolysis of subendothelial adhesive glycoproteins (fibronectin, thrombospondin, and von Willebrand factor) by plasmin, leukocyte cathepsin G, and elastase. *Thromb Res* 2000; **98**:323-32.

6. Brodsky S, Chen J, Lee A, Akassoglou K, Norman J, Goligorsky MS. Plasmin-dependent and -independent effects of plasminogen activators and inhibitor-1 on ex vivo angiogenesis. *Am J Physiol Heart Circ Physiol* 2001; **281**:H1784-92.

7. Chazaud B, Bonavaud S, Plonquet A, Pouchelet M, Gherardi RK, Barlovatz-Meimon G. Involvement of the [uPAR:uPA:PAI-1:LRP] complex in human myogenic cell motility. *Exp Cell Res* 2000; **258**:237-44.

8. Dellas C, Loskutoff DJ. Historical analysis of PAI-1 from its discovery to its potential role in cell motility and disease. *Thromb Haemost* 2005; **93**:631-40.

9. Andreasen PA, Egelund R, Petersen HH. The plasminogen activation system in tumor growth, invasion, and metastasis. *Cell Mol Life Sci* 2000; **57**:25-40.

10. Lawrence DA, Palaniappan S, Stefansson S, Olson ST, Francis-Chmura AM, Shore JD, Ginsburg D. Characterization of the binding of different conformational forms of plasminogen activator inhibitor-1 to vitronectin. Implications for the regulation of pericellular proteolysis. *J Biol Chem* 1997; **272**:7676-80.

11. Stratikos E, Gettins PG. Formation of the covalent serpin-proteinase complex involves translocation of the proteinase by more than 70 A and full insertion of the reactive center loop into beta-sheet A. *Proc Natl Acad Sci U S A* 1999; **96**:4808-13.

12. Levin EG, Santell L. Conversion of the active to latent plasminogen activator inhibitor from human endothelial cells. *Blood* 1987; **70**:1090-8.

13. Hekman CM, Loskutoff DJ. Endothelial cells produce a latent inhibitor of plasminogen activators that can be activated by denaturants. *J Biol Chem* 1985; **260**:11581-7.

14. Carrell RW, Evans DL, Stein PE. Mobile reactive centre of serpins and the control of thrombosis. *Nature* 1991; **353**:576-8.

15. Seiffert D, Ciambrone G, Wagner NV, Binder BR, Loskutoff DJ. The somatomedin B domain of vitronectin. Structural requirements for the binding and stabilization of active type 1 plasminogen activator inhibitor. *J Biol Chem* 1994; **269**:2659-66.

16. Heaton JH, Dlakic WM, Gelehrter TD. Posttranscriptional regulation of PAI-1 gene expression. *Thromb Haemost* 2003; **89**:959-66.

17. Montuori N, Rossi G, Ragno P. Post-transcriptional regulation of gene expression in the plasminogen activation system. *Biol Chem* 2002; **383**:47-53.

18. Latron Y, Alessi MC, George F, Anfosso F, Poncelet P, Juhan-Vague I. Characterization of epitheloid cells from human omentum: comparison with endothelial cells from umbilical veins. *Thromb Haemost* 1991; **66**:361-7.

19. Hill SA, Shaughnessy SG, Joshua P, Ribau J, Austin RC, Podor TJ. Differential mechanisms targeting type 1 plasminogen activator inhibitor and vitronectin into the storage granules of a human megakaryocytic cell line. *Blood* 1996; **87**:5061-73.

20. Lang IM, Schleef RR. Calcium-dependent stabilization of type I plasminogen activator inhibitor within platelet alpha-granules. *J Biol Chem* 1996; **271**:2754-61.

21. Schleef RR, Podor TJ, Dunne E, Mimuro J, Loskutoff DJ. The majority of type 1 plasminogen activator inhibitor associated with cultured human endothelial cells is located under the cells and is accessible to solution-phase tissue-type plasminogen activator. *J Cell Biol* 1990; **110**:155-63.

22. Brogren H, Karlsson L, Andersson M, Wang L, Erlinge D, Jern S. Platelets synthesize large amounts of active plasminogen activator inhibitor 1. *Blood* 2004; **104**:3943-8.

23. Nagai N, Van Hoef B, Lijnen HR. Plasminogen activator inhibitor-1 contributes to the deleterious effect of obesity on the outcome of thrombotic ischemic stroke in mice. *J Thromb Haemost* 2007; **5**:1726-31.

24. Haapaniemi E, Tatlisumak T, Soinne L, Syrjala M, Kaste M. Plasminogen activator inhibitor-1 in patients with ischemic stroke. *Acta Neurochir Suppl* 2000; **76**:277-8.

25. Yamamoto K, Saito H. A pathological role of increased expression of plasminogen activator inhibitor-1 in human or animal disorders. *Int J Hematol* 1998; **68**:371-85.

26. Huber K. Plasminogen activator inhibitor type-1 (part one): basic mechanisms, regulation, and role for thromboembolic disease. *J Thromb Thrombolysis* 2001; **11**:183-93.

27. Ma GM, Halayko AJ, Stelmack GL, Zhu F, Zhao R, Hillier CT, Shen GX. Effects of oxidized and glycated low-density lipoproteins on transcription and secretion of plasminogen activator inhibitor-1 in vascular endothelial cells. *Cardiovasc Pathol* 2006; **15**:3-10.

28. Gombau L, Schleef RR. Processing of type 1 plasminogen activator inhibitor (PAI-1) into the regulated secretory pathway. *J Biol Chem* 1994; **269**:3875-80.

29. Schleef RR, Loskutoff DJ, Podor TJ. Immunoelectron microscopic localization of type 1 plasminogen activator inhibitor on the surface of activated endothelial cells. *J Cell Biol* 1991; **113**:1413-23.

30. Hakkert BC, Rentenaar JM, van Mourik JA. Monocytes enhance the bidirectional release of type I plasminogen activator inhibitor by endothelial cells. *Blood* 1990; **76**:2272-8.

31. Trost S, Pratley R, Sobel B. Impaired fibrinolysis and risk for cardiovascular disease in the metabolic syndrome and type 2 diabetes. *Curr Diab Rep* 2006; **6**:47-54.

32. DeYoung MB, Tom C, Dichek DA. Plasminogen activator inhibitor type 1 increases neointima formation in balloon-injured rat carotid arteries. *Circulation* 2001; **104**:1972-1.

33. Kaikita K, Fogo AB, Ma L, Schoenhard JA, Brown NJ, Vaughan DE. Plasminogen activator inhibitor-1 deficiency prevents hypertension and vascular fibrosis in response to long-term nitric oxide synthase inhibition. *Circulation* 2001; **104**:839-44.

34. Carmeliet P, Moons L, Lijnen R, Janssens S, Lupu F, Collen D, Gerard RD. Inhibitory role of plasminogen activator inhibitor-1 in arterial wound healing and neointima formation: a gene targeting and gene transfer study in mice. *Circulation* 1997; **96**:3180-91.

35. Rupin A, Martin F, Vallez MO, Bonhomme E, Verbeuren TJ. Inactivation of plasminogen activator inhibitor-1 accelerates thrombolysis of a platelet-rich thrombus in rat mesenteric arterioles. *Thromb Haemost* 2001; **86**:1528-31.

36. Zhu Y, Carmeliet P, Fay WP. Plasminogen activator inhibitor-1 is a major determinant of arterial thrombolysis resistance. *Circulation* 1999; **99**:3050-5.

37. Seiffert D, Crain K, Wagner NV, Loskutoff DJ. Vitronectin gene expression in vivo. Evidence for extrahepatic synthesis and acute phase regulation. *J Biol Chem* 1994; **269**:19836-42.

38. Kobayashi J, Yamada S, Kawasaki H. Distribution of vitronectin in plasma and liver tissue: relationship to chronic liver disease. *Hepatology* 1994; **20**:1412-7.

39. Dawes J. Interactions of heparins in the vascular environment. *Haemostasis* 1993; **23 Suppl 1**:212-9.

40. Ishikawa-Sakurai M, Hayashi M. Two collagen-binding domains of vitronectin. *Cell Struct Funct* 1993; **18**:253-9.

41. Arroyo De Prada N, Schroeck F, Sinner EK, Muehlenweg B, Twellmeyer J, Sperl S, Wilhelm OG, Schmitt M, Magdolen V. Interaction of plasminogen activator inhibitor type-1 (PAI-1) with vitronectin. *Eur J Biochem* 2002; **269**:184-92.

42. Kost C, Stuber W, Ehrlich HJ, Pannekoek H, Preissner KT. Mapping of binding sites for heparin, plasminogen activator inhibitor-1, and plasminogen to vitronectin's heparin-binding region reveals a novel vitronectin-dependent feedback mechanism for the control of plasmin formation. *J Biol Chem* 1992; **267**:12098-105.

43. Underwood PA, Kirkpatrick A, Mitchell SM. New insights into heparin binding to vitronectin: studies with monoclonal antibodies. *Biochem J* 2002; **365**:57-67.

44. Madsen CD, Ferraris GM, Andolfo A, Cunningham O, Sidenius N. uPAR-induced cell adhesion and migration: vitronectin provides the key. *J Cell Biol* 2007; **177**:927-39.

45. Milis L, Morris CA, Sheehan MC, Charlesworth JA, Pussell BA. Vitronectin-mediated inhibition of complement: evidence for different binding sites for C5b-7 and C9. *Clin Exp Immunol* 1993; **92**:114-9.

46. Preissner KT, Anders E, Grulich-Henn J, Muller-Berghaus G. Attachment of cultured human endothelial cells is promoted by specific association with S protein (vitronectin) as well as with the ternary S protein-thrombin-antithrombin III complex. *Blood* 1988; **71**:1581-9.

47. Royle G, Deng G, Seiffert D, Loskutoff DJ. A method for defining binding sites involved in protein-protein interactions: analysis of the binding of plasminogen activator inhibitor 1 to the somatomedin domain of vitronectin. *Anal Biochem* 2001; **296**:245-53.

48. Zhuang P, Chen AI, Peterson CB. Native and multimeric vitronectin exhibit similar affinity for heparin. Differences in heparin binding properties induced upon denaturation are due to self-association into a multivalent form. *J Biol Chem* 1997; **272**:6858-67.

49. Tomasini BR, Owen MC, Fenton JW, 2nd, Mosher DF. Conformational lability of vitronectin: induction of an antigenic change by alpha-thrombin-serpin complexes and by proteolytically modified thrombin. *Biochemistry* 1989; **28**:7617-23.

50. Izumi M, Yamada KM, Hayashi M. Vitronectin exists in two structurally and functionally distinct forms in human plasma. *Biochim Biophys Acta* 1989; **990**:101-8.

51. Zanetti A, Conforti G, Hess S, Martin-Padura I, Ghibaudi E, Preissner KT, Dejana E. Clustering of vitronectin and RGD peptides on microspheres leads to engagement of integrins on the luminal aspect of endothelial cell membrane. *Blood* 1994; **84**:1116-23.

52. Podor TJ, Campbell S, Chindemi P, Foulon DM, Farrell DH, Walton PD, Weitz JI, Peterson CB. Incorporation of vitronectin into fibrin clots. Evidence for a binding interaction between vitronectin and gamma A/gamma' fibrinogen. *J Biol Chem* 2002; **277**:7520-8.

53. Podor TJ, Singh D, Chindemi P, Foulon DM, McKelvie R, Weitz JI, Austin R, Boudreau G, Davies R. Vimentin exposed on activated platelets and platelet microparticles localizes vitronectin and plasminogen activator inhibitor complexes on their surface. *J Biol Chem* 2002; **277**:7529-39.

54. Seiffert D, Loskutoff DJ. Kinetic analysis of the interaction between type 1 plasminogen activator inhibitor and vitronectin and evidence that the bovine inhibitor binds to a thrombin-derived amino-terminal fragment of bovine vitronectin. *Biochim Biophys Acta* 1991; **1078**:23-30.

55. Schvartz I, Seger D, Shaltiel S. Vitronectin. *Int J Biochem Cell Biol* 1999; **31**:539-44.

56. Ill CR, Ruoslahti E. Association of thrombin-antithrombin III complex with vitronectin in serum. *J Biol Chem* 1985; **260**:15610-5.

57. Jenne D, Stanley KK. Nucleotide sequence and organization of the human S-protein gene: repeating peptide motifs in the "pexin" family and a model for their evolution. *Biochemistry* 1987; **26**:6735-42.

58. Liang OD, Preissner KT, Chhatwal GS. The hemopexin-type repeats of human vitronectin are recognized by Streptococcus pyogenes. *Biochem Biophys Res Commun* 1997; **234**:445-9.

59. Gibson AD, Lamerdin JA, Zhuang P, Baburaj K, Serpersu EH, Peterson CB. Orientation of heparin-binding sites in native vitronectin. Analyses of ligand binding to the primary glycosaminoglycan-binding site indicate that putative secondary sites are not functional. *J Biol Chem* 1999; **274**:6432-42.

60. Gechtman Z, Belleli A, Lechpammer S, Shaltiel S. The cluster of basic amino acids in vitronectin contributes to its binding of plasminogen activator inhibitor-1: evidence from

thrombin-, elastase- and plasmin-cleaved vitronectins and anti-peptide antibodies. *Biochem J* 1997; **325 (Pt 2)**:339-49.

61.   Podor TJ, Shaughnessy SG, Blackburn MN, Peterson CB. New insights into the size and stoichiometry of the plasminogen activator inhibitor type-1.vitronectin complex. *J Biol Chem* 2000; **275**:25402-10.

62.   Preissner KT. Self-association of antithrombin III relates to multimer formation of thrombin-antithrombin III complexes. *Thromb Haemost* 1993; **69**:422-9.

63.   Podor TJ, Joshua P, Butcher M, Seiffert D, Loskutoff D, Gauldie J. Accumulation of type 1 plasminogen activator inhibitor and vitronectin at sites of cellular necrosis and inflammation. *Ann N Y Acad Sci* 1992; **667**:173-7.

64.   Rus HG, Niculescu F, Vlaicu R. Presence of C5b-9 complement complex and S-protein in human myocardial areas with necrosis and sclerosis. *Immunol Lett* 1987; **16**:15-20.

65.   Dahlback K, Lofberg H, Dahlback B. Immunohistochemical studies on vitronectin in elastic tissue disorders, cutaneous amyloidosis, lichen ruber planus and porphyria. *Acta Derm Venereol* 1988; **68**:107-15.

66.   Dahlback K, Lofberg H, Dahlback B. Immunohistochemical demonstration of vitronectin in association with elastin and amyloid deposits in human kidney. *Histochemistry* 1987; **87**:511-5.

67.   Reilly JT, Nash JR. Vitronectin (serum spreading factor): its localisation in normal and fibrotic tissue. *J Clin Pathol* 1988; **41**:1269-72.

68.   Zheng X, Saunders TL, Camper SA, Samuelson LC, Ginsburg D. Vitronectin is not essential for normal mammalian development and fertility. *Proc Natl Acad Sci U S A* 1995; **92**:12426-30.

69.   Fay WP, Parker AC, Ansari MN, Zheng X, Ginsburg D. Vitronectin inhibits the thrombotic response to arterial injury in mice. *Blood* 1999; **93**:1825-30.

70.   Lazar MH, Christensen PJ, Du M, Yu B, Subbotina NM, Hanson KE, Hansen JM, White ES, Simon RH, Sisson TH. Plasminogen activator inhibitor-1 impairs alveolar epithelial repair by binding to vitronectin. *Am J Respir Cell Mol Biol* 2004; **31**:672-8.

71.   Rosenson RS. Myocardial injury: the acute phase response and lipoprotein metabolism. *J Am Coll Cardiol* 1993; **22**:933-40.

72.   Seiffert D, Geisterfer M, Gauldie J, Young E, Podor TJ. IL-6 stimulates vitronectin gene expression in vivo. *J Immunol* 1995; **155**:3180-5.

73.   van Leeuwen MA, van Rijswijk MH. Acute phase proteins in the monitoring of inflammatory disorders. *Baillieres Clin Rheumatol* 1994; **8**:531-52.

74.   Young E, Podor TJ, Venner T, Hirsh J. Induction of the acute-phase reaction increases heparin-binding proteins in plasma. *Arterioscler Thromb Vasc Biol* 1997; **17**:1568-74.

75.   Rosenblum G, Carsons S. Quantitation and distribution of vitronectin in synovial fluid and tissue of patients with rheumatic disease. *Clin Exp Rheumatol* 1996; **14**:31-6.

76.   Gladson CL, Dennis C, Rotolo TC, Kelly DR, Grammer JR. Vitronectin expression in differentiating neuroblastic tumors: integrin alpha v beta 5 mediates vitronectin-dependent adhesion of retinoic-acid-differentiated neuroblastoma cells. *Am J Pathol* 1997; **150**:1631-46.

77.   Geiger B. Intermediate filaments. Looking for a function. *Nature* 1987; **329**:392-3.

78.   Carmo-Fonseca M, David-Ferreira JF. Interactions of intermediate filaments with cell structures. *Electron Microsc Rev* 1990; **3**:115-41.

79.   Klymkowsky MW, Bachant JB, Domingo A. Functions of intermediate filaments. *Cell Motil Cytoskeleton* 1989; **14**:309-31.

80.   Shah SB, Peters D, Jordan KA, Milner DJ, Friden J, Capetanaki Y, Lieber RL. Sarcomere number regulation maintained after immobilization in desmin-null mouse skeletal muscle. *J Exp Biol* 2001; **204**:1703-10.

81.   Traub P, Kuhn S, Grub S. Separation and characterization of homo and hetero-oligomers of the intermediate filament proteins desmin and vimentin. *J Mol Biol* 1993; **230**:837-56.

82.   Wickert U, Mucke N, Wedig T, Muller SA, Aebi U, Herrmann H. Characterization of the in vitro co-assembly process of the intermediate filament proteins vimentin and desmin: mixed polymers at all stages of assembly. *Eur J Cell Biol* 2005; **84**:379-91.

83.   Beuttenmuller M, Chen M, Janetzko A, Kuhn S, Traub P. Structural elements of the amino-terminal head domain of vimentin essential for intermediate filament formation in vivo and in vitro. *Exp Cell Res* 1994; **213**:128-42.

84.   Coulombe PA, Chan YM, Albers K, Fuchs E. Deletions in epidermal keratins leading to alterations in filament organization in vivo and in intermediate filament assembly in vitro. *J Cell Biol* 1990; **111**:3049-64.

85.   Geisler N, Kaufmann E, Weber K. Proteinchemical characterization of three structurally distinct domains along the protofilament unit of desmin 10 nm filaments. *Cell* 1982; **30**:277-86.

86. Perides G, Kuhn S, Scherbarth A, Traub P. Probing of the structural stability of vimentin and desmin-type intermediate filaments with Ca2+-activated proteinase, thrombin and lysine-specific endoproteinase Lys-C. *Eur J Cell Biol* 1987; **43**:450-8.

87. Bang H, Egerer K, Gauliard A, Luthke K, Rudolph PE, Fredenhagen G, Berg W, Feist E, Burmester GR. Mutation and citrullination modifies vimentin to a novel autoantigen for rheumatoid arthritis. *Arthritis Rheum* 2007; **56**:2503-11.

88. Vossenaar ER, Despres N, Lapointe E, van der Heijden A, Lora M, Senshu T, van Venrooij WJ, Menard HA. Rheumatoid arthritis specific anti-Sa antibodies target citrullinated vimentin. *Arthritis Res Ther* 2004; **6**:R142-50.

89. Clarke EJ, Allan V. Intermediate filaments: vimentin moves in. *Curr Biol* 2002; **12**:R596-8.

90. Helfand BT, Chang L, Goldman RD. Intermediate filaments are dynamic and motile elements of cellular architecture. *J Cell Sci* 2004; **117**:133-41.

91. Hansson GK, Starkebaum GA, Benditt EP, Schwartz SM. Fc-mediated binding of IgG to vimentin-type intermediate filaments in vascular endothelial cells. *Proc Natl Acad Sci U S A* 1984; **81**:3103-7.

92. Hansson GK, Lagerstedt E, Bengtsson A, Heideman M. IgG binding to cytoskeletal intermediate filaments activates the complement cascade. *Exp Cell Res* 1987; **170**:338-50.

93. Lijnen HR. Pleiotropic functions of plasminogen activator inhibitor-1. *J Thromb Haemost* 2005; **3**:35-45.

94. Wu YP, Bloemendal HJ, Voest EE, Logtenberg T, de Groot PG, Gebbink MF, de Boer HC. Fibrin-incorporated vitronectin is involved in platelet adhesion and thrombus formation through homotypic interactions with platelet-associated vitronectin. *Blood* 2004; **104**:1034-41.

95. Dvorak HF. Tumors: wounds that do not heal. Similarities between tumor stroma generation and wound healing. *N Engl J Med* 1986; **315**:1650-9.

96. Kokkinos MI, Wafai R, Wong MK, Newgreen DF, Thompson EW, Waltham M. Vimentin and epithelial-mesenchymal transition in human breast cancer--observations in vitro and in vivo. *Cells Tissues Organs* 2007; **185**:191-203.

97. Hendrix MJ, Seftor EA, Chu YW, Trevor KT, Seftor RE. Role of intermediate filaments in migration, invasion and metastasis. *Cancer Metastasis Rev* 1996; **15**:507-25.

98.   Sanchez A, Ossorio C, Alvaro-Gracia JM, Padilla R, Avila J. A subset of antibodies from the sera of patients with systemic lupus erythematosus react with vimentin and DNA. *J Rheumatol* 1990; **17**:205-9.

99.   Alcover A, Ramirez-Lafita F, Hernandez C, Nieto A, Avila J. Antibodies to vimentin intermediate filaments in sera from patients with SLE and RA: quantitation by solid phase radioimmunoassay. *J Rheumatol* 1985; **12**:233-6.

100.   Rose ML. De novo production of antibodies after heart or lung transplantation should be regarded as an early warning system. *J Heart Lung Transplant* 2004; **23**:385-95.

101.   Vazquez-Doval J, Sanchez-Ibarrola A. Defective mononuclear phagocyte function in systemic lupus erythematosus: relationship of FcRII (CD32) with intermediate cytoskeletal filaments. *J Investig Allergol Clin Immunol* 1993; **3**:86-91.

102.   Yan X, Kuhn S, Traub P. A complex of intermediate filament protein-DNA: a target for autoantibodies in systemic lupus erythematosus? *Chin Med Sci J* 1995; **10**:90-2.

103.   Xue C, Takahashi M, Hasunuma T, Aono H, Yamamoto K, Yoshino S, Sumida T, Nishioka K. Characterisation of fibroblast-like cells in pannus lesions of patients with rheumatoid arthritis sharing properties of fibroblasts and chondrocytes. *Ann Rheum Dis* 1997; **56**:262-7.

104.   Hayry P, Isoniemi H, Yilmaz S, Mennander A, Lemstrom K, Raisanen-Sokolowski A, Koskinen P, Ustinov J, Lautenschlager I, Taskinen E, et al. Chronic allograft rejection. *Immunol Rev* 1993; **134**:33-81.

105.   Moien-Afshari F, Choy JC, McManus BM, Laher I. Cyclosporine treatment preserves coronary resistance artery function in rat cardiac allografts. *J Heart Lung Transplant* 2004; **23**:193-203.

106.   Moien-Afshari F, McManus BM, Laher I. Immunosuppression and transplant vascular disease: benefits and adverse effects. *Pharmacol Ther* 2003; **100**:141-56.

107.   Boucek MM, Aurora P, Edwards LB, Taylor DO, Trulock EP, Christie J, Dobbels F, Rahmel AO, Keck BM, Hertz MI. Registry of the International Society for Heart and Lung Transplantation: tenth official pediatric heart transplantation report--2007. *J Heart Lung Transplant* 2007; **26**:796-807.

108.   Hruban RH, Beschorner WE, Baumgartner WA, Augustine SM, Ren H, Reitz BA, Hutchins GM. Accelerated arteriosclerosis in heart transplant recipients is associated with a T-lymphocyte-mediated endothelialitis. *Am J Pathol* 1990; **137**:871-82.

109.   Oni AA, Ray J, Hosenpud JD. Coronary venous intimal thickening in explanted cardiac allografts. Evidence demonstrating that transplant coronary artery disease is a manifestation of a diffuse allograft vasculopathy. *Transplantation* 1992; **53**:1247-51.

110. Shirakawa I, Sata M, Saiura A, Kaneda Y, Yashiro H, Hirata Y, Makuuchi M, Nagai R. Atorvastatin attenuates transplant-associated coronary arteriosclerosis in a murine model of cardiac transplantation. *Biomed Pharmacother* 2007; **61**:154-9.

111. Kobashigawa JA. Statins in solid organ transplantation: is there an immunosuppressive effect? *Am J Transplant* 2004; **4**:1013-8.

112. Eisen H, Ross H. Optimizing the immunosuppressive regimen in heart transplantation. *J Heart Lung Transplant* 2004; **23**:S207-13.

113. Smith JD, Rose M. Detection and clinical relevance of antibodies after transplantation. *Methods Mol Biol* 2006; **333**:227-46.

114. Kamoun M. Mechanisms of chronic allograft dysfunction. *Ther Drug Monit* 2006; **28**:14-8.

115. Opelz G. Effect of HLA matching in heart transplantation. Collaborative Heart Transplant Study. *Transplant Proc* 1989; **21**:794-6.

116. Hutchinson IV. Cellular mechanisms of allograft rejection. *Curr Opin Immunol* 1991; **3**:722-8.

117. Ascher NL, Hoffman RA, Hanto DW, Simmons RL. Cellular basis of allograft rejection. *Immunol Rev* 1984; **77**:217-32.

118. Schutz A, Breuer M, Kemkes BM. Antimyosin antibodies in cardiac rejection. *Ann Thorac Surg* 1997; **63**:578-81.

119. Burlingham WJ, Love RB, Jankowska-Gan E, Haynes LD, Xu Q, Bobadilla JL, Meyer KC, Hayney MS, Braun RK, Greenspan DS, Gopalakrishnan B, Cai J, Brand DD, Yoshida S, Cummings OW, Wilkes DS. IL-17-dependent cellular immunity to collagen type V predisposes to obliterative bronchiolitis in human lung transplants. *J Clin Invest* 2007; **117**:3498-3506.

120. Murata K, Fox-Talbot K, Qian Z, Takahashi K, Stahl GL, Baldwin WM, 3rd, Wasowska BA. Synergistic Deposition of C4d by Complement-Activating and Non-activating Antibodies in Cardiac Transplants. *Am J Transplant* 2007; **7**:2605-14.

121. Wehner J, Morrell CN, Reynolds T, Rodriguez ER, Baldwin WM, 3rd. Antibody and complement in transplant vasculopathy. *Circ Res* 2007; **100**:191-203.

122. Wheeler CH, Collins A, Dunn MJ, Crisp SJ, Yacoub MH, Rose ML. Characterization of endothelial antigens associated with transplant-associated coronary artery disease. *J Heart Lung Transplant* 1995; **14**:S188-97.

123. Jurcevic S, Ainsworth ME, Pomerance A, Smith JD, Robinson DR, Dunn MJ, Yacoub MH, Rose ML. Antivimentin antibodies are an independent predictor of transplant-associated coronary artery disease after cardiac transplantation. *Transplantation* 2001; **71**:886-92.

124. Barber LD, Whitelegg A, Madrigal JA, Banner NR, Rose ML. Detection of vimentin-specific autoreactive CD8+ T cells in cardiac transplant patients. *Transplantation* 2004; **77**:1604-9.

125. Carter V, Shenton BK, Jaques B, Turner D, Talbot D, Gupta A, Chapman CE, Matthews CJ, Cavanagh G. Vimentin antibodies: a non-HLA antibody as a potential risk factor in renal transplantation. *Transplant Proc* 2005; **37**:654-7.

126. Cailhier JF, Laplante P, Hebert MJ. Endothelial apoptosis and chronic transplant vasculopathy: recent results, novel mechanisms. *Am J Transplant* 2006; **6**:247-53.

127. Rose ML. Activation of autoimmune B cells and chronic rejection. *Transplantation* 2005; **79**:S22-4.

128. Vincenti F, Luggen M. T cell costimulation: a rational target in the therapeutic armamentarium for autoimmune diseases and transplantation. *Annu Rev Med* 2007; **58**:347-58.

129. Quadri SM, Segall L, de Perrot M, Han B, Edwards V, Jones N, Waddell TK, Liu M, Keshavjee S. Caspase inhibition improves ischemia-reperfusion injury after lung transplantation. *Am J Transplant* 2005; **5**:292-9.

130. Nakanishi K, Maruyama M, Shibata T, Morishima N. Identification of a caspase-9 substrate and detection of its cleavage in programmed cell death during mouse development. *J Biol Chem* 2001; **276**:41237-44.

131. Moisan E, Girard D. Cell surface expression of intermediate filament proteins vimentin and lamin B1 in human neutrophil spontaneous apoptosis. *J Leukoc Biol* 2006; **79**:489-98.

CHAPTER II: RATIONALE, HYPOTHESIS, AND EXPERIMENTAL AIMS

2.1. Rationale

The extracellular distribution of PAI-1 has been determined to be governed by its interactions with VN and vimentin, and together they form a ternary complex that localizes onto the surface of activated cells. What is not understood is how intracellular stores of PAI-1 from platelets become localized to the surface of activated platelets and platelet microparticles and the source of vimentin for this surface distribution. What is also unknown is the conformation of vitronectin required for the formation of the ternary complex: monomeric or multimeric VN. Although the extracellular presentation of vimentin cytoskeleton is prerequisite for ternary complex formation, the manner of vimentin presentation the mechanism of vimentin auto-antibody formation is unknown. Lastly, do these anti-vimentin antibodies have downstream effects on cells that naturally express vimentin in the circulation?

2.2. Hypothesis

Ternary complex formation is dependent on the formation and release of microparticles from the activated cell, morphologically termed microparticles. At the broken junction between a platelet microparticle (PMP) and platelet that released the PMP, vimentin becomes briefly exposed and vulnerable to, 1) vitronectin multimerization followed by, 2) PAI-1 and PAI-1:complex incorporation into the VN multimer aggregate. This exposed vimentin cytoskeleton becomes the site of anti-vimentin antibody binding, leading to complement-mediated lysis.

2.3. Specific Aims

1. To develop a fluorescently red form of PAI-1 protein and to characterize this fusion protein and verify its functionality as a PAI-1 analogue. This protein will be used to track the intracellular and extracellular fate of endogenously synthesized PAI-1 upon stimulation of various transfected cell lines.

2. To visualize the ultrastructure of purified ternary complex components and these components on activated platelets and platelet microparticles.

3. To determine what cell type anti-vimentin antibodies bind to and what effects these antibodies exert on those cells.

2.4. Methodology Overview

In the first project, cell culture, RT-PCR, nucleic acid ligation, subcloning, selective bacterial culture and DNA sequencing to construct the fusion vector of PAI-1-dsRed was performed. Following this, cell transfection on cultured cells, confocal microscopy and live cell culture wide field fluorescence microvideography to track the PAI-1-dsRed protein intracellularly and extracellularly was performed. To validate the protein chimera, western immunoblotting and ligand immunoblotting was performed to characterize the binding interactions of the fusion protein. *In vitro* fibrin clot formation was used to characterize PAI-1-dsRed binding and fibrinolysis. In the second project, flow cytometry and atomic force microscopy to select platelet microparticles that expressed some if not all components of the ternary complex was performed. In the third project, a variety of *in vitro* treatments on whole blood were performed to compare the effects of anti-vimentin antibodies compared to positive-

control complement-fixing antibodies which were subsequently analyzed by flow cytometry. Cell cytotoxicity tests were used to assess cell type specificity of antibodies.

2.5. Potential Relevance of Findings

The cytoskeleton of platelets, neutrophils and endothelial cells is gaining more respect as a cause and effector for a variety of diseases and pathological processes. This thesis provides a novel look at how vimentin can interact with components of hemostatic mechanisms and immune mechanisms by virtue of its biochemical properties. Proteins that interact and associate with vimentin will gain more importance and provide insights in the treatment and management of disease. Although many questions remain due to the conventional intracellular understandings of vimentin, this research combined with heightened understandings of it within various cellular contexts such as cell activation or senescence [53, 131] will provide an impetus to focus on the cytoskeleton's role in natural processes and disease.

CHAPTER III: TARGETING OF RECOMBINANT PAI-1-dsRED AND VITRONECTIN TO STORAGE GRANULES IN ENDOTHELIAL AND MEGAKARYOCYTE CELL LINES

3.1. Introduction:

Plasminogen activator inhibitor type-1 (PAI-1) is a serpin inhibitor family and an inhibitor of both urokinase-type and tissue-type plasminogen activator (uPA/tPA) [1, 2]. PAI-1 plays a pivotal role in clot stabilization by inhibiting the fibrinolytic activities of fibrin-bound tPA. PAI-1 is expressed by a number of cell types, most notably endothelial cells [3-5], megakaryocytes [6, 7] and platelets [8, 9]. The active form of PAI-1 is stabilized when it forms a complex with vitronectin (VN), which prevents the re-insertion of the PAI-1 reactive center loop back into the body of the molecule [10]. PAI-1-VN complexes are present in α-granules of platelets, and this complex assembly occurs when VN is endocytosed into α-granules that contain endogenously synthesized PAI-1 [7, 11].

In platelets and megakaryocytes, PAI-1 is organized into α-granules, along with other resident α-granule proteins such as VN, vWF and P-selectin [7, 9, 11]. Exocytosis of α-granules and hence PAI-1, has also demonstrated to be secretogogue dependent [12]. In the context of endothelial cells, studies to date do not report compartmentalization of PAI-1 to storage granules such as Weibel-Palade bodies (WPB's) [13]. However, both endothelial cells and megakaryocytes are of mesenchymal lineage, and their storage granules - Weibel-Palade bodies

---

[1]A version of this chapter will be submitted for publication. Leong, HS, Bateman RB, Walinski H, and Podor T.J. Targeting of Recombinant PAI-1-dsRed and Vitronectin to Storage Granules in Endothelial and Megakaryocyte Cell Lines.

and α-granules, contain similar resident proteins such as vWF and P-selectin. Although PAI-1 is present within α-granules, it has not been determined to reside in an endothelial storage vacuole, except for the Golgi. For example, Rosnoblet et al. have demonstrated that intracellular stores of PAI-1 are confined to the Golgi, with a more recent report describing PAI-1 colocalization with Giantin, a Golgi protein marker in HUVEC cells [14].

In this study, a fluorescent form of PAI-1 was developed to examine its intracellular compartmentalization in endothelial and megakaryocytic cell lines without the use of epitope specific antibodies. Intracellular PAI-1 may evade antibody detection because epitopes may be masked due to complex formation with VN. We constructed a red fluorescent form of PAI-1 which exhibits a spectral excitation/emission profile of 553/584 nm. This fusion protein consists of a dsRed fluorescent protein fused to the C-terminus of the PAI-1 protein. The possibility of protein-tag interference and its potential impact on PAI-1 active-inactive states was addressed by assessment of the ability of PAI-1-dsRed to bind to tissue-type plasminogen activator (tPA) and vitronectin (VN), and its ability to attenuate fibrin clot lysis. Following this assessment, we then determined PAI-1 compartmentalization in an endothelial cell line (Eahy926) and subsequently its fate after TNF-α treatment. These properties were then compared in a transfected megakaryocyte cell line (MEG-01) in which PAI-1 organization into storage granules had been previously described.

3.2. Materials and Methods:

3.2.1. PAI-1-dsRed plasmid construction

RNA isolation was performed with Trizol reagent (Invitrogen Inc., Carlsbad, CA) on Eahy926 cell culture grown to 80% confluency. Human plasminogen activator inhibitor type-1 cDNA (PAI-1; GI accession number: 189541) was amplified via RT-PCR (Forward: 5' GGA TCC GGG TTC CAT CAC TTG GCC CA 3' Reverse: 5'GAA TTC GTC TTT GGT GAA GGG TCT GC 3') using SuperScript II RNaseH⁻ RT and Platinum HiFi Taq polymerase (Invitrogen Inc.). PCR product was ligated into a TOPO vector (Invitrogen Inc.) and upon transformation into chemically competent cells, the PAI-1 cDNA was subcloned into the pDsRedN1 plasmid (Clontech Inc., Mountain View, CA) in which PAI-1-dsRed transgene expression is transcriptionally controlled by a pCMV promoter. Sequencing was performed to verify the identity and frame of the insert into the pDsRedN1 plasmid.

3.2.2. Transfection of Eahy926 and MEG-01 cell cultures

Human endothelial hybridoma Eahy926 were used because it is an endothelial cell line that can be transfected (obtained from Dr. C Edgell, University of North Carolina) and were cultured on 30 mm six well plates grown to ~70% confluency with DMEM supplemented with 10% FBS. For transfections, ~1 μg of PAI-1-dsRed plasmid and 3 μL of FuGENE6 (Roche Diagnostics Inc., Indianapolis, IN) was used per well, and was incubated without serum for 24 hours. After 24 hours, the cells were washed and replenished with DMEM + 10% FBS. At specified timepoints post-transfection (0, 6, 12, 24, 48, 72 hours), 1 mL conditioned media was collected for immunoblot analysis.

3.2.3. Immunoblot analysis of conditioned media from transfected Eahy926 cells

SDS-PAGE of samples of conditioned media on 8% polyacrylamide gels was followed by transfer onto nitrocellulose membrane using a Bio-Rad mini-gel and transfer apparatus (BioRad Inc., Hercules, CA). Membranes blocked with 5% dry milk powder in TBS+0.05% Tween were subsequently probed with either: sheep α human PAI-1 IgG (1:1000 dilution; Affinity Biologicals Inc., Ancaster, ON), mouse α dsRed IgG (1:500 dilution; Clontech Inc.), sheep α human tPA IgG (1:1000 dilution – Affinity Biologicals Inc.), or sheep α human VN (1:1000 dilution – Affinity Biologicals Inc.). This was followed by secondary antibody detection with IgG-linked AP antibodies (Santa Cruz Biotechnology, Santa Cruz, CA) and the AP developing kit (BioRad Inc).

VN ligand blots were performed by running lanes of 50 ng purified vitronectin (Affinity Biologicals Inc.) in 8% SDS-PAGE gels with the mini-gel apparatus and then transferred onto nitrocellulose membrane. Individual strips of membrane each representing a lane of electrophoresed VN were individually cut, incubated and shaken overnight with 1 mL of conditioned medium at room temperature. After incubation, the strips were immunoblotted with antibodies specific for PAI-1 or dsRed. Positive and negative controls were strips that were immunoblotted with antibodies specific for VN and IgG-AP respectively.

3.2.4. Confocal microscopy of tPA-Pacific Blue:PAI-1-dsRed complexes in fibrin clot lysis

To assess PAI-1-dsRed functionality in terms of binding to tPA and its ability to attenuate fibrin clot lysis, tPA (Alteplase, Genentech, South San Francisco, CA) was labeled with Pacific Blue-Maleimide agent as previously described (Molecular Probes Inc., Eugene, OR) [15].

Conditioned media containing PAI-1-dsRed (~2 mg/mL total protein) was incubated with 10 nM tPA-Pacific Blue for 5 minutes at 37°C and then added to a reaction mix consisting of 3 mM purified fibrinogen, 0.1 mM fibrinogen-alexa488 (Molecular Probes Inc.) in Tyrode's buffer at pH 7.4. The clot was formed on a 24 × 50 mm coverslip by addition of 1.0 µL of 10 U/mL thrombin and then quickly overlaid with a 22 × 22 mm coverslip and incubated at 37°C in the dark for 30 minutes. The 22 × 22 mm coverslip was cleaved off the larger coverslip and confocal microscopy used to visualize the distribution of PAI-1-dsRed and tPA-Pacific Blue on the Alexa488-labeled fibrin lattice. To initiate clot lysis, 100 uL of platelet-poor plasma (PPP) warmed to 37°C was overlaid onto the clot and field of view. Immediately after addition of PPP, confocal scans of PAI-1-dsRed, tPA-Pacific Blue and fibrinogen-Alexa488 were acquired sequentially every 30 seconds for 20 minutes. For confocal microscopy, a Leica inverted DMIRE2 microscope fitted with a TCS SP2 AOBS scanner was used. A Leica 63X/NA=1.20 HCS PL APO objective for water immersion optics (cat. # - 506131) was used for all widefield and confocal microscopy.

3.2.5. Immunofluorescence staining of transfected MEG-01and Eahy926 cultured cells

The human megakaryoblastic cell line MEG-01 (ATCC, Manassas, VA) was cultured onto fibronectin coated glass coverslips with RPMI 1640 media supplemented with 10% FBS and 1 mM sodium pyruvate. Cells were pre-treated with 1.0 nM of phorbol 12-myristate 13-acetate (PMA) (Sigma-Aldrich Inc., Oakville, ON) prior to transfection to induce cell flattening and maturation(8001904). The transfection protocol is as described above. Transfected cells were fixed with 4% paraformaldehyde for 10 minutes and then incubated with PBS+ 0.01% Triton-X for 10 minutes. Immunofluorescence staining was performed with the previously

described primary antibodies at the same dilutions. Alexa488 conjugated secondary antibodies were used according to the primary antibody used (Molecular Probes Inc.). Cells were counterstained with Hoechst 33342 nuclear stain.

Eahy926 cells were cultured onto coverslips in 30mm six well culture plates to a 75-80% confluency and transfected as described above. Transfected cells were fixed with 4% paraformaldehyde for 10 minutes and then incubated with PBS+ 0.01% Triton-X for 10 minutes. Transfected cells were stained with these antibodies: rabbit anti-human vWF (1:250 dilution, Dako, Mississauga, ON) with donkey anti-rabbit IgG-Alexa488 (Molecular Probes Inc.), or with goat anti-human CD62P (1:500 dilution, Biovision, MountainView, CA) with donkey anti-goat IgG-Alexa633 (Molecular Probes Inc.).

3.2.6. Immunofluorescence staining of TNF-α activated transfected Eahy926 cell cultures

Eahy926 cells were cultured onto glass coverslips and cultured to 70% confluency with DMEM supplemented with 10% FBS. Three days following transfection with PAI-1-dsRed vector, cells were activated with 100 ng/mL of TNF-α for 12 hours prior to paraformaldehyde fixation and staining. After blocking with sheep and donkey normal serum (5% in PBS), wells were immunostained with sheep α-human VN IgG and donkey anti-sheep IgG-Alexa488 or mouse α-human vimentin (3B4) IgG with goat anti-mouse IgG-Alexa488. Sheep IgG or mouse IgG was used as isotype antibody controls. A Hoechst 33342 nuclear counterstain was used at 1:1000 dilution post-antibody labeling.

3.2.7. Videomicroscopic analysis of exocytosis of fibrinogen-Alexa488 and PAI-1-dsRed from α-granules in MEG-01 cells

To examine whether stored PAI-1-dsRed could be rapidly released upon thrombin stimulation in megakaryocytes, stably transfected PMA-treated MEG-01 cells were cultured with Alexa488-labeled fibrinogen (50nM final) for 6 hours. Fibrinogen-Alexa488 is known to be endocytosed into α-granules via glycoprotein IIb-IIIa [16], and was used as a positive control for α-granule exocytosis. Endocytosis tracing of fluorescently labeled VN was impractical for these studies that required monomeric, native VN due to the multimerization of the protein during conjugation, thus fibrinogen was used as a surrogate marker for an internalized α-granule protein. The cells were then counterstained with Hoechst 33342 for 10 minutes and then gently washed with RPMI 1640 media. A temperature and CO_2 gas regulated stage specimen setup was used to allow for time-lapse fluorescence imaging of exocytosis of PAI-1-dsRed and fibrinogen-Alexa488. Cells were stimulated by the addition of 100 μL of thrombin (1.0 U/mL in PBS pH 7.2). For wide-field fluorescence microscopy, a Leica DMIRE2 inverted microscope fitted with a 515-560/580/590 (nm) dichroic filter set for dsRed excitation/emission, and a 450-490/510/515 (nm) dichroic filter set for Alexa488 excitation/emission was used. Wide field images were sequentially acquired every 5 seconds for 10 minutes with a Retiga EXi mono CCD camera (QImaging, Inc., Burnaby, BC) with an exposure time of 20 milliseconds per frame and the camera set on automatic gain. Heat mirrors and a neutral density filter (3% transmittance) minimized sample overheating and fluorophore photobleaching.

3.3. Results

3.3.1. PAI-1-dsRed synthesis and secretion by transfected Eahy926 cell culture

Human PAI-1 cDNA was cloned by RT-PCR amplification using mRNA from cultured Eahy926 cells to generate a ~1.2 kb PCR product that was ligated into the pDsRedN1 vector. Restriction enzyme digest analysis confirmed successful insertion (Figure 1A). DNA sequence analysis of this insert confirmed 100% identity with the published amino acid sequence of PAI-1 (GI accession number: 189541). The resulting vector was named pDsRed-PAI-1 in which the PAI-1 cDNA sequence was fused with a 6 alanine residue sequence followed by the dsRed sequence (5' to 3' end).

Transfection of Eahy926 cells with the pDsRed-PAI-1 vector resulted in the synthesis and secretion of two distinct forms of PAI-1, native PAI-1 (~45 kDa) and PAI-1-dsRed (~70 kDa). As shown in Figure 3.1, conditioned media was collected at various time points post-transfection and upon western immunoblot analysis with a polyclonal antibody specific for PAI-1, both forms of PAI-1, PAI-1-dsRed and native PAI-1 were detected. Since both forms of PAI-1 are under different transcriptional control, detection of PAI-1-dsRed protein expression and secretion was not evident until 24 hours post-transfection. There was gradual accumulation of native PAI-1 over all time points as well as PAI-1-dsRed accumulation in later time points as evidenced by increasing intensity of bands over time at the 45kDa and 65kDa size level. To assess potential bleedthrough for each fluorophore used, spectral control images were acquired by collecting signal in wavelength ranges lower than the incident light used to excite the fluorophore or higher than the predicted emission range. For example, spectral controls for dsRed were: 530-560nm when using 563nm incident light; 600-650nm when using 488nm incident light for FITC/Alexa488.
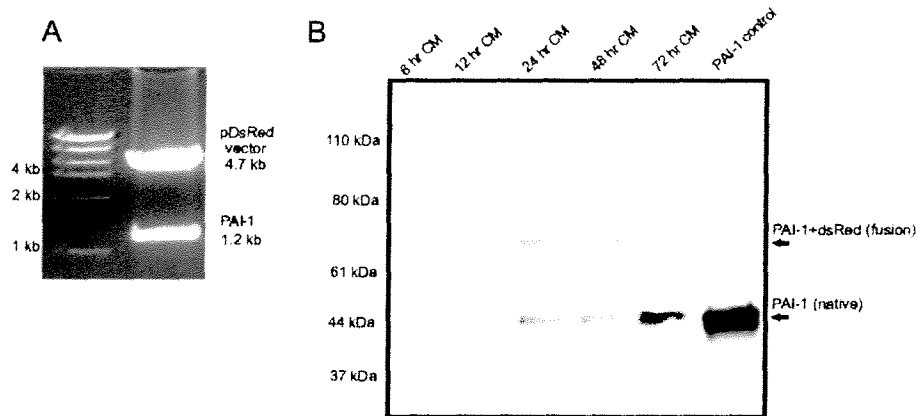
Figure 3.1. Construction of pDsRed-PAI-1 vector and synthesis of chimeric PAI-1-dsRed protein in transfected cells. Panel A) is a restriction digest of pDsRed-PAI-1 vector to confirm insertion of human PAI-1 cDNA clone. Panel B) is an immunoblot of conditioned media from cultured Eahy926 cells transfected with the pDsRed-PAI-1 vector. A PAI-1 polyclonal antibody detected both native PAI-1 and PAI-dsRed in conditioned media.

3.3.2. PAI-1-dsRed forms a complex with addition of exogenous tPA

Purified tPA (200 ng) was added to 40 uL of conditioned media from the 48 hour time point, to determine if exogenous tPA could form complexes with both secreted PAI-1-dsRed and native PAI-1. Upon immunoblotting with a tPA primary antibody, a doublet band was observed at the ~110 and ~135 kDa size range (Figure 3.2), thus representing tPA complex formation with native PAI-1 (~110 kDa) and PAI-1-dsRed (~135 kDa). Moreover, immunoblotting with the dsRed primary antibody only recognized the PAI-1-dsRed fusion protein which was the upper band of the doublet. The matching intensities of both bands at ~110 kDA and ~130 kDa also indicates that exogenous tPA has similar binding affinities to both PAI-1 and PAI-1-dsRed.
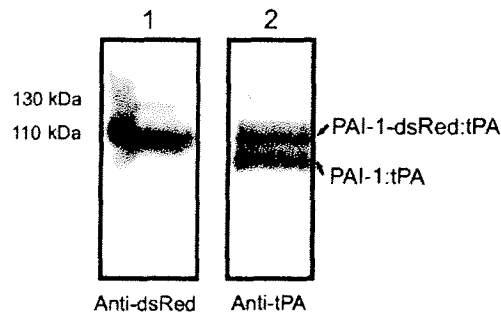
Figure 3.2. PAI-1-dsRed chimeric protein forms covalent complexes with exogenous tPA. Lane 1 was immunoblotted with a dsRed monoclonal antibody and lane 2 was immunoblotted with a tPA polyclonal antibody. The dsRed antibody detected one band representing PAI-1-dsRed-tPA complexes, whereas the tPA antibody detected both PAI-1-tPA and PAI-1-dsRed-tPA complexes.

3.3.3. PAI-1-dsRed binds to immobilized vitronectin (VN)

A VN ligand blot was performed to determine if the dsRed tag on the PAI-1-dsRed molecule could hinder PAI-1-dsRed binding to immobilized VN [9]. Figure 3.3 demonstrates PAI-1-dsRed binding interaction with immobilized VN as confirmed by dsRed and PAI-1 antibodies. Nitrocellulose lanes of electophoresed VN were incubated with conditioned media so that both PAI-1 and PAI-1-dsRed could bind to immobilized VN. The positive control in the first lane was not incubated with conditioned media and was stained with VN primary antibody to demarcate the doublet banding pattern of VN. The doublet pattern present in the lane as stained by the polyclonal PAI-1 antibody suggests that both native and fusion forms of PAI-1 binded to the immobilized VN. The third lane was immunoblotted with dsRed antibody and the doublet banding pattern confirmed the ability of PAI-1-dsRed to bind to both bands of immobilized VN. The negative control was a lane of immobilized VN incubated with mouse IgG followed by secondary antibody detection with goat anti-mouse IgG AP.
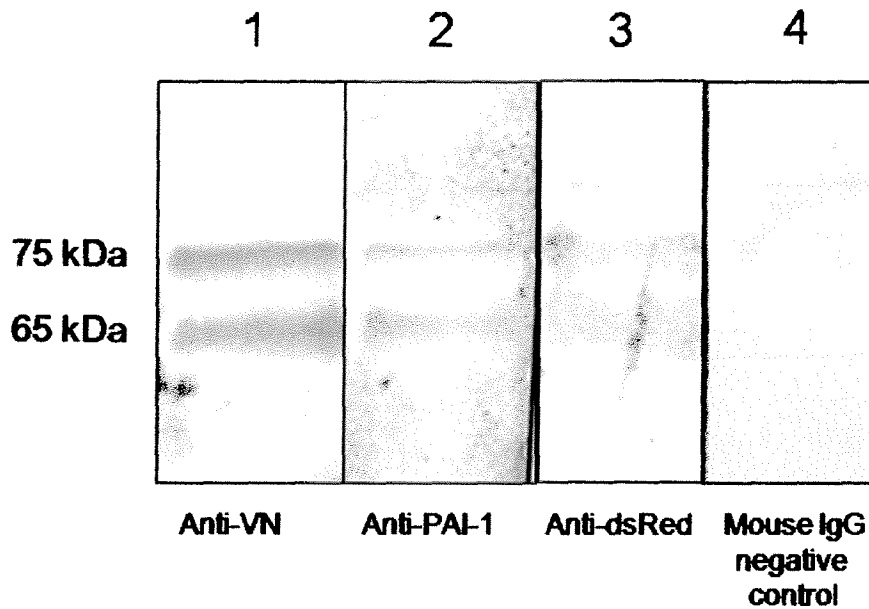
Figure 3.3. PAI-1-dsRed chimeric protein binds to immobilized vitronectin.
Purified VN was electrophoresed and transfected to nitrocellulose. Each individual strip was then incubated with conditioned media from transfected Eahy926 cells and then immunoblotted with antibodies specific for (lane 1) vitronectin, or PAI-1(lane 2), or dsRed (lane 3), or a mouse IgG$_1$ isotype control (lane 4). Lane 1 highlights the position of immobilized two-chain vitronectin (75- and 65-kDa). Lane 2 demonstrates the binding of both PAI-1 and PAI-1-dsRed present in the conditioned media that binded to immobilized vitronectin. Lane 3 demonstrates the binding of only PAI-1-dsRed to immobilized vitronectin from conditioned media.

3.3.4. PAI-1-dsRed attenuates clot lysis in the presence of exogenous tPA

For production of PAI-1-dsRed alone, CHO cells were grown to ~90% confluency and transfected with the vector according to transfection protocols used for Eahy926 cells. Conditioned media was collected and used as a source of PAI-1-dsRed in these experiments. Fibrin clots were formed with purified human fibrinogen and trace amounts of fibrinogen-Alexa488, tPA-Pacific Blue, and in some clots to inhibit tPA-Pacific Blue, PAI-1-dsRed was also added. To initiate tPA-Pacific Blue mediated clot lysis, platelet poor plasma (PPP) was

41

overlaid onto these fibrin clots to initiate plasminogen conversion into plasmin, leading to clot lysis. Three channel fluorescence images of tPA-Pacific Blue, fibrinogen-Alexa488, and PAI-1-dsRed were acquired every 30 seconds to determine the effect of PAI-1-dsRed on tPA-mediated clot lysis. Figure 3.4 illustrates the distribution of tPA-Pacific Blue, PAI-1-dsRed on an Alexa488-fibrin clot (Figure 3.4A-E) and the rate of clot lysis (Figure 3.4F) as measured by the amount of Alexa488-fibrinogen fluorescence intensity in the field of view remaining at each time point. Confocal microscopy revealed PAI-1-dsRed co-localization to areas of tPA-Pacific Blue signal which were present intermittently throughout the fibrin clot as a punctate signal (Figure 3.4C). Figures 3.4A-B depict the distribution of tPA-Pacific Blue and PAI-1-dsRed respectively and a composite of these channels in Figure 3.4C, demonstrates a high degree of colocalization. Figure 3.4E represents a composite of PAI-1-dsRed and fibrin-Alexa488 channels, and yellow signal represents PAI-1-dsRed bound to Alexa488-labelled fibrils. In an experiment to determine rates of clot lysis with or without PAI-1-dsRed (Figure 3.4F), clots supplemented with PAI-dsRed prior to PPP addition displayed a lower rate of clot lysis compared to the clot supplemented with just tPA-Pacific Blue. At 10 minutes, fibrinolysis as mediated by tPA-Pacific Blue resulted in ~80% dissolution of the original clot (black plot line) compared to ~10% dissolution of the clot supplemented with both tPA-Pacific Blue and PAI-1-dsRed (red plot line). The difference in initial RFI of Alexa488-fibrinogen/area is explained by the greater amount of Alexa488-fibrin present within the field of view (black plot line vs. red plot line) prior to addition of plasma.
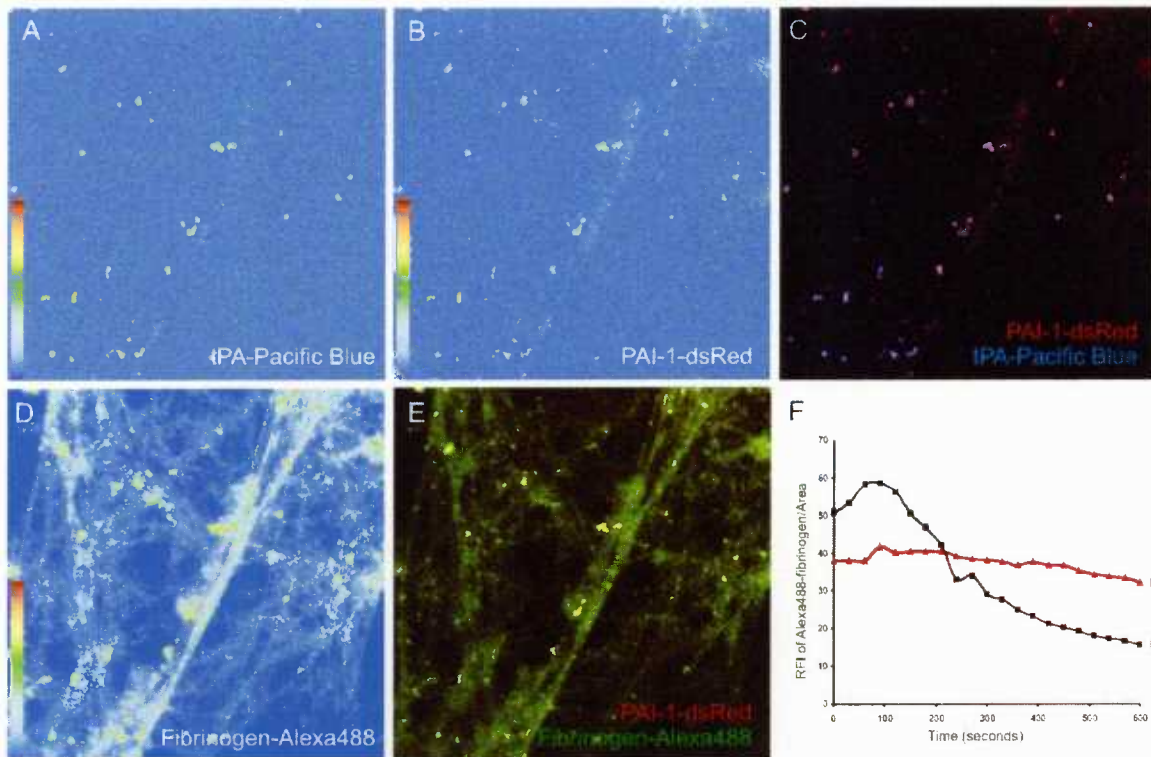
Figure 3.4. PAI-1-dsRed attenuates t-PA mediated fibrin clot lysis. Figures 4A-B depict the distribution of tPA-Pacific Blue and PAI-1-dsRed respectively in the fibrin clots formed with 0.1 U/mL thrombin, and trace amounts of fibrinogen-Alexa488 and 0.1 mM tPA-Pacific Blue. Figure 3.4C depicts a composite of the pseudocolored Figures 3.4A-B and reveals the colocalization of tPA-Pacific Blue and PAI-1-dsRed (depicted as magenta signal). Figure 3.4D is a pseudocolor image of the Alexa488-fibrin clot, and again depicted in green in Figure 3.4E which is a composite of Figure 3.4B & D with yellow signal indicating areas of colocalization of PAI-1-dsRed on fibrin fibrils. In Figure 3.4F, (ii) is the rate of fibrinolysis in a fibrin clot treated with tPA-Pacific Blue (n=1), while (i) is the rate of fibrinolysis in a fibrin clot treated with t-PA and PAI-1–dsRed (n=1). Lysis was measured by the total relative fluorescence intensity of Alexa488-fibrin(ogen) in a randomly selected field of view.

3.3.5. PAI-1-dsRed localizes with P-selectin and vWF in Eahy926 cells

Figure 3.5 depicts the intracellular localization of PAI-1-dsRed protein in relation to vWF (Figure 3.5A) and P-selectin (Figure 3.5B) in Triton X-100 permeabilized Eahy926 cells. PAI-1-dsRed was shown to significantly co-localize to granules containing P-selectin and vWF, both resident Weibel-Palade body (WPB) proteins. Calculations to assess colocalization determined that PAI-1-dsRed demonstrated strong colocalization correlations for P-selectin (R=0.65) and

43

vWF (R=0.77) (Figures 3.5A-B). Colocalization correlation values were determined with ImageJ software.
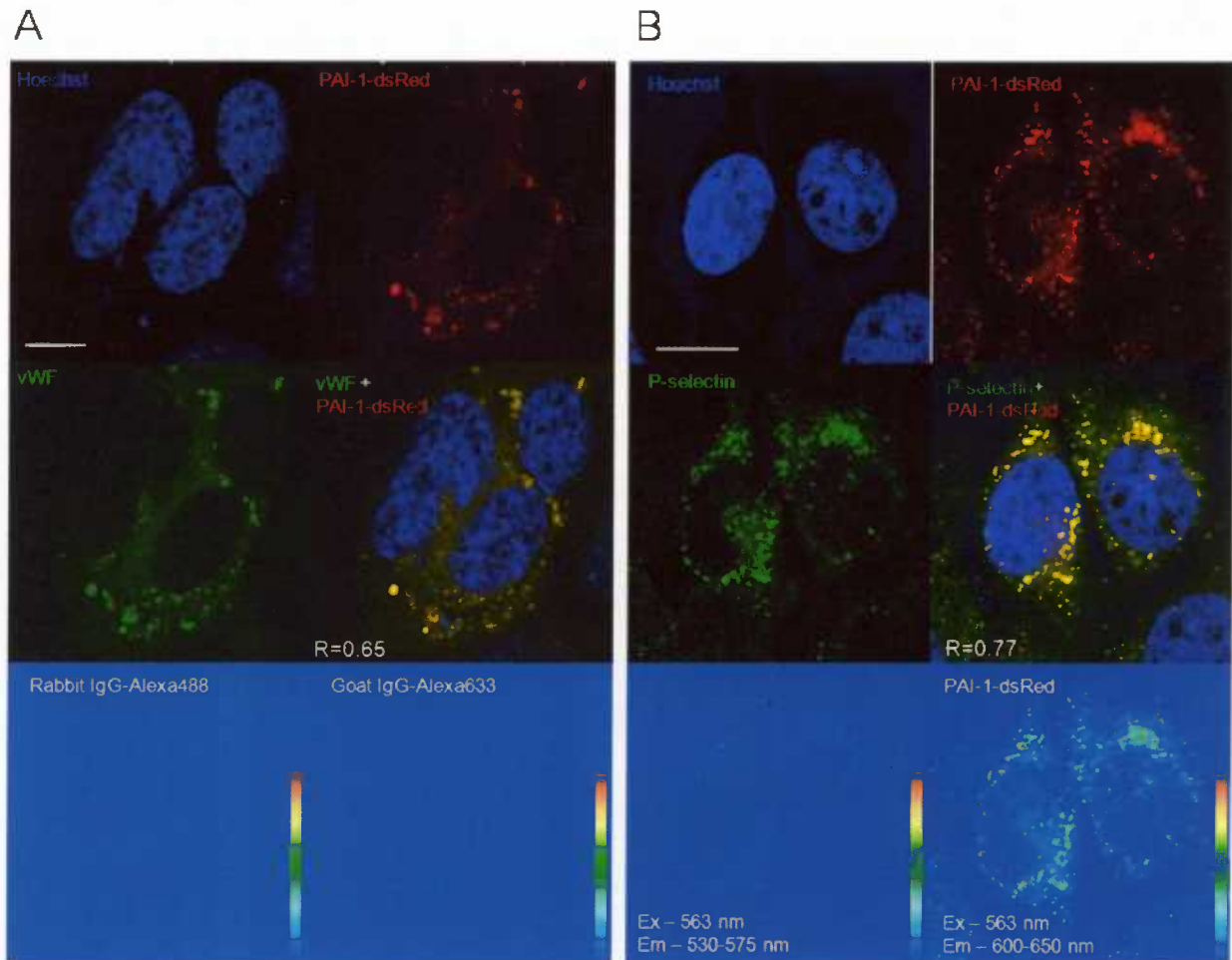
Figure 3.5. Intracellular compartmentalization of PAI-1-dsRed in Eahy926 cells. Confocal microscopy of immunofluorescence stained Eahy926 cells transfected with the PAI-1-dsRed vector. Figure 3.5A depicts colocalization of PAI-1-dsRed (red) to granules containing vWF (green). The composite image reveals colocalization of R=0.65 between vWF and PAI-1-dsRed. Figure 3.5B depicts colocalization of PAI-1-dsRed (red) to granules containing P-selectin (green) in another transfected Eahy926 cell. The composite image reveals a colocalization R=0.77 between P-selectin and PAI-1-dsRed. Each scale bar represents 10.0 μm. The bottom images represent spectral controls for PAI-1-dsRed (two bottom right) and isotype labeling controls (Rabbit IgG for vWF and Goat IgG for P-selectin).

3.3.6. *Activated endothelial cells express extracellular PAI-1-dsRed associated with vimentin*

Transfected Eahy926 cells were activated with TNF-α to induce PAI-1 exocytosis and to determine the nature of extracellular PAI-1 distribution on the activated endothelial cell surfaces [17-20]. In Figure 3.6A, PAI-1dsRed was found to co-localize with VN present on the surface of non-permeabilized activated Eahy926 cells, suggesting that PAI-1 is bound to the surface via a PAI-1:VN complex interaction. Figure 3.6B demonstrates the distribution of surface exposed vimentin on non-permeabilized Eahy926 cells which is exposed as a result of cell activation by TNF-α treatment. PAI-1-dsRed was shown to co-localize with VN (Figure 3.6A) and was associated with exposed vimentin intermediate filaments (Figure 3.6B) suggesting that VN and vimentin surface expression is a requirement for PAI-1 binding on cell surfaces [9].
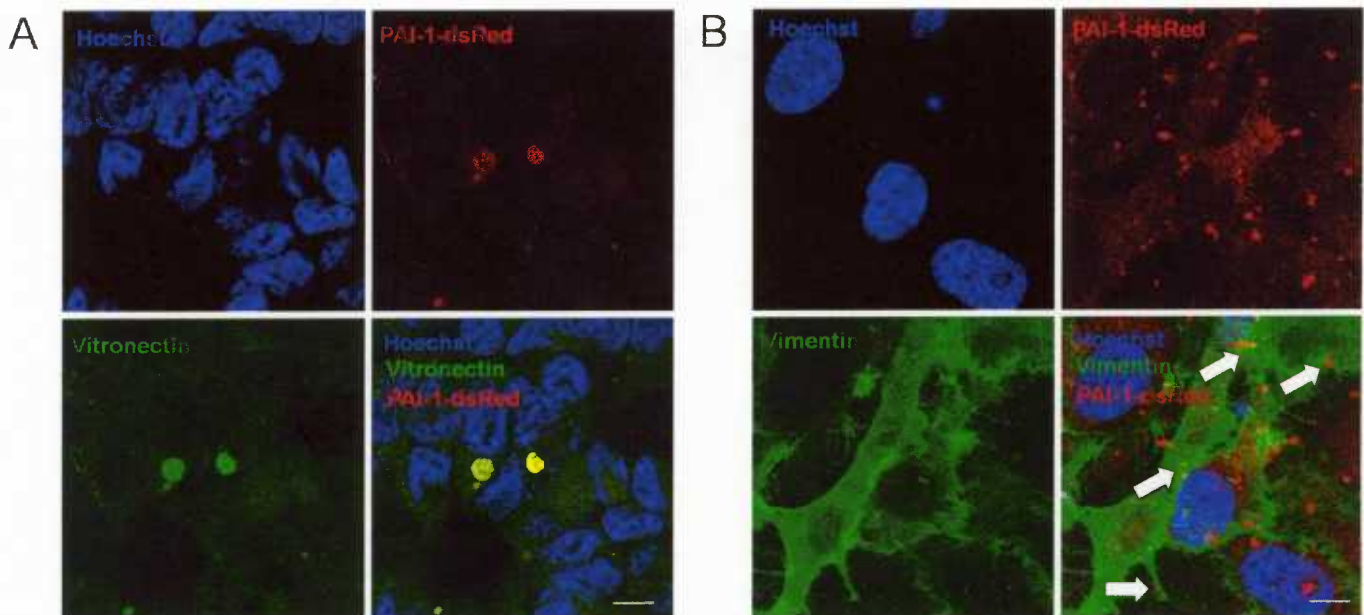
Figure 3.6. TNF-α treated Eahy926 cells express PAI-1-dsRed:vitronectin:vimentin complexes on their cell surface. Eahy926 cells transfected with the PAI-1-dsRed vector were activated with 12 hours incubation of 100 ng/mL TNF-α. Non-permeabilized cells were immunostained for either vitronectin or vimentin (green) and a Hoechst 33342 counterstain. Figure 3.6A represents a TNF-α activated transfected Eahy926 cell revealing colocalization of vitronectin (green) and PAI-1-dsRed (red) on the cell surface. Figure 3.6B represents the distribution of PAI-1-dsRed relative to exposed vimentin (green) on the surface of the activated Eahy926 cells. The arrow heads highlight sites of PAI-1-dsRed binding to exposed vimentin cytoskeleton. Scale bar, 7.0 μm.

3.3.7. PAI-1-dsRed is targeted to α-granules in MEG-01 cells for rapid exocytosis

Transfected MEG-01 cells were also stained with a variety of antibodies to confirm PAI-1-dsRed co-localization to resident α-granule proteins such as VN (Figure 3.7). The PAI-1 polyclonal antibody was able to detect the majority of PAI-1-dsRed as shown by the strong yellow colocalization signal in the channel composite image. The disparate signal in Figure 3.7A is due to the pseudopodial extensions on that particular cell. Staining with VN and vWF antibodies demonstrated strong yellow colocalization signal in both channel composite images, confirming that PAI-dsRed is compartmentalized to α-granules. PAI-1-dsRed fluorescence signal did not appear alone and was generally found to colocalize with PAI-1, VN and vWF.
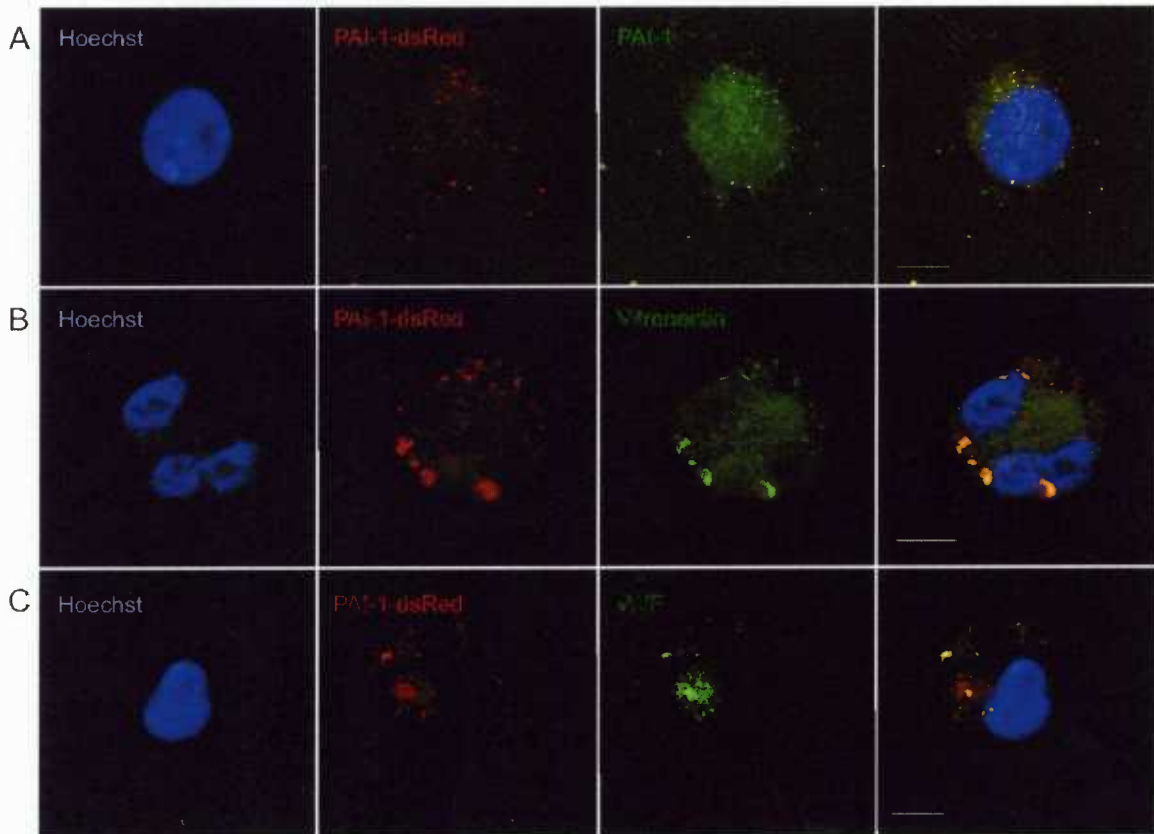
Figure 3.7.   Intracellular compartmentalization of PAI-1-dsRed in MEG-01 cells.
As represented in whole image projections, transfected MEG-01 cells were stained with antibodies specific for PAI-1 (A), vitronectin (B), and vWF (C) and each antigen was localized to α-granules. The far right image of each panel is the overlay composite in which yellow signal denotes colocalization of PAI-1-dsRed and the antibody stain. Scale bar, 10.0 μm.

3.3.8. Exocytosis of α-granules containing stores of PAI-1-dsRed in MEG-01 cells

To examine real-time exocytosis of PAI-1-dsRed from storage granules, transfected MEG-01 cells were incubated with 0.1 mM Alexa488-fibrinogen overnight to use as a positive marker for the dynamics of a α-granule protein. MEG-01 cells endocytosed Alexa488-fibrinogen into α-granules and exhibited significant colocalization with PAI-1-dsRed stores (Figure 3.8A-B). Thrombin-induced (1.0 U/mL) exocytosis resulted in rapid (~1 minute) release of large granules containing both fibrinogen–Alexa488 and PAI-1-dsRed.

In contrast, a second subpopulation of granules positive for both fluorophores within the cytosol demonstrated signal depletion over a longer time period (~5 minutes); suggesting mobilization and externalization of this second subpopulation of granules. Additionally, a third subpopulation of granules positive for both fibrinogen-Alexa488 and PAI-1-dsRed remained stationary throughout the acquisition time period. In Scan A&B, the peaks of the line scan represent the signal of granules containing both Alexa488-fibrinogen (in green) and PAI-1-dsRed (in red). Scan A represents granules that eventually become exocytosed and another granule that remains stationary throughout the acquisition period. This stationary granule may represent immature granules that are not able to undergo exocytosis. Scan B represents two granules that become exocytosed by depletion of signal and loss of a doublet peak.
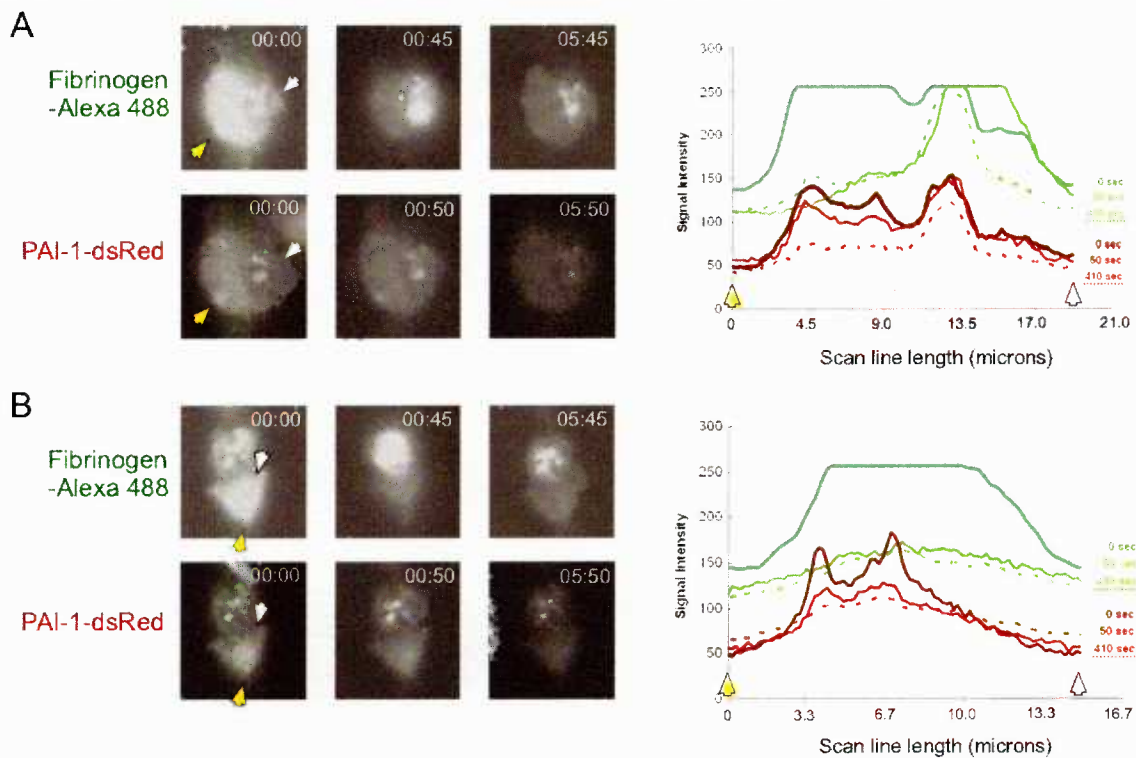
Figure 3.8. Exocytosis of PAI-1-dsRed and Alexa 488-fibrinogen from MEG-01 α-granules. MEG-01 cells with stores of Alexa 488-fibrinogen and PAI-1-dsRed were activated with thrombin (10 U/mL) to observe exocytosis of granules containing PAI-1-dsRed. Figures 3.8A-B depict wide-field fluorescence images of fibrinogen-Alexa 488 (upper panels in 3.8A-B) and PAI-1-dsRed (lower panels in 3.8A-B) in two different MEG-01 cells at various time points (min:sec) after thrombin stimulation. The accompanying graphs (right side) for Figures 3.8A-B depict spectral line scans of PAI-1-dsRed signal (deep red curve: t=0 secs, red curve: t=45 secs, red dashed curve: t=405 secs) and Alexa488-fibrinogen signal (deep green curve: t=0 secs, green curve: t=50 secs, dashed green curve: t=410 secs). The yellow and white arrowheads in the images represent the scan line used to analyze the image, and this data is presented in the graphs to the right of the images.

3.4. Discussion:

3.4.1. Overview

In this report, we reveal that a novel PAI-1-dsRed fusion protein is targeted to granules containing vitronectin within endothelial and megakaryocyte cell lineages respectively. PAI-1-dsRed was able to form complexes with VN on nitrocellulose, formed SDS-stable complexes with tPA in conditioned media, and on the fibrin fibril surface PAI-1-dsRed attenuated clot lysis. Moreover, PAI-1-dsRed was sorted into α-granules in megakaryocytic cell cultures, and was exocytosed upon thrombin stimulation. Interestingly, in the context of the Eahy926 cells, PAI-1-dsRed was found to colocalize with vWF- and P-selectin- containing granules, which has not been previously described. Upon TNF-α activation, PAI-1 was found to translocate to surface bound VN, and exposed vimentin intermediate filaments. These findings are consistent with previous flow cytometry and immunogold studies on activated human and bovine endothelium *in vitro* [19]. The vitronectin-dependent binding of PAI-1 to vimentin has also been demonstrated in activated platelets and platelet microparticles generated *in vitro* and in subjects with heart disease undergoing acute exercise stress [9].

PAI-1-dsRed is the first fluorescent protein form of PAI-1 for investigating protein-protein binding interactions, biogenesis and maturation of secretory granules, and the constitutive and regulated pathways of exocytosis in megakaryocytic cells and endothelium. Our finding of PAI-1-dsRed colocalizing with vWF and P-selectin in WPB-like granules in Eahy926 cells raises the question regarding the role of the fluorescent dsRed protein in regulating the sorting of the fusion protein. As a protein tag, dsRed was significantly large enough (~23 kDa) to cast concerns about its potential steric interference effect on PAI-1, a serpin highly dependent on the position of its reactive center loop (RCL) relative to its body. However, recognition of

both native and fused forms of PAI-1 by a polyclonal specific for PAI-1 now suggests that the dsRed tag does not interfere with the PAI-1 antibody binding epitopes. In terms of VN binding interactions with PAI-1-dsRed, positioning the dsRed tag at the C-terminus end of the PAI-1 enabled the VN binding site (aa 115-167) [21] to remain unobstructed, thereby allowing active to inactive latent phases of the PAI-1 molecule to be primarily dependent on its interactions with VN. Similar strategies in fusing a GFP tag with vimentin and cathepsin B also preserved functionality [22, 23].

Previous studies for tracking PAI-1 entailed the chemical conjugation of FITC or biotin to the PAI-1 molecule [24, 25]. In detail, specific conjugation of fluorophores such as FITC to the P1' [26], P3 and P18 domain of PAI-1 [27] by insertion of a cysteine residue by site-directed mutagenesis permitted labeling of this sulfhydryl group with iodoacetamide derivatives of fluorophores such as FITC without any observed inhibition of PAI-1:tPA interactions; in fact, these strategies further stabilized PAI-1 activity [24]. Biotinylation of PAI-1 also resulted in minimal loss of PAI-1 inhibitory activity as determined by VN ligand blotting and ELISA [7]. In terms of protein tags, we have previously constructed a recombinant human PAI-1 fusion protein containing the 6 residual peptide consensus sequences for heart muscle kinase (HMK) at the amino terminus and shown it to be fully functional, while also allowing for radiolabelling with ^{32}P for quantitative binding studies [25]. However, our use of the PAI-1-dsRed fusion now gives us the same advantages as all the other forms of labeled PAI-1 plus the advantage of its use in real-time secretory granule biogenesis tracking studies.

3.4.2. Thrombin induced MEG-01 cell α-granule exocytosis

Time-lapse video microscopy confirmed that thrombin stimulation of MEG-01 cells induced rapid exocytosis of a large majority of α-granules storing PAI-1, PAI-1-dsRed and fibrinogen within <45 seconds. A second population of α-granules containing PAI-1-dsRed remained static but demonstrated depletion of signal over a longer period of time. It appears that there are two classes of α-granules: larger more mature α-granules which possessed both fibrinogen and PAI-1-dsRed stores primed for exocytosis, and smaller more peri-nuclear vesicles that only contained PAI-1-dsRed. It is conceivable that the lack of fibrinogen in these smaller granules may suggest an immature stage of these granules, perhaps containing freshly synthesized PAI-1 shuttled from the Golgi apparatus. Therefore, it is a possibility that PAI-1-VN complexes are assembled in fully mature granules nearest the cell membrane because VN would be expected to follow a similar endocytotic fate as fibrinogen [9, 28]. Similar observations regarding differential fates of storage granules have been found in cultured HUVECs and their WPB's when activated by thrombin. Vinogradova et al., observed two main fates of vWF-containing Weibel-Palade bodies, immediate exocytosis or centrosome-directed translocation to the peri-nuclear space [29].

3.4.3. PAI-1 colocalizes with vWF in Eahy926 cells

After establishing the properties of PAI-1-dsRed as a native equivalent of PAI-1, we determined that it colocalizes with vWF and P-selectin in large, heterogeneous shaped granules in Eahy926 cells. Given that vWF and P-selectin are well-described Weibel-Palade body (WPB) resident proteins, it is apparent that PAI-1-dsRed is internalized into these granules just as it is in megakaryocytic cells and platelets [7]. Perhaps more relevant is that these results challenge

previous reports describing PAI-1 intracellular distribution [13, 14], in that our technique of PAI-1 intracellular colocalization does not require antibody detection of PAI-1. This is an advantage for *in vitro* and *in vivo* tracing studies given the disadvantages of using an antibody that may have a poor binding signal because of steric hinderance from VN or other WPB proteins, masking binding epitopes on the PAI-1 molecule. Using the PAI-1-dsRed protein, we were able to observe the punctate or ring-like distribution of exposed vimentin [32] and the distribution of vimentin-vitronectin-PAI-1 ternary complexes at these sites on the surface of TNF-α activated Eahy926 cells. More specifically, PAI-1-dsRed was found to be primarily associated with VN and the exposed vimentin intermediate filament cytoskeleton, a finding only previously observed on activated platelets and platelet microparticles [9]. Overall, the punctate distribution of PAI-1-dsRed and VN (Figure 3.6A) indicates that cell activation results in the binding of PAI-1-dsRed:VN complexes from the conditioned media binding to this exposed vimentin cytoskeleton, forming the ternary complex as previously described [9]. To validate the ring-like, punctate distribution of VN and PAI-1, previous reports have also described this observation of surface exposed vimentin in a ring-like morphology [32, 33]. Surface vimentin exposed to plasma, will act as a site for VN multimerization [9] and to an extent, PAI-1-dsRed:VN complex incorporation into this VN multimer via VN-VN homotypic interactions [34].

The construction of the first endogenous red fluorescent form of functionally active human PAI-1 is a catalyst for studying the cell biology of PAI-1 and its role in vascular fibrinolysis. In addition to real-time fluorescence imaging in cultured cells, the PAI-1-dsRed fusion protein can be used for *in vivo* applications with transgenic mice, and as purified protein for ELISA assay design, and for studying interactions between PAI-1 and target ligands.

3.5 References for Chapter III:

1. Gils A, Declerck PJ. Plasminogen activator inhibitor-1. Curr Med Chem 2004; 11:2323-34.

2. Lindahl TL, Ohlsson PI, Wiman B. The mechanism of the reaction between human plasminogen-activator inhibitor 1 and tissue plasminogen activator. Biochem J 1990; 265:109-13.

3. Schleef RR, Wagner NV, Loskutoff DJ. Detection of both type 1 and type 2 plasminogen activator inhibitors in human cells. J Cell Physiol 1988; 134:269-74.

4. MacGregor IR, Booth NA. An enzyme-linked immunosorbent assay (ELISA) used to study the cellular secretion of endothelial plasminogen activator inhibitor (PAI-1). Thromb Haemost 1988; 59:68-72.

5. van den Berg EA, Sprengers ED, Jaye M, Burgess W, Maciag T, van Hinsbergh VW. Regulation of plasminogen activator inhibitor-1 mRNA in human endothelial cells. Thromb Haemost 1988; 60:63-7.

6. Konkle BA, Schick PK, He X, Liu RJ, Mazur EM. Plasminogen activator inhibitor-1 mRNA is expressed in platelets and megakaryocytes and the megakaryoblastic cell line CHRF-288. Arterioscler Thromb 1993; 13:669-74.

7. Hill SA, Shaughnessy SG, Joshua P, Ribau J, Austin RC, Podor TJ. Differential mechanisms targeting type 1 plasminogen activator inhibitor and vitronectin into the storage granules of a human megakaryocytic cell line. Blood 1996; 87:5061-73.

8. Brogren H, Karlsson L, Andersson M, Wang L, Erlinge D, Jern S. Platelets synthesize large amounts of active plasminogen activator inhibitor 1. Blood 2004; 104:3943-8.

9. Podor TJ, Singh D, Chindemi P, et al. Vimentin exposed on activated platelets and platelet microparticles localizes vitronectin and plasminogen activator inhibitor complexes on their surface. J Biol Chem 2002; 277:7529-39.

10. Zhou A, Huntington JA, Pannu NS, Carrell RW, Read RJ. How vitronectin binds PAI-1 to modulate fibrinolysis and cell migration. Nat Struct Biol 2003; 10:541-4.

11. Preissner KT, Holzhuter S, Justus C, Muller-Berghaus G. Identification of and partial characterization of platelet vitronectin: evidence for complex formation with platelet-derived plasminogen activator inhibitor-1. Blood 1989; 74:1989-96.

12. Mousa SA, Bozarth J, Forsythe M, Tsao P, Pease L, Reilly TM. Role of platelet GpIIb/IIIa receptors in the modulation of platelet plasminogen activator inhibitors type-1 (PAI-1) release. Life Sci 1994; 54:1155-62.

13. Rosnoblet C, Vischer UM, Gerard RD, Irminger JC, Halban PA, Kruithof EK. Storage of tissue-type plasminogen activator in Weibel-Palade bodies of human endothelial cells. Arterioscler Thromb Vasc Biol 1999; 19:1796-803.

14. Ma GM, Halayko AJ, Stelmack GL, et al. Effects of oxidized and glycated low-density lipoproteins on transcription and secretion of plasminogen activator inhibitor-1 in vascular endothelial cells. Cardiovasc Pathol 2006; 15:3-10.

15. Novokhatny VV, Ingham KC, Medved LV. Domain structure and domain-domain interactions of recombinant tissue plasminogen activator. J Biol Chem 1991; 266:12994-3002.

16. Handagama P, Scarborough RM, Shuman MA, Bainton DF. Endocytosis of fibrinogen into megakaryocyte and platelet alpha-granules is mediated by alpha IIb beta 3 (glycoprotein IIb-IIIa). Blood 1993; 82:135-8.

17. Schleef RR, Loskutoff DJ, Podor TJ. Immunoelectron microscopic localization of type 1 plasminogen activator inhibitor on the surface of activated endothelial cells. J Cell Biol 1991; 113:1413-23.

18. Hill SA, Podor TJ. Serum-dependent modulation of the type 1 plasminogen activator inhibitor binding to endothelial cell surfaces. Ann N Y Acad Sci 1992; 667:42-5.

19. Podor TJ, Loskutoff DJ. Immunoelectron microscopic localization of type 1 plasminogen activator inhibitor in the extracellular matrix of transforming growth factor-beta-activated endothelial cells. Ann N Y Acad Sci 1992; 667:46-9.

20. Podor TJ, Joshua P, Butcher M, Seiffert D, Loskutoff D, Gauldie J. Accumulation of type 1 plasminogen activator inhibitor and vitronectin at sites of cellular necrosis and inflammation. Ann N Y Acad Sci 1992; 667:173-7.

21. Padmanabhan J, Sane DC. Localization of a vitronectin binding region of plasminogen activator inhibitor-1. Thromb Haemost 1995; 73:829-34.

22. Linke M, Herzog V, Brix K. Trafficking of lysosomal cathepsin B-green fluorescent protein to the surface of thyroid epithelial cells involves the endosomal/lysosomal compartment. J Cell Sci 2002; 115:4877-89.

23. Lochner JE, Kingma M, Kuhn S, Meliza CD, Cutler B, Scalettar BA. Real-time imaging of the axonal transport of granules containing a tissue plasminogen activator/green fluorescent protein hybrid. Mol Biol Cell 1998; 9:2463-76.

24. Shore JD, Day DE, Francis-Chmura AM, et al. A fluorescent probe study of plasminogen activator inhibitor-1. Evidence for reactive center loop insertion and its role in the inhibitory mechanism. J Biol Chem 1995; 270:5395-8.

25.   Podor TJ, Peterson CB, Lawrence DA, et al. Type 1 plasminogen activator inhibitor binds to fibrin via vitronectin. J Biol Chem 2000; 275:19788-94.

26.   Shore JD, Vandenberg, E., Day, D., Olson, S.T., Sherman, R., Ginsburg, D., Kvassman, J. Fibrinolysis 1992; 6, Suppl. 2:Abstract 292.

27.   Strandberg L, Johansson, L. B.-A., Ny, T. Fibrinolysis 1992; 6 Suppl. 2.

28.   Wencel-Drake JD, Boudignon-Proudhon C, Dieter MG, Criss AB, Parise LV. Internalization of bound fibrinogen modulates platelet aggregation. Blood 1996; 87:602-12.

29.   Vinogradova TM, Roudnik VE, Bystrevskaya VB, Smirnov VN. Centrosome-directed translocation of Weibel-Palade bodies is rapidly induced by thrombin, calyculin A, or cytochalasin B in human aortic endothelial cells. Cell Motil Cytoskeleton 2000; 47:141-53.

30.   Volker W, Hess S, Vischer P, Preissner KT. Binding and processing of multimeric vitronectin by vascular endothelial cells. J Histochem Cytochem 1993; 41:1823-32.

31.   de Boer HC, Preissner KT, Bouma BN, de Groot PG. Internalization of vitronectin-thrombin-antithrombin complex by endothelial cells leads to deposition of the complex into the subendothelial matrix. J Biol Chem 1995; 270:30733-40.

32.   Hansson GK, Starkebaum GA, Benditt EP, Schwartz SM. Fc-mediated binding of IgG to vimentin-type intermediate filaments in vascular endothelial cells. Proc Natl Acad Sci U S A 1984; 81:3103-7.

33.   Hansson GK, Lagerstedt E, Bengtsson A, Heideman M. IgG binding to cytoskeletal intermediate filaments activates the complement cascade. Exp Cell Res 1987; 170:338-50.

34.   Wu YP, Bloemendal HJ, Voest EE, et al. Fibrin-incorporated vitronectin is involved in platelet adhesion and thrombus formation through homotypic interactions with platelet-associated vitronectin. Blood 2004; 104:1034-41.

CHAPTER IV: DISTRIBUTION OF PAI-1:VITRONECTIN:VIMENTIN TERNARY COMPLEXES ON ACTIVATED PLATELETS AND PLATELET MICROPARTICLES BY ATOMIC FORCE MICROSCOPY.

4.1. Introduction:

Elevated plasma levels of plasminogen activator inhibitor type-1 (PAI-1) have been found to be correlated with thrombotic events, a likely association due to its ability to inhibit the fibrinolytic branch of hemostasis [1-6]. PAI-1 can attenuate fibrinolytic breakdown of thrombi by inhibiting the key initiators of fibrinolysis, tissue-type and urokinase-type plasminogen activators (tPA and uPA) [7], and the inhibitory activity of PAI-1 is further prolonged when it forms a complex with vitronectin (VN), an abundant plasma protein [8]. While VN can stabilize PAI-1 activity, VN can also direct PAI-1 localization in thrombi by mediating its binding to two major components: the surfaces of activated platelets and fibrin [9, 10].

The assembly of the PAI-1:VN:vimentin ternary complex is largely responsible for the majority of cell-surface bound PAI-1 on activated cells, namely activated platelets and platelet microparticles (PMP's). In detail, VN binds with high affinity to vimentin [9], a cytoskeletal intermediate filament protein expressed by mesenchymal cell lineages such as platelets [9, 11], endothelial cells [12, 13] and leukocytes [14]. We have previously determined that the head domain of vimentin is exposed on the surface of activated platelets, acting as a site for multimerization of VN and incorporation of PAI-1:VN complexes [9]. In theory, PAI-1:VN complexes can also be incorporated into these vimentin-induced multimers due to homotypic

---

VN-VN interactions [15]. Although the exact proportion of each component is not fully understood, the extent of vimentin-induced multimerization of VN is thought to dictate the extent of PAI-1 localization onto activated cell surfaces.

Platelet microparticles (PMP's) are vesicular bodies that are released during platelet activation and have been postulated to play a pro-thrombotic role in acute coronary syndromes [16 , 17]. It is thought that PMP's are shed from the tip or median of platelet pseudopodia [18, 19], therefore we hypothesized that vimentin exposure occurs at the broken junction between the released PMP and the pseudopod of the activated platelet, which subsequently becomes available for PAI-1:VN:vimentin ternary complex formation. To understand this exposure of vimentin, we used atomic force microscopy to visualize PMP's that expressed some, if not all, components of the ternary complex. To do this, we isolated and imaged PMP's generated from expired platelet concentrates or platelet-poor plasma (PPP) from post-myocardial infarction patients. PMP's were isolated by FACS and their topography visualized by atomic force microscopy (AFM). A similar strategy was performed on isolated activated platelets in order to visualize VN-vimentin multimers on the activated platelet surface. Finally, we used AFM to visualize VN-vimentin multimers formed *in vitro* in a cell-free preparation to understand the ultrastructure of VN-vimentin multimers and to determine if these multimers have a distinct molecular organization that allows them to be recognized on the surface of activated platelets and PMP's.

4.2. Materials and Methods:

4.2.1. Ethics, blood preparation and PAI-1 ELISA

Ethics approval was obtained from the University of British Columbia Clinical Research Ethics Committee to collect whole blood from patients at 24, 48, and 72 hours post-myocardial infarction. Whole blood was collected into 4.5 mL acid citrate dextrose vacutainers (BD Biosciences, Mississauga ON). Blood samples were then centrifuged at 1500×g for 15 minutes and the upper layer representing the platelet-poor plasma (PPP) fraction was removed and stored at -80°C. Expired platelet concentrates (10 days post-preparation) were provided by the National Blood Service (UK, Harefield Hospital). An ELISA kit to measure active PAI-1 in patient PPP was used, in which 5 μL of PPP diluted in 20 μL of reaction buffer was assayed for in triplicate (Molecular Innovations, Ann Arbor, MI).

4.2.2. Electrophoresis of High Molecular Weight Protein Complexes from Patient Plasma Samples

Diluted PPP samples (4 μL PPP + 16 μL of PBS + 4 μL 6X sample buffer) and electrophoresed on a native 8% acrylamide gel with a 5% acrylamide stacker gel. Native protein separation was visualized by staining with Coomassie blue, and acrylamide gel pieces with positive staining in the stacker well interface were excised and then incubated in 400 μL of elution buffer (0.25 mM Tris-HCl buffer, pH=6.8; 0,1% (w/v) SDS) at 4°C overnight. This preparation was then ultrafiltrated with a Nanosep Centrifuge tube column (0.28 μm pore size; Pall Life Sciences, Ann Arbor, MI) by centrifugation at 8000×g for 20 minutes. After elution, the samples were boiled in sample buffer containing 5% 2-mercaptoethanol, and fractionated in 10% SDS-PAGE gels. Separated proteins were transferred to nitrocellulose membrane, and after

blocking with blotting buffer (1X PBS, pH 7.4, containing 2% milk powder and 0.05% w/v Tween-20), the membranes were incubated for 1 hour with antibodies directed against PAI-1, VN, and vimentin at a final concentration of 5 μg/mL (Affinity Biologicals Inc., Hamilton, ON). After washing, membranes were incubated with a 1:2000 dilution of alkaline phosphatase-conjugated rabbit anti-sheep IgG (Santa Cruz Biotechnology Inc., Santa Cruz, CA) for 1 hour and then developed with AP Color Development Reagent Kit (BioRad Corporation Inc., Hercules, CA).

4.2.3. FACS isolation of platelet microparticles and activated platelets expressing ternary complex

FACS analysis was used to assay PMP populations in PPP collected from patients at 48 hours post-AMI. PPP (20 μL) was incubated for 15 minutes with a combination of: 1) mouse α-human CD41a IgG$_1$-RPE (BD Biosciences, Burlington, ON), sheep α-human vimentin IgG (Affinity Biologicals Inc, Hamilton, ON) with donkey α-sheep-FITC IgG (BD Biosciences), and rabbit α-human VN IgG (Affinity Biologicals Inc.) with goat α-rabbit Alexa633 IgG (Molecular Probes, Eugene, OR); or 2) mouse α-human CD41a IgG$_1$-RPE (BD Biosciences), sheep α-human vimentin (Affinity Biologicals Inc.) with donkey α-sheep FITC IgG (BD Biosciences) and mouse α-human PAI-1 IgG (Molecular Innovations, Ann Arbor, MI), or mouse α-human CD62P IgG$_1$(BD Biosciences) both labeled with goat α-mouse Alexa633 IgG (Molecular Probes Inc.) secondary antibody. The forward scatter (FS) PMT threshold was minimized to measure all particles of any size with both significant FITC and Alexa633 fluorescence. Microspheres with a 1.0 μm diameter (Molecular Probes Inc.) were analyzed to define a size standard in terms of forward scatter of microparticles. For PMP sample isolation, only particles that exhibited an FS

below that of the 1.0 μm microsphere forward scatter with significant dual FITC+Alexa633 fluorescence was sorted onto mica for AFM imaging.

Human blood was drawn into ACD tubes and PRP was prepared by centrifugation of anti-coagulated blood at 200×g for 10 minutes and the supernatant transferred into another tube. This PRP fraction was centrifuged at 1000×g for 10 minutes, the resulting supernatant removed and the platelet-rich pellet was gently washed twice with calcium-free Tyrodes buffer and resuspended with modified Tyrodes buffer to a final cell concentration of 1×10^4 platelets/μL. One aliquot of diluted washed platelets was activated with 2 μL of 10 U/mL of thrombin and incubated for 30 minutes. Activated platelets were incubated for 15 minutes with a combination of mouse α-human CD41a IgG1-RPE (BD Biosciences, Burlington, ON), sheep α-human vimentin IgG (Affinity Biologicals Inc, Hamilton, ON) with donkey α-sheep-FITC IgG (BD Biosciences), and rabbit α-human VN IgG (Affinity Biologicals Inc.) with goat α-rabbit Alexa633 IgG (Molecular Probes). CD41+ve platelets with the highest FITC+Alexa633 dual signal were gated and isolated by FACS.

4.2.4. Atomic Force Microscope (AFM) Specifications

The instrument used for atomic force microscopy was a BioScope (Digital Instruments Inc., Santa Barbara, CA), which is an AFM head piece mounted onto an inverted microscope (Axiovert 100, Zeiss Inc.). For sample preparation, proteins and cells were adsorbed onto a piece of freshly cleaved mica (2 cm^2, Ted Pella Inc., Redding, CA). Tapping mode AFM was used for all microscopy and was performed in ambient temperature and humidity using Veeco Tapping Mode Etched Silicon cantilevers (k=40 N/m). A slow scan rate of 1–3 Hz was used to minimize sample disturbances giving a scan rate that was much slower (<25 000×) than the tap

rate. A maximum resolution of 512×512 pixels was used. The x- and y-scan directions were calibrated with a 10×10 μm2 grid. The z-direction was calibrated with 5 nm diameter gold particles (Ted Pella Inc.) on a cleaved mica surface. The scans were tested for imaging artifact by varying scan direction, scan size, and by rotating the sample.

4.2.5. Atomic force microscopy of platelet microparticles, VN-vimentin multimers and activated platelets

PMP's and activated platelets that presented significant expression of antibodies used were gated and sorted directly onto freshly cleaved mica sheets for AFM imaging (Ted Pella, Inc.). Approximately 200 particles were absorbed onto the mica sheet. AFM imaging of protein-protein interactions of VN and vimentin required pretreatment of mica sheets with a dH2O wash, then adsorption of 10 μL of 5 mM MgCl$_2$ on the center of the mica sheet for 5 minutes. Excess MgCl$_2$ was washed off with dH$_2$O and then gently blow dried with dry nitrogen gas. To form vitronectin-vimentin multimers, purified human VN (Molecular Innovations Inc., Southfield, MI) and purified vimentin head domain protein [9] were incubated at varying molar ratios and the multimerization reactions were carried out in PBS (pH 7.4) at 37 °C for 24 hours. To prepare protein samples for AFM imaging, 20 μL of sample was plated on the center of the coverslip and then left to adsorb onto the mica at room temperature for 10 minutes. Protein was fixed by addition of 2 μL of EM grade 0.025% w/v paraformaldehyde for 5 minutes. The sample was gently washed three times with 0.1 M ammonium acetate (Ultrasigma grade, Sigma-Aldrich, St. Louis, MO) and then gently dried with dry nitrogen gas. To quantify VN-VIM multimer structure, images were processed using MATLAB and quantified by fractal analysis. The image processing algorithm consisted of background signal subtraction, median filter, image

thresholding (Otsu's method [20]) and binarization. Fractal dimension was calculated using the box dimension estimation method. The box dimension, Db, is defined as the exponent of N(d) ~ 1/dDb, where N(d) is the number of boxes of linear size (d) required to cover a set of points distributed in a 2D plane.

4.2.6. Platelet-Rich Clot Formation and Staining for Vimentin, Vitronectin and PAI-1

Human blood was drawn into ACD tubes and PRP was prepared by centrifugation of anti-coagulated blood at 200×g for 10 minutes and the supernatant transferred into another tube. This supernatant was recalcified with 1 M $CaCl_2$ to a final concentration of 10 mM Ca^{2+} prior to clot formation. To generate a platelet-rich clot, 2 μL of 10 U/mL human thrombin (Chronolog, Havertown, PA) was added to 20 μL of platelet-rich plasma and then quickly pipetted onto a 1 mm thickness glass coverslip and left to incubate for 60 minutes at 37°C. The clot was incubated for 1 hour for both primary and secondary antibody incubations with these antibodies: sheep anti-human vimentin IgG antibody with donkey anti-sheep IgG-FITC secondary antibody, and mouse anti-human VN IgG (clone - 1244) with goat anti-mouse IgG-Alexa594 secondary antibody. After several PBS washes (1X, pH=7.4), the sample was mounted with a coverslip and anti-fade mounting media (Molecular Probes, Eugene, OR).

4.4. Results:

4.4.1. High molecular weight complexes in post-AMI platelet-poor plasma contains elevated PAI-1, vitronectin, and vimentin

Two PPP sets of patient samples (samples collected at t=24, 48, 72 hours post-AMI) were electophoresed on a non-reducing, native PAGE gel in order to separate the high molecular weight protein fraction from plasma, which also contains platelet microparticles. Coomassie blue stain revealed the accumulation of HMW protein complexes in the stacker gel (Figure 4.1A). These HMW complexes were eluted from the native gel and further fractionated by SDS-PAGE and subjected to Western blot analysis. At all three time points, levels of PAI-1, VN and vimentin expression were greater or equal to levels found in normal human plasma. The multiple bands (>47kDa) detected by the PAI-1 polyclonal antibody represents cleavage fragments of covalently-formed complexes that contain some of the PAI-1 molecule. Table 1 presents the levels of active PAI-1 in the PPP in a group of patients 48 hours post-AMI. Patient #1 and #2 are part of this group. Levels of active PAI-1 in control PPP are <2.0 U/mL.

Number of subjects (N)	6
Male/Female	6/0
Age (yrs)	57±3.3
Cigarette smoker	16.70%
Complications post-analysis	33.30%
Patient plasma Active PAI-1 (U/mL)	5.2±1.1
Control plasma Active PAI-1 (U/mL) N=9	1.1±0.1

Table 4.1. Clinical data of patients with Acute Myocardial Infarction (AMI).
Active PAI-1 levels were determined in PPP collected from patients 48 hours post-AMI with an ELISA assay specific for PAI-1.
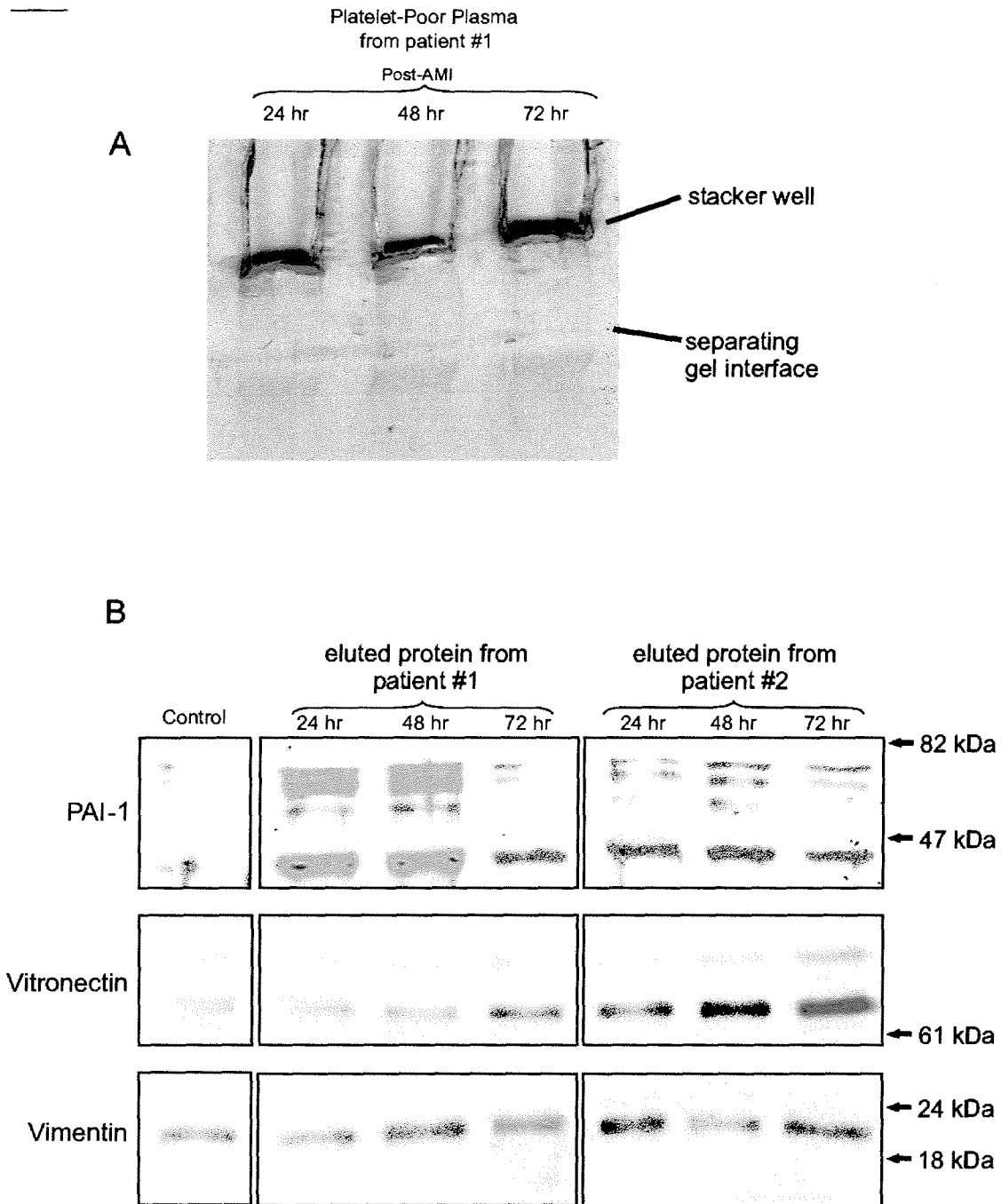
Figure 4.1. Platelet poor plasma (PPP) from post-acute ischemic infarction (post-AMI) patients contain high molecular weight protein complexes consisting of vimentin, vitronectin and PAI-1. A) illustrates the migration of PPP in a native PAGE gel and the entrapment of high molecular weight protein complexes in the stacker well interface. Following excision and elution of this high molecular weight fraction, immunoblot analysis in a 8% SDS-PAGE in B) demonstrates vimentin, vitronectin and PAI-1 protein levels to be higher in both post-AMI patients compared to control PPP.

4.4.2. Platelet microparticles express vitronectin, vimentin and PAI-1 on their surface as determined by FACS Analysis

Figure 4.2 is an overview of the FACS analysis performed on a representative 48 hour post-AMI PPP sample (Figure 4.2A) and a control PPP sample (Figure 4.2B). In the left panel, use of a CD41 antibody detected a population of CD41-positive particles with lower forward and side light scatter compared to beads with a diameter of ~1.0 μm, representing PMP's. With this gating, a minimum of 10,000 counts were analyzed. The middle and right panels represent co-expression scatter plots of these CD41-positive PMP's that also co-express vimentin and vitronectin (middle histoplot); as well as vimentin and PAI-1 (right histoplot). These histoplots suggest that at least two components of the ternary complex are present on a subpopulation of CD41-positive PMP's in greater quantities (Figure 4.2A) compared to control PPP (Figure 4.2B).
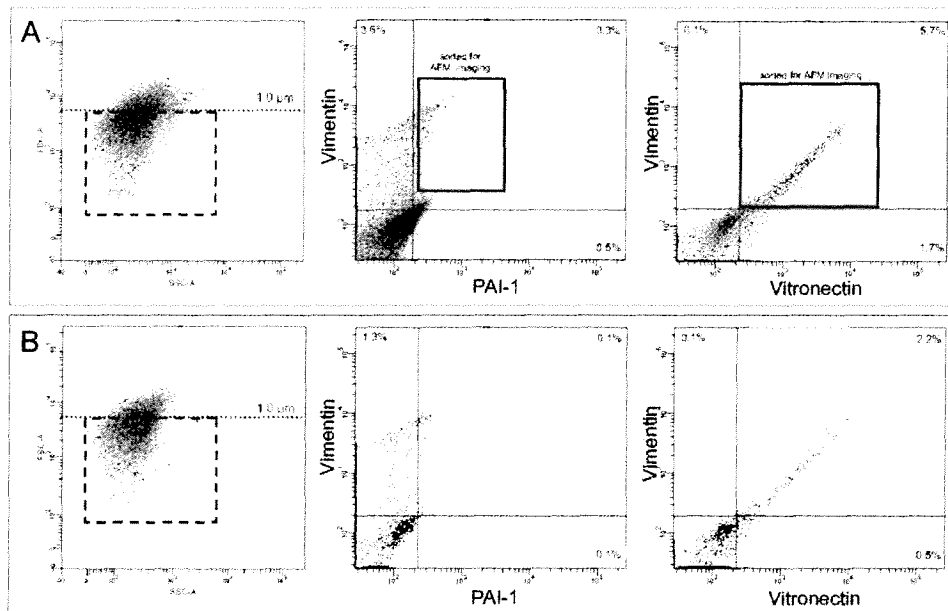
Figure 4.2. Flow Cytometric Analysis of PPP from post-AMI patients. Flow cytometry was performed to determine the amount of vitronectin, vimentin and PAI-1 on CD41-positive particles present in platelet-poor plasma. Each forward/side scatter histogram represents a combination of PAI-1, vitronectin, vimentin vs. CD41 or vimentin co-expression. Each inset box in the FS vs. SS histrogram depicts the cell population sorted for atomic force microscopy as determined by the upper limit of forward scatter of UV microspheres with a diameter of 1.0 μm.

4.4.3. AFM ultrastructural analysis of PMP's positive for ternary complex

As determined in Figure 4.2, PMP's positive for vimentin-vitronectin or vimentin-PAI-1 were sorted onto mica coverslips for atomic force microscopy. Image analysis of these patient PMP's reveal a heterogeneous population of granular, round and vesicular particles with a diameter range of 350-900 nm. In Figure 4.3A, AFM images of PMP's expressing CD41+vimentin, as well as VN (top), or PAI-1 (second from top) or P-selectin (third from top) are presented in two images: a *height dimension channel* with a pseuodocolour LUT (nm) and a *amplitude channel* in grayscale that represents the topographical detail of the PMP. A substantial proportion of sorted patient PMP's exhibited extensive surface protein aggregation which may in part, reflect localization of the antigen-antibody complexes specific for multimeric VN, vimentin and PAI-1. In these sample patient samples, a population of PMP's expressing CD41+vimentin+VN exhibited minor phospholipid membrane appendages extending from base of the microparticle (Figure 4.3A second from top). These short membrane appendages or "skirts" had a low height approximating ~5-7 nm and attached to the base of the microparticle.

PMP's isolated from post-AMI patient PPP exhibited substantial surface topography as manifest by the presence of many proteinaceous structures on the surface of the PMP's. In contrast, PMP's generated *in vitro* by expired platelets did not present with such topography and permitted ultrastructural analysis in assessing expression of ternary complex on the surface of PMP's. In Figure 4.3B, PMP's co-expressing vimentin or vimentin-vitronectin also exhibited extensive phospholipid appendage-like structures attached to the base of the microparticle. It was determined that 68% (17/25) of PMP's expressing VN+VIM had membrane flaps that exhibited an average thickness of 6.3±1.3 nm. Moreover, 45% (5/11) of PMP's expressing

vimentin exhibited membrane flaps with a thickness of 5.8±0.2 nm. Figure 4.3C demonstrates the manner in which a PMP expressing CD41+vimentin is analyzed in terms of (panel from left to right) a height dimension, amplitude dimension, a scan line of the height dimension of the PMP, and a 3-dimensional perspective of the PMP depicting the height difference between the PMP and its membrane flaps. In this particular PMP, the scan line graph reveals that the membrane thickness to be ~5.6 nm thick, which is within the 4-7 nm thickness range determined by previous observations [21].

In Figure 4.4, one particular PMP that expressed CD41 and vimentin was chosen for height profile analysis because of filamentous structures associated with membrane flaps attached to the PMP (As seen in Figure 4.3B second from the top). In Figure 4.4A&B, these filamentous were analyzed via scan line analysis (green scan line in A and grey scan line in B). Figure 4.4C represents the height profile of this scan line and when compared to the membrane height of 6.3nm, the two major peaks had thickness values of 11.3 and 9.1 nm, which is within the range of reported diameters of vimentin intermediate filaments (9 – 11 nm)[22].

4.4.4. Microscopy of vitronectin-vimentin multimers on activated platelets

As previously described in [9], a subpopulation of activated platelets are known to express high amounts of vimentin and vitronectin on their surface, observations that lead to a proposed mechanism wherein vimentin expression is requisite for vitronectin multimerization and consequent ternary complex formation. Extracellular distribution of the ternary complex on activated platelets was imaged with confocal microscopy as shown in Figure 4.5A-D and with AFM in Figure 4.5E. Panels B and C illustrate the staining distribution of vimentin and vitronectin of an activated platelet and in panel D, yellow signal represents areas of co-
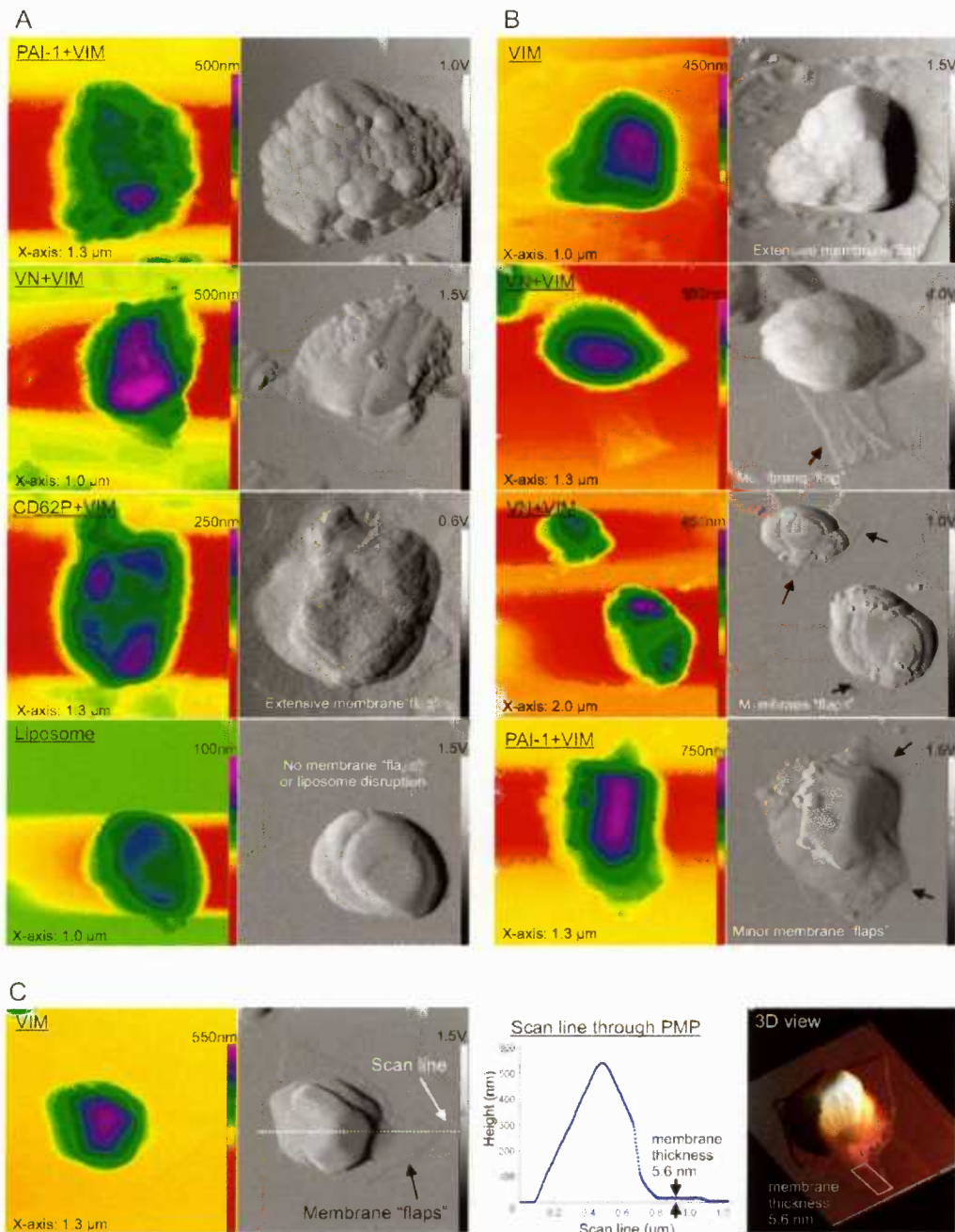
Figure 4.3. Atomic force microscopy on platelet microparticles isolated from platelet-poor plasma. A) depicts images of PMP's as isolated from post-AMI plasma that express CD41+PAI-1+vimentin (VIM), CD41+VN+VIM, CD41+CD62P+VIM, (top to bottom). B) depicts images of PMP's isolated from expired platelet concentrates that express CD41+VIM, CD41+VN+VIM, CD41+PAI-1+VIM (top to bottom). In B), the majority of PMP's expressing CD41+VIM presented membrane appendages at the base of the PMP. Each PMP is presented as two types of images, the left column a height image channel as measured in nanometers (nm) and the right column an amplitude channel as measured in volts (V). The height channel provides a quantitative Z-plane perspective while the amplitude channel provides a superficial topographical perspective.
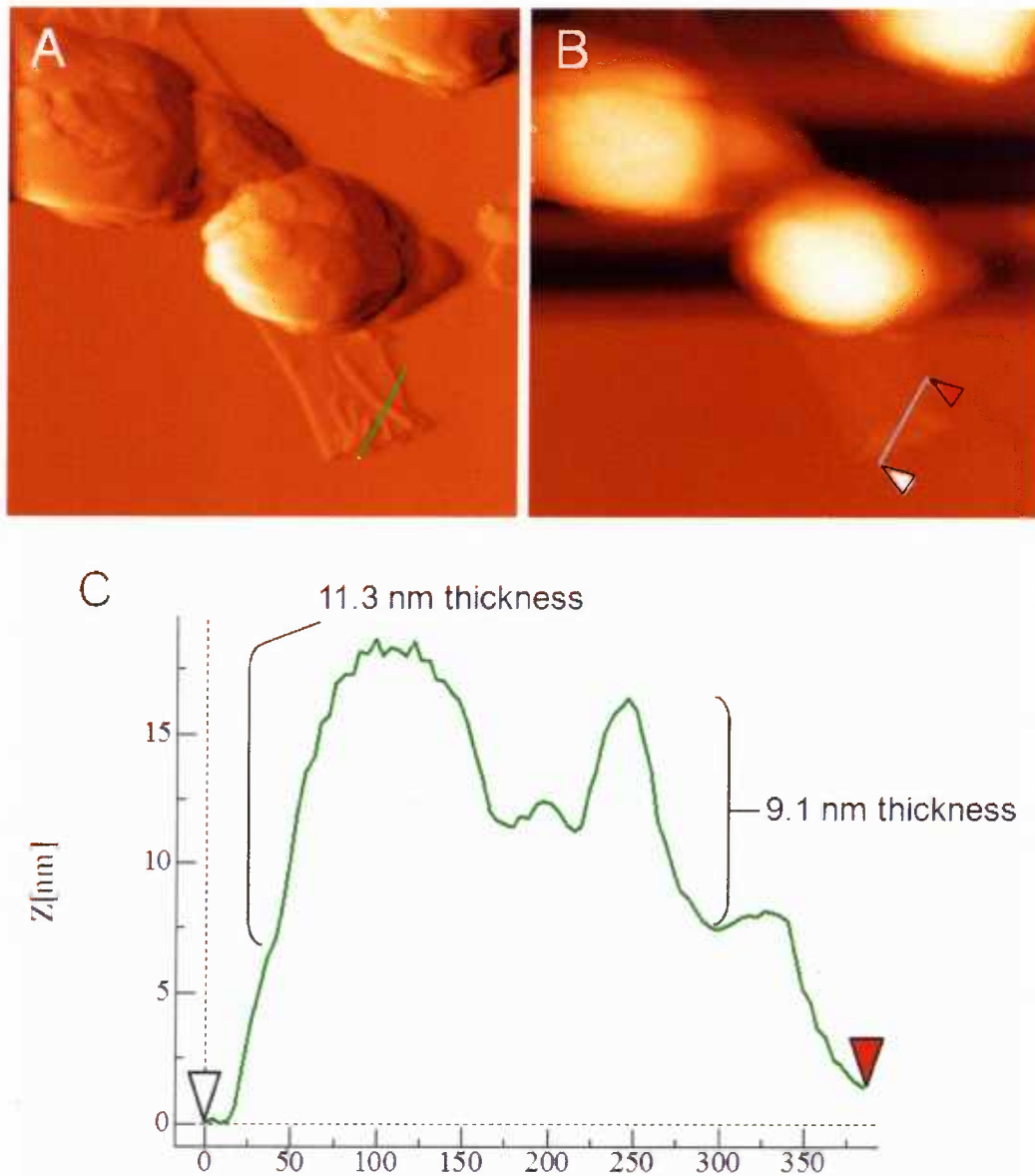
Figure 4.4 – Scan line analysis of filament-like structures present within membrane flaps of PMP's expressing CD41+vimentin. A) depicts the amplitude channel of PMP and B) depicts the height dimension of the PMP. The green and grey scan line in A) and B) respectively marks the scan line used to analyze the filamentous structures. In C), the peaks represent the heights of the filaments when the membrane height is considered. The two major peaks identified represent filament structures with a diameter of 11.3 and 9.1 nm (left to right). This is within the reported diameters of intermediate filaments (9-11 nm in diameter).

localization of vimentin and VN throughout the activated platelet. In this same image, discrete VN signal was also observed as minor protrusions extending from the vimentin cytoskeleton. This latter observation is consistent with our previous findings demonstrating multimerized VN at sites of exposed vimentin intermediate filaments [9]. Panel A represents another activated platelet stained with isotype negative controls with their respective FITC- and RPE- IgG conjugates. Ultrastructural analysis using AFM was performed on thrombin-activated platelets coexpressing vimentin and vitronectin as shown in Figure 4.5E. Height dimension analysis identified the structures as being two platelets adhering to the mica surface, each having a maximal height of ~720 nm (data not shown). Panel E is a merged image of the trace and

retrace deflection channel. An organized field of globular proteins can be observed on the highest plateau of each platelet, and this distribution of protein is distinct from rest of the flat surface of the platelet. It is believed that the distribution of vimentin-VN complexes is represented on the cortical region of the activated platelet and similar to the distribution of vimentin-VN complexes in Panel D. In general, activated platelets with strong VN and vimentin surface immunoreactivity exhibited a disc-like morphology with a central depression. Furthermore, the perimeter of these activated platelets was elevated and supported a distribution of carpet-like vimentin and VN multimers disproportionate to one side of the platelet.

4.4.5. Multimers of vitronectin-vimentin form a highly ordered ultrastructure

Cell-free experiments with purified proteins were performed to simulate the formation of VN multimers bound to the platelet vimentin cytoskeleton that become exposed during platelet activation. The AFM was used to visualize the ultrastructure of the polymeric VN-vimentin
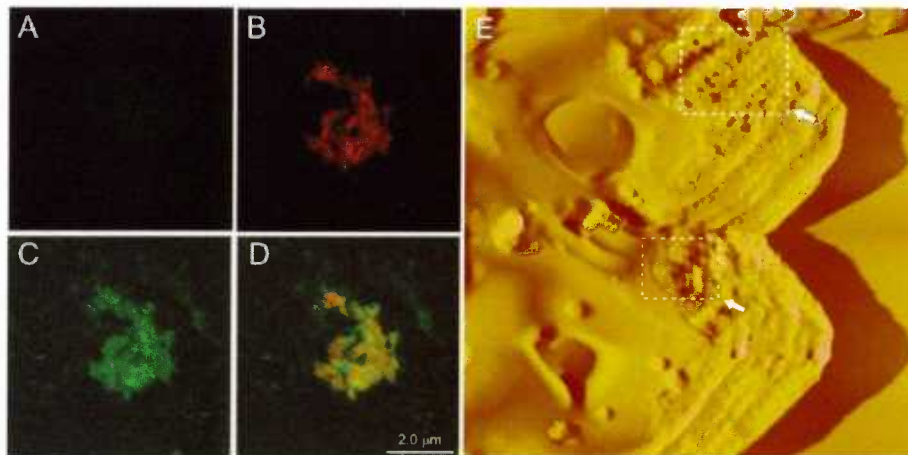
Figure 4.5. Distribution of vitronectin-vimentin multimers on the cell surface of activated platelets. A-D) depicts images of an activated platelet as acquired by confocal microscopy. A) is an isotype antibody stained activated platelet, red signal B) represents vimentin and green signal C) represents vitronectin. The formation of vitronectin-vimentin multimers is highlighted by yellow colocalization in D). E) is a merged AFM image of the trace and retrace deflection channel of an aggregate of activated platelets. Washed platelets were activated with thrombin and then stained with antibodies for vimentin and vitronectin. Only dual-labelled platelets were isolated by flow cytometry sorting for AFM imaging. The distribution of vimentin-vitronectin complexes on the cortical regions of the activated platelets as highlighted by the inset boxes is analogous to the distribution of the vimentin-vitronectin complexes in D).

complex at a nanometer resolution. The reaction was primarily carried out in PBS (pH 7.4), while similar results were achieved with distilled water. Moreover, varying the incubation times from 15 minutes to 24 hours did not affect the overall ultrastructure of the VN-vimentin multimers (data not shown). Figure 4.6A demonstrates an AFM image of monomeric VN plated at a concentration of 5 μg/mL (1.3 μM). VN monomers on average are ~3 nm in height as seen in the corresponding scan line height analysis graph (right). Figure 4.6B represents vimentin head domain protein (VIM133) which is approximately 13 kDa, at a height dimension of ~0.8 nm. Polymeric VN-vimentin aggregates as imaged by AFM illustrated a highly organized lattice

71
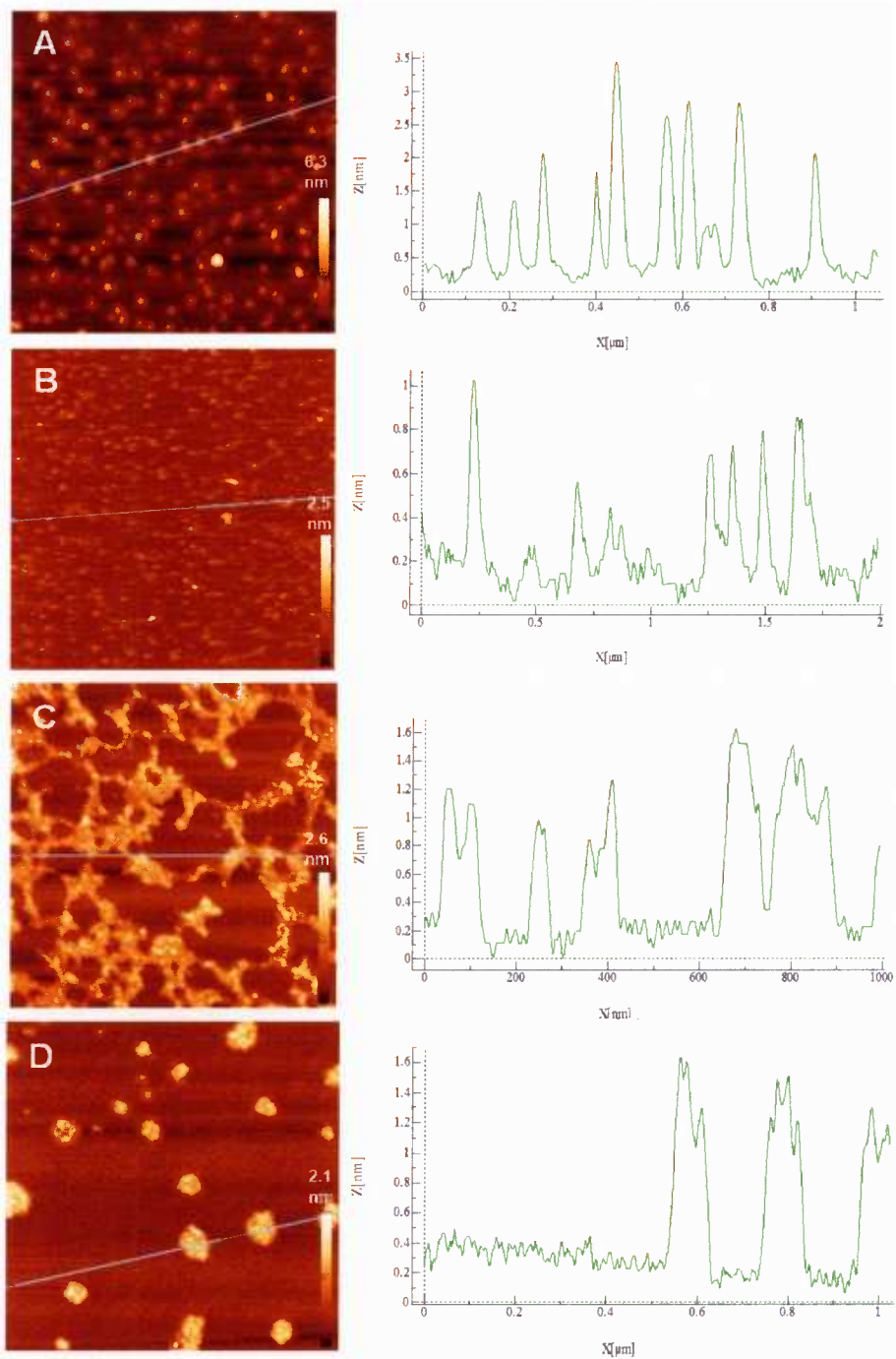
Figure 4.6. AFM analysis of the ultrastructure of vitronectin-vimentin multimers.
The head domain of vimentin (VIM133) and purified vitronectin was used to form vitronectin-vimentin multimers. The above images represent height dimensions. A) represents monomeric vitronectin (0.8 nM) and B) represents monomeric VIM133 (0.6 nM). Fractal dimension analysis (Db) of A) and B) are 1.32 and 1.11 respectively. C) Represents ultrastructure of vitronectin-vimentin multimers at a 3:2 molar ratio with a fractal dimension of 1.74. D) represents vitronectin-vimentin multimers formed at a molar ratio of 6:1 with a fractal dimension analysis of 1.20.

ultrastructure in which no free protein was found unbound to the lattice (Figure 4.6C). In this image, no structures had a height that exceeded ~3nm, suggesting that vimentin induces a conformational change such that VN height becomes <1.6 nm. This would indicate that vimentin induces a structural change in VN that destabilizes its intramolecular structure.

Fractal dimension analysis calculations were performed to determine the order and organization of imaged structures by AFM. Fractal dimension analysis of monomeric VN and VIM133 protein generates Db's of 1.32 ± 0.30, 1.11 ± 0.30 indicating that the images have no significant structural organization. The image of polymeric VN-VIM aggregates (Figure 4.6C&D) has a fractal Db value of 1.74 ± 0.21, 1.63 ± 0.70 exceeding the minimum Db value of 1.5 required for significant order and degree of organization and thus suggesting the polymeric structures contain a high degree of structural organization. Figures 4.6E&F also had Db values lower than 1.5, indicating that there was no major structural organization or pattern of multimerization.

4.5. Discussion

This study is a continuation of previous work describing the manner in which vitronectin mediates the binding of PAI-1 to the surface of activated platelets and PMP's by binding to exposed vimentin on the surface of activated platelets and PMP's [9]; moreover, the expression of vimentin and vitronectin on PMP's has been verified by proteomic analysis [23]. We provide further support for this mechanism with observations regarding the ultrastructure of PMP's and the nature of vimentin exposure. The source of PMP's for these experiments was platelet-poor plasma from expired platelet concentrates [24, 25] and platelet-poor plasma from post-acute myocardial infarction patients [26]. In summary, vimentin may become exposed when a PMP is
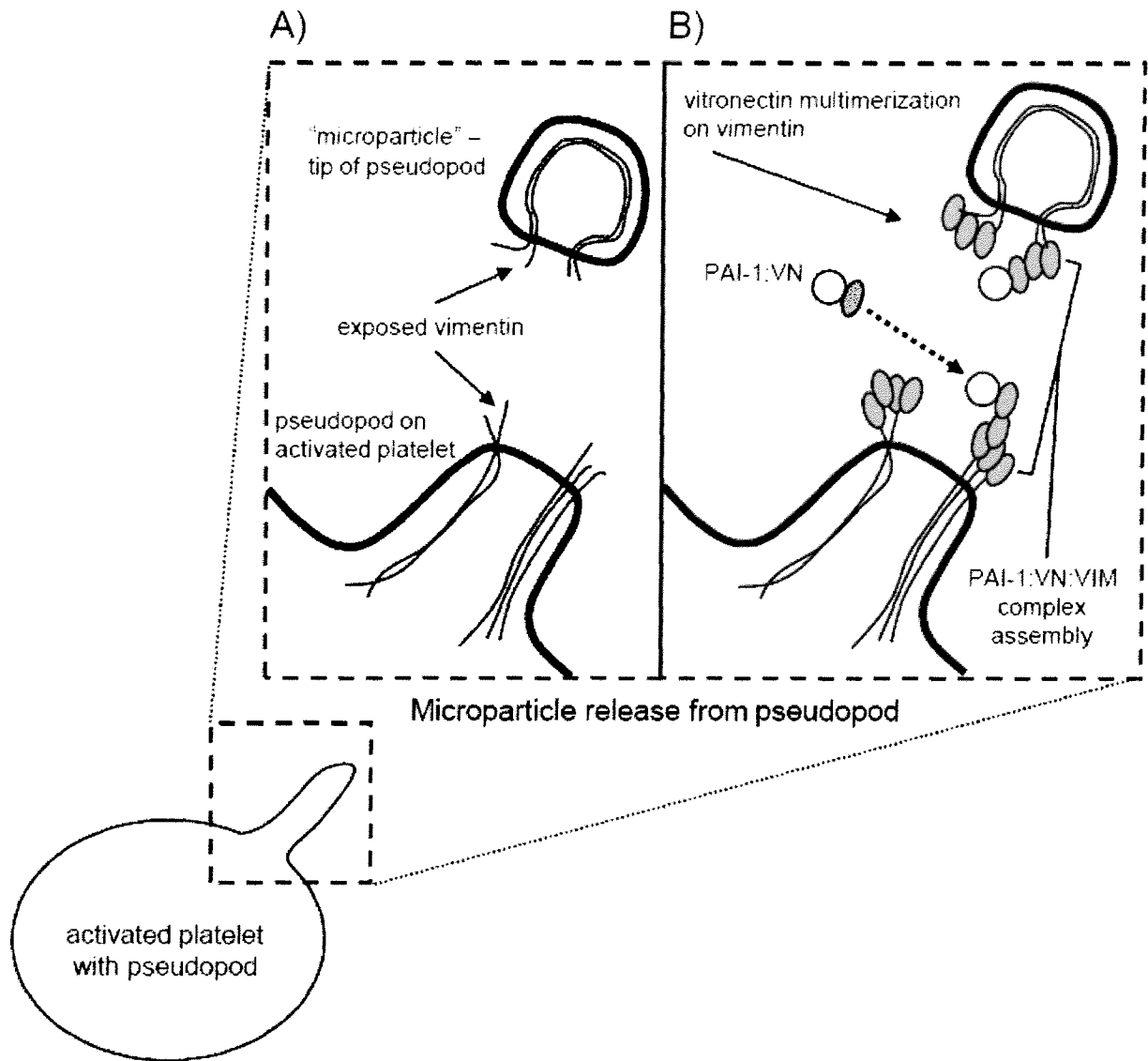
Figure 4.7. Proposed model of vimentin exposure on activated platelets and platelet microparticles and subsequent assembly of the PAI-1:VN:vimentin ternary complex. Microparticles can be released at the tip of pseudopods in activated platelets, A). We describe vimentin exposure at the interface of the broken junction between the pseudopod and PMP. This exposure of vimentin will cause plasma-derived VN to undergo multimerization, which will be followed by incorporation of either free PAI-1 or PAI-1:VN complexes to this multimerized VN. This assembly of ternary complex can occur on both the microparticle and activated platelet.

released from the pseudopod of an activated platelet, resulting in a broken junction between the two vesicular bodies. This broken junction can then lead to a very brief disruption of membrane at which there is exposure of vimentin cytoskeleton to the lumen. However, any membrane disruption will immediately re-seal due to the hydrophobic nature of the phospholipid tail in bilayer membranes, but some vimentin may become partially exposed as illustrated in a proposed model in Figure 4.7. Exposed vimentin on both the PMP and activated platelet becomes the assembly site of vitronectin multimerization and subsequent PAI-1 incorporation, hence the formation of the PAI-1:VN:vimentin ternary complexes. We have also visualized the ultrastructure of vimentin-vitronectin multimers in a cell-free environment to further understand the organization of the ternary complex when assembled on activated platelets and PMP's.

Despite the wealth of literature supporting PMP counts as a potential diagnostic marker, the ultrastructure of PMP's and their formation from platelets is somewhat unclear due to optical limitations of real-time imaging of microparticle release (diameter <1.0μm) from cells as small as platelets (diameter of approximately 3 μm). However, various reports utilizing scanning electron microscopy and confocal microscopy have described PMP formation occurring at the tip and/or median of platelet pseudopodia [18, 19, 27], as well as at the edge of the platelet body [28, 29]. Currently, flow cytometry is the primary methodology for high-throughput analysis of PMP's but this methodology is beset by a major caveat wherein the incident light (488 nm) and forward scatter detector in commercially available flow cytometry instruments do not accurately analyze and size particles with diameters smaller than the incident wavelength [30-33]. The angular distribution of light scatter from sub-micron particles analyzed by the 488nm incident light does not accurately yield consistent size readouts [31, 33]. However, impedance flow cytometry instruments can overcome this physical limitation to permit accurate quantification of

PMP size dimensions [34] and is based on a technology that is free of optical limitations. Despite the physical limitations associated with conventional flow cytometry, we performed a FACS isolation of CD41(+)ve particles with a diameter < 1.0 μm that expressed vimentin, vitronectin and PAI-1 which were then imaged by AFM to provide accurate morphological analysis.

Vimentin intermediate filaments are not normally present on the surface of viable cells. Vimentin intermediate filaments are intracellular with a cortical distribution underneath the cell membrane with intimate associations with microfilament and microtubule networks [35-37]. During platelet activation, cytoskeleton reorganization results in the formation of platelet pseudopods, as evidenced by filamentous rings at the greatest circumference of the pseudopod [38-40] and treatment with cytoskeleton inhibitors such as cytochalasin D can prevent pseudopod formation and microparticle formation [19, 41]. In this report, we isolated vimentin-positive PMP's from expired platelet concentrates and observed minor phospholipid membrane appendages attached to the base of the PMP as visualized by AFM. Topographically, the surfaces of these vesicles were smooth and continuous, with little suggestion of filament-like structures on their surface. We infer that these vesicles are the tips of pseudopods and the origin of vimentin lies at the base of the PMP between the phospholipid membrane flaps at the base of the PMP as visualized by AFM. In Figure 4.5, intermediate filament-like structures were observed within these membrane flaps, providing insight as to how vimentin may be exposed underneath the base of the PMP.

The membrane flaps observed via AFM are of artifactual nature, because the amphipathic nature of phospholipid molecules in aqueous solutions strongly dictates an arrangement that accommodates the non-polar hydrophobic tails so that they are oriented towards each other while

the polar hydrophilic heads are oriented outside. In the event of membrane disruption, gaps will quickly re-seal as hydrophobic tails rearrange themselves and membrane is reorganized to maintain surface continuity and minimize phospholipid tail interactions with water.

One key requirement for membrane sealing is the presence of free Ca^{2+}, in which Ca^{2+}-dependent exocytosis mechanisms within a cell recruit internal stores of phospholipid in the form of endomembranes to the cell surface, providing more phospholipid for re-sealing [42, 43]. However, PMP's formed in expired platelet concentrates contain citrate (~9 mM), which neutralizes the ability of Ca^{2+} to recruit and mobilize stores of endomembrane, if exists within the PMP to its surface [44]. Most importantly, PMP's formed *in vivo* will not express membrane appendages at their base because physiological concentrations of Ca^{2+} will contribute to resealing of membrane over or around vimentin. The membrane appendages visualized at the base of PMP's isolated in expired platelet concentrates (Figure 4.3) are artifactual due to: 1) the spreading of PMP membrane adjacent which is adjacent to exposed vimentin spreading on the mica coverslip and to a lesser extent, 2) storage conditions such as high citrate plasma concentrations that retard recruitment of phospholipid to the surface of PMP's. However, these artifacts have also provided some insight regarding a potential mechanism describing vimentin expression on PMP's and activated platelets.

The ultrastructure of *in vitro* formed VN-vimentin multimers revealed a tightly knit lattice structure that rapidly incorporated all free VN and vimentin molecules. The AFM is an excellent means to understand protein-protein interactions, particularly the manner in which vimentin can induce structural changes in VN, a normally globular protein stabilized by its di-sulfide bridges into a tertiary structure ~3 nm in height. It is concievable that the ionic interactions between the highly charged VIM133 peptide and VN resulted in the unravelling of

vitronectin into a more linear structure, thus resulting in a VN monomer height of <1.6nm. Furthermore, the unravelling of VN from a globular to a linear structure could reveal cryptic binding sites for other ligands. The AFM has the potential to explore these possibilities of how proteins can induce tertiary structure change without the use of epitope-specific antibodies combined with ELISA or surface plasmon resonance analysis. Considering that no structure in the VN-vimentin multimers produced a height >3nm, it is clear that vimentin is a key activator or "unraveling" agent for vitronectin and warrants further experimentation onto itself.

The VN-vimentin multimer is a tightly knit and highly organized lattice and resembled other similar patterns of VN and vimentin distribution as imaged by confocal and AFM on activated platelets expressing high amounts of VN and vimentin (Figure 4.6). In particular, the uniform fields of protein-like structures distributed over the surface of the vitronectin-rich platelet in Figure 4.5E are analogous to this tightly knit lattice. However, no such lattice-type structures are observed on VN-positive PMP's as imaged by AFM (Figure 4.3B and 4.4), indicating that activated platelets are more likely to present with VN-vimentin multimers due to a greater availability of vimentin on a cell much larger than a PMP. Although the lattice is highly organized, an obvious structural signature representing VN-vimentin multimers was not delineated. However, it can be concluded that PMP's may be limited in the amount of PAI-1 expressed on their surface because of the low proportion of vimentin that may be extracellularly presented, while activated platelets have both a higher capacity of vimentin extracellular presentation and a larger surface for which VN-vimentin multimers can spread out onto.

Vimentin exposure may be relevant when considered in the context of thrombus formation, in which PAI-1 is bound to the surface of activated platelets and PMP's by way of multimerized VN. Presumably, the extent of vimentin exposure dictates the amount of PAI-1

presentation within thrombi which will determine the extent of thrombus stabilization against plasminogen activators. It also dictates the amount of multimerized VN within the thrombus, possibly contributing to thrombus structural integrity by homotypic interactions with other cells or fibrin with multimerized VN on its surface [15]. Recent murine studies of intravital imaging models of photochemically-induced thrombosis have highlighted the requirement of VN for clot stabilization. Photochemically induced clots require more time to reach vessel occlusion in VN-/- mice and these clots are unstable and have earlier clot dissolution times compared to wild type models [45]. However, mice with both a VN-/- and PAI-1 -/- genotype generate comparable clot formation and clot lysis times when compared to VN-/- mice [46] but the basis for this similarity is still unclear. It was previously hypothesized that VN had dual contributory roles in inhibiting fibrinolysis as well as stabilizing thrombi by binding to integrins $\alpha_{IIb}\beta_3$ and $\alpha_5\beta_3$. The lack of variation between PAI-1-/- & VN-/- mice and their single gene knockout counterparts strongly suggests that VN plays a primary, if not central role in fibrinolysis and that perhaps absence of VN leads to inactive PAI-1 and subsequent lack of clot stabilization. These intravital studies also support the requirement of VN multimerization for the deposition of active PAI-1 onto the surface of activated platelets as a means to contribute to the stability of a growing thrombus during blood shear and plasminogen activator secretion by endothelium.

Due to the high affinity of PAI-1-VN complexes to vimentin intermediate filaments, thromboembolic fragments with high PAI-1 content can resist significant clot lysis despite treatment with thrombolytic therapy [47-50]. Moreover, PAI-1 present on platelet microparticles (PMP's) may act as a secondary pool of active PAI-1 and potentiate other downstream thrombogenic events due to their sub-micron size and clot stabilizing properties [9]. However, the extent of these clot stabilitory properties on activated platelets and platelet microparticles will

be dependent on the extent of VN-vimentin multimerization on the activated cell surface and the amount of PAI-1-VN incorporation into this ternary complex. Hence, the expression and proportion of ternary complex will differ between PMP's and activated platelet populations due to cell surface availability and vimentin exposure.

4.6. References for Chapter IV:

1.	Pandolfi A, Cetrullo D, Polishuck R, Alberta MM, Calafiore A, Pellegrini G, Vitacolonna E, Capani F, Consoli A. Plasminogen activator inhibitor type 1 is increased in the arterial wall of type II diabetic subjects. *Arterioscler Thromb Vasc Biol* 2001; 21:1378-82.

2.	Vaughan DE. PAI-1 and atherothrombosis. *J Thromb Haemost* 2005; 3:1879-83.

3.	Muller JE, Tofler GH, Stone PH. Circadian variation and triggers of onset of acute cardiovascular disease. *Circulation* 1989; 79:733-43.

4.	Kohler HP, Grant PJ. Plasminogen-activator inhibitor type 1 and coronary artery disease. *N Engl J Med* 2000; 342:1792-801.

5.	Hamsten A, de Faire U, Walldius G, Dahlen G, Szamosi A, Landou C, Blomback M, Wiman B. Plasminogen activator inhibitor in plasma: risk factor for recurrent myocardial infarction. *Lancet* 1987; 2:3-9.

6.	Sobel BE, Woodcock-Mitchell J, Schneider DJ, Holt RE, Marutsuka K, Gold H. Increased plasminogen activator inhibitor type 1 in coronary artery atherectomy specimens from type 2 diabetic compared with nondiabetic patients: a potential factor predisposing to thrombosis and its persistence. *Circulation* 1998; 97:2213-21.

7.	Gils A, Declerck PJ. Plasminogen activator inhibitor-1. *Curr Med Chem* 2004; 11:2323-34.

8.	Wun TC, Palmier MO, Siegel NR, Smith CE. Affinity purification of active plasminogen activator inhibitor-1 (PAI-1) using immobilized anhydrourokinase. Demonstration of the binding, stabilization, and activation of PAI-1 by vitronectin. *J Biol Chem* 1989; 264:7862-8.

9.	Podor TJ, Singh D, Chindemi P, Foulon DM, McKelvie R, Weitz JI, Austin R, Boudreau G, Davies R. Vimentin exposed on activated platelets and platelet microparticles localizes vitronectin and plasminogen activator inhibitor complexes on their surface. *J Biol Chem* 2002; 277:7529-39.

10.	Podor TJ, Campbell S, Chindemi P, Foulon DM, Farrell DH, Walton PD, Weitz JI, Peterson CB. Incorporation of vitronectin into fibrin clots. Evidence for a binding interaction between vitronectin and gamma A/gamma' fibrinogen. *J Biol Chem* 2002; 277:7520-8.

11.	Muszbek L, Adany R, Glukhova MA, Frid MG, Kabakov AE, Koteliansky VE. The identification of vimentin in human blood platelets. *Eur J Cell Biol* 1987; 43:501-4.

12. Franke WW, Schmid E, Osborn M, Weber K. Different intermediate-sized filaments distinguished by immunofluorescence microscopy. *Proc Natl Acad Sci U S A* 1978; 75:5034-8.

13. Franke WW, Schmid E, Osborn M, Weber K. Intermediate-sized filaments of human endothelial cells. *J Cell Biol* 1979; 81:570-80.

14. Dellagi K, Brouet JC. Redistribution of intermediate filaments during capping of lymphocyte surface molecules. *Nature* 1982; 298:284-6.

15. Wu YP, Bloemendal HJ, Voest EE, Logtenberg T, de Groot PG, Gebbink MF, de Boer HC. Fibrin-incorporated vitronectin is involved in platelet adhesion and thrombus formation through homotypic interactions with platelet-associated vitronectin. *Blood* 2004; 104:1034-41.

16. Katopodis JN, Kolodny L, Jy W, Horstman LL, De Marchena EJ, Tao JG, Haynes DH, Ahn YS. Platelet microparticles and calcium homeostasis in acute coronary ischemias. *Am J Hematol* 1997; 54:95-101.

17. Tan KT, Lip GY. The potential role of platelet microparticles in atherosclerosis. *Thromb Haemost* 2005; 94:488-92.

18. Hughes M, Hayward CP, Warkentin TE, Horsewood P, Chorneyko KA, Kelton JG. Morphological analysis of microparticle generation in heparin-induced thrombocytopenia. *Blood* 2000; 96:188-94.

19. Yano Y, Kambayashi J, Shiba E, Sakon M, Oiki E, Fukuda K, Kawasaki T, Mori T. The role of protein phosphorylation and cytoskeletal reorganization in microparticle formation from the platelet plasma membrane. *Biochem J* 1994; 299 (Pt 1):303-8.

20. Otsu N. A threshold selection method from gray-level histograms. *IEEE Trans. on Sys., Man, and Cybern* 1979; 9:62-66.

21. Frankel DJ, Pfeiffer JR, Surviladze Z, Johnson AE, Oliver JM, Wilson BS, Burns AR. Revealing the topography of cellular membrane domains by combined atomic force microscopy/fluorescence imaging. *Biophys J* 2006; 90:2404-13.

22. Guzman C, Jeney S, Kreplak L, Kasas S, Kulik AJ, Aebi U, Forro L. Exploring the mechanical properties of single vimentin intermediate filaments by atomic force microscopy. *J Mol Biol* 2006; 360:623-30.

23. Garcia BA, Smalley DM, Cho H, Shabanowitz J, Ley K, Hunt DF. The platelet microparticle proteome. *J Proteome Res* 2005; 4:1516-21.

24. Cauwenberghs S, van Pampus E, Curvers J, Akkerman JW, Heemskerk JW. Hemostatic and signaling functions of transfused platelets. *Transfus Med Rev* 2007; 21:287-94.

25. Keuren JF, Magdeleyns EJ, Govers-Riemslag JW, Lindhout T, Curvers J. Effects of storage-induced platelet microparticles on the initiation and propagation phase of blood coagulation. *Br J Haematol* 2006; 134:307-13.

26. van der Zee PM, Biro E, Ko Y, de Winter RJ, Hack CE, Sturk A, Nieuwland R. P-selectin- and CD63-exposing platelet microparticles reflect platelet activation in peripheral arterial disease and myocardial infarction. *Clin Chem* 2006; 52:657-64.

27. Reininger AJ, Heijnen HF, Schumann H, Specht HM, Schramm W, Ruggeri ZM. Mechanism of platelet adhesion to von Willebrand factor and microparticle formation under high shear stress. *Blood* 2006; 107:3537-45.

28. Cauwenberghs S, Feijge MA, Harper AG, Sage SO, Curvers J, Heemskerk JW. Shedding of procoagulant microparticles from unstimulated platelets by integrin-mediated destabilization of actin cytoskeleton. *FEBS Lett* 2006; 580:5313-20.

29. Rotman A, Makov N, Luscher EF. Isolation and partial characterization of proteins from platelet pseudopods. *Proc Natl Acad Sci U S A* 1982; 79:4357-61.

30. Furie B, Furie BC. Cancer-associated thrombosis. *Blood Cells Mol Dis* 2006; 36:177-81.

31. Hercher M, Mueller W, Shapiro HM. Detection and discrimination of individual viruses by flow cytometry. *J Histochem Cytochem* 1979; 27:350-2.

32. Steen HB. Flow cytometer for measurement of the light scattering of viral and other submicroscopic particles. *Cytometry A* 2004; 57:94-9.

33. Born M WE. Principles of Optics. New York: Pergamon, 1959:652ff.

34. Cheng X, Liu YS, Irimia D, Demirci U, Yang L, Zamir L, Rodriguez WR, Toner M, Bashir R. Cell detection and counting through cell lysate impedance spectroscopy in microfluidic devices. *Lab Chip* 2007; 7:746-55.

35. Ho CL, Martys JL, Mikhailov A, Gundersen GG, Liem RK. Novel features of intermediate filament dynamics revealed by green fluorescent protein chimeras. *J Cell Sci* 1998; 111 (Pt 13):1767-78.

36. Esue O, Carson AA, Tseng Y, Wirtz D. A direct interaction between actin and vimentin filaments mediated by the tail domain of vimentin. *J Biol Chem* 2006; 281:30393-9.

37. Kuroda M, Porter KR. Cytoskeleton in vitro: preparation of isolated cytoskeletons with three-dimensional architecture. *J Biochem (Tokyo)* 1987; 101:1413-27.

38. Schliwa M. Action of cytochalasin D on cytoskeletal networks. *J Cell Biol* 1982; 92:79-91.

39.   Debus E, Weber K, Osbom M. The cytoskeleton of blood platelets viewed by immunofluorescence microscopy. *Eur J Cell Biol* 1981; 24:45-52.

40.   Taylor RG, Lewis JC. Microfilament reorganization in normal and cytochalasin B treated adherent thrombocytes. *J Supramol Struct Cell Biochem* 1981; 16:209-20.

41.   Carroll RC, Butler RG, Morris PA, Gerrard JM. Separable assembly of platelet pseudopodal and contractile cytoskeletons. *Cell* 1982; 30:385-93.

42.   Terasaki M, Miyake K, McNeil PL. Large plasma membrane disruptions are rapidly resealed by Ca2+-dependent vesicle-vesicle fusion events. *J Cell Biol* 1997; 139:63-74.

43.   Steinhardt RA, Bi G, Alderton JM. Cell membrane resealing by a vesicular mechanism similar to neurotransmitter release. *Science* 1994; 263:390-3.

44.   Hirayama J, Azuma H, Fujihara M, Homma C, Yamamoto S, Ikeda H. Storage of platelets in a novel additive solution (M-sol), which is prepared by mixing solutions approved for clinical use that are not especially for platelet storage. *Transfusion* 2007; 47:960-5.

45.   Reheman A, Gross P, Yang H, Chen P, Allen D, Leytin V, Freedman J, Ni H. Vitronectin stabilizes thrombi and vessel occlusion but plays a dual role in platelet aggregation. *J Thromb Haemost* 2005; 3:875-83.

46.   Koschnick S, Konstantinides S, Schafer K, Crain K, Loskutoff DJ. Thrombotic phenotype of mice with a combined deficiency in plasminogen activator inhibitor 1 and vitronectin. *J Thromb Haemost* 2005; 3:2290-5.

47.   Zunker P, Schick A, Padro T, Kienast J, Phillips A, Ringelstein EB. Tissue plasminogen activator and plasminogen activator inhibitor in patients with acute ischemic stroke: relation to stroke etiology. *Neurol Res* 1999; 21:727-32.

48.   Nicholls SC, Hoffer EK, Chandler WL. Failure of peripheral arterial thrombolysis due to elevated plasminogen activator inhibitor type 1. *Blood Coagul Fibrinolysis* 2003; 14:729-33.

49.   Huber K. Plasminogen activator inhibitor type-1 (part two): role for failure of thrombolytic therapy. PAI-1 resistance as a potential benefit for new fibrinolytic agents. *J Thromb Thrombolysis* 2001; 11:195-202.

50.   Potter van Loon BJ, Rijken DC, Brommer EJ, van der Maas AP. The amount of plasminogen, tissue-type plasminogen activator and plasminogen activator inhibitor type 1 in human thrombi and the relation to ex-vivo lysibility. *Thromb Haemost* 1992; 67:101-5.

CHAPTER V: VIMENTIN AUTO-ANTIBODIES INDUCE PLATELET ACTIVATION AND FORMATION OF PLATELET-LEUKOCYTE CONJUGATES VIA PLATELET-ACTIVATING FACTOR

5.1. Introduction

Auto-antibodies to the intermediate filament vimentin are associated with rheumatoid arthritis (1), systemic lupus erythematosus (SLE) (2-4) and rejection of solid organ transplants (5-9). Vimentin is a cytoskeleton intermediate filament protein present in cells of mesenchymal origin; these include leukocytes, endothelial cells and smooth muscle cells. More recently, vimentin has been observed on the cell surface of apoptotic cells (10-12) and thrombin-activated platelets (13). The production of anti-vimentin antibodies (AVA) in certain diseases is probably caused by excessive exposure to vimentin on apoptotic cells, since it is known that caspase dependent cleavage of vimentin, with exposure of vimentin on the cell surface, are necessary requisites for apoptosis (14). The functions of AVA are unknown, and in particular whether they have an active role in disease pathogenesis.

Prevalence of coronary artery disease in SLE patients is high, with heightened states of immune activation and pro-thrombotic activity thought to be key contributory factors to disease pathogenesis in these patients (15). Lupus autoantibodies have been implicated as observed by immune deposits present in kidney and heart (16). In the context of transplantation, AVA have been associated with a different type of atherosclerosis, namely graft vascular disease (GVD) (9). GVD is the most common complication following heart or renal transplantation; it is

---

characterized by intimal occlusion and fibrosis of donor arteries and veins (17;18).

A pro-coagulant microvasculature is associated with pathogenesis of GVD. The presence of fibrin deposition (19) and depletion of t-PA (20) in the microvessels of the heart, is predictive of heart transplant recipients who will develop GVD. Similarly, deposition of the complement component C4d within allografts is characteristic of GVD (21). These studies suggest that synergy between thrombotic events and complement fixing antibodies contribute to GVD and possibly to atherosclerosis in patients with autoimmune diseases. We hypothesize that antibodies to the autoantigen vimentin, particularly of the IgM subclass, may interact with vimentin expressing platelets with possible pathogenic consequences. This hypothesis was tested *in vitro,* by adding AVA to normal whole blood, platelet-rich plasma and leukocyte-rich plasma, and investigating its effect on formation of platelet/leukocyte conjugates and platelet microparticles.

5.2. Materials and Methods:

5.2.1. Blood collection and patient serum

MHC (major histocompatibility complex) Class I HLA A2+ve A3-ve subtype individuals consented to provide normal whole blood which was collected into 4.5mL CTAD tubes and then diluted 1/10X in Tyrodes buffer. Platelet-rich plasma (PRP) was obtained by collecting the supernatant fraction of blood centrifuged at 200g for 10mins. Post-transplant serum collected from cardiac transplant recipients for diagnostic reasons was used with permission from Royal Brompton and Harefield Hospital ethics committee and University of British Columbia ethics board. Patient serum had been screened for presence of anti-vimentin and HLA antibodies as previously described (9;22).

5.2.2. Preparation of recombinant human vimentin

The cDNA for human vimentin was isolated from a human umbilical vein endothelial cell cDNA expression library by PCR, introducing a 5' NdeI restriction site and a BamHI site at the 3' end of the cDNA (Primers: forward 5' ATA GAG CAT ATG TCC ACC AGG TCC GTG TCC; reverse 5' GCG CTC GGA TCC TCT TAT TCA AGG TCA TCG TG). The PCR product was sub-cloned into NdeI / BamHI of pET15b (Novagen; Merck Biosciences, Nottingham, UK), a bacterial expression vector, and transformed into BL21 *E.coli* (BL21/vimentin; Novagen). Crude preparations of recombinant human vimentin were prepared and extracted according to the pET System Manual (Novagen) and purified on a His-Bind resin column under denaturing conditions, using a His-Bind Purification Kit (Novagen). Purification was confirmed by SDS PAGE (a single band at 58kD was observed) and mass spectrometry (not shown).

5.2.3. Depletion of AVA's from patient sera

Recombinant human vimentin protein (1 mg/mL in 6 M urea, preparation) was conjugated to agarose beads as described in kit instructions (AminoLink Plus Immobilization Kit). Vimentin-conjugated agarose beads (50μL) were incubated with 50 μL of patient serum at 25°C overnight and then centrifuged at 1000g for 10mins and the supernatant fraction and was collected, termed depleted patient serum. ELISA assays [10] demonstrated that this treatment reduced AVA titres to ~15% of original titres (Mean non-depleted 1061±52.9; mean depleted 160±29.3).

5.2.4. Flow cytometry and monoclonal antibodies (mAb)

Equal amounts (25 μg/mL final concentration) of mAb mouse IgM antibody (to A2, A3, from One Lambda), anti-vimentin antibodies (AVA) 13.2-IgM, V9-IgG (both mouse anti-human - Sigma) or sheep anti-vimentin (Affinity Biologicals) were added to 20μL of diluted (1/10X) whole blood and incubated at 37°C for 30 or 45mins. 20μL of patient sera was added to 20μL of diluted blood for 30 or 45mins. CD41-RPE, C3d-FITC, or fibrinogen-FITC antibodies (mouse anti-human, rabbit anti-human, rabbit anti-human respectively - BD Biosciences) at a final concentration of 25μg/ml were used to label each sample to detect platelets and expression of C3d or fibrin. CD62P-APC (mouse anti-human - BD Biosciences) and tissue factor-FITC antibodies (rabbit anti-human - American Diagnostica) were also added to blood at similar concentrations. Isotype controls, FITC rabbit IgG (Beckman Coulter), APC-mouse IgG1 (Beckman Coulter) and RPE-mouse IgG1 (BD Biosciences), were added at the same concentrations. To label leukocytes, Hoechst 33342 (Molecular Probes) diluted in PBS (1 μg/L

final concentration) was subsequently added for another 30mins. Labelled leukocytes were identified as 'Hoechst-positive cells' during flow cytometric analysis. To track binding of mAb IgM antibodies in whole blood, FITC-donkey-anti-mouse IgM (Sigma) was added at a final concentration of 25 µg/mL. In order to determine numbers of vimentin-positive cells in whole blood, 13.2 IgM was added to washed buffy coat leukocytes. Washing buffy coat leukocytes were resuspended in 100µL of PBS, to which 13.2 IgM was added at a final concentration of 25 µg/mL. After 30 mins incubation at 4°C, cells were washed again and FITC-goat anti-mouse IgM was added (final concentration 10 µg/mL) for another 30 mins at 4°C. Cells were analyzed using a BD FACS-Aria instrument with 405, 488 and 635 nm single line lasers was used and >30,000 events were analyzed for every sample. Measurement of platelet microparticles was performed using 1.0 µm beads (Invitrogen cat#F13080). The PAF inhibitor, CV-6209, was obtained from Calbiochem (Nottingham, UK).

5.2.5. Complement dependent cytotoxic assay on AVA treated purified leukocytes

To prevent contamination by platelets, a modified method of purifying leukocytes was performed. Normal blood was collected into acid citrate dextrose tubes (BD Biosciences) and leukocyte-rich preparation (LRP) was prepared by centrifugation of 10 mL of whole blood for 10 minutes at 200g and the platelet rich plasma (PRP) supernatant removed. An additional 1.0 mL of Tyrodes buffer was added to the remaining whole blood, mixed by inversion and then centrifuged again under the same conditions. The supernatant was again removed and remaining blood was lightly layered onto Lympholyte H solution (Cedarlane Labs, Hornby, ON) in a 15 mL Falcon tube. This was centrifuged at 200g for 20 minutes. Upon centrifugation, four layers were present and a Pasteur pipette was used to suction out the leukocyte layer (typically 2 mL

from a 10 mL whole blood preparation). This layer was centrifuged at 200g for 5 minutes to remove residual platelets which was confirmed by flow cytometry. The supernatant containing platelets was discarded and the pellet was resuspended in modified Tyrodes buffer. Flow cytometry demonstrated that these leukocytes were ~60% neutrophils; the remainder were monocytes and lymphocytes and used for two tests, the cytotoxic assay and preparation of supernatants from AVA activated neutrophils.

Leukocytes were diluted with modified Tyrodes buffer to 5×10^5 cells/μL and 1μL aliquots were placed in single wells of a Terasaki plate. To these were added 1 μL of HLA-A2 IgM, HLA-A3 IgM or 13.2-IgM antibody (0.5 μg/mL) in each well in duplicate. After 30mins, 5μL of rabbit complement (Cedarlane Labs) was added and incubated for another 30mins. Cell viability was assessed by adding 2μL of FluoroQuench (One Lambda) to each well. A Zeiss inverted microscope fitted with a QImaging Retiga EXi colour cooled camera and QCapture Pro software (QImaging Inc.) was used to acquire images. A live/dead filter set (Chroma Technology Corp) was used to visualize the ethidium bromide and acridine orange viability stains in which viable cells demonstrated a fluorescent green nuclear signal and dead cells demonstrated a fluorescent orange nuclear signal.

5.3. Results:

5.3.1. Effect of monoclonal and patient AVA's on whole blood

Treatment of whole blood with AVA 13.2-IgM resulted in a depletion of platelet counts (determined by numbers of CD41-positive cells) as well as an increase in %platelet:leukocyte conjugates (calculated as a percentage of CD41+Hoechst cells/ Hoechst-positive cells) compared

to whole blood treated with AVA V9-IgG antibody or not (Figs 5.1A vs. 5.1B&C). The effect of AVA 13.2 IgM was inhibited in the presence of recombinant human vimentin (Fig 5.1D).

Fibrinogen and C3d deposition was evaluated on leukocytes and platelets before and after treatment with AVA 13.2 IgM. Post AVA13.2-IgM treatment, fibrin(-ogen) expression on leukocytes increased from $9.6\pm1.3\%$ to $33.0\pm8.6\%$ and fibrin(-ogen)expression on platelets increased from $7.8\pm1.2\%$ to $89.3\pm2.2\%$ (Fig 5.1E). When assessing C3d expression, increases from $12.9\pm2.1\%$ to $59.2\pm6.3\%$ on leukocytes and increases from $4.2\pm1.2\%$ to $41.1\pm13.6\%$ were observed after AVA 13.2-IgM treatment (Fig 5.1E). Control experiments showed that AVA 13.2 IgM treated blood cells do not non-specifically bind FITC rabbit IgG (Fig 5.1F&G). These results demonstrate that whole blood treatment with AVA induces platelet:leukocyte (P:L) conjugate formation, and deposition of fibrin and C3d on platelets and leukocytes. For negative control, A3 IgM did not induce deposition of fibrin and C3d on platelets and leukocytes (data not shown).

To compare the activity of the AVA monoclonal with AVA from transplant patient sera, normal blood was then treated with patient sera containing high titre IgM AVA (mean titre 1061 ± 52.9) or the same sera depleted of AVA (mean titre 160 ± 29.3), using vimentin coated agarose beads. These sera did not contain alloantibodies of AVA of the IgG subclass. Patient sera containing high AVA titre lead to a decrease in the ratio of free platelets to leukocytes compared to whole blood treated with control serum or sera depleted of AVA IgM (Fig 5.2A). In Fig 5.2B, an increase in platelet/leukocyte conjugates was observed when whole blood was treated with patient sera with high AVA IgM compared to normal blood incubated with control serum (from a transplant patient negative for AVA) or sera depleted of AVA IgM. To control for the possibility that vimentin coated beads may remove immunoglobulin non-specifically, we
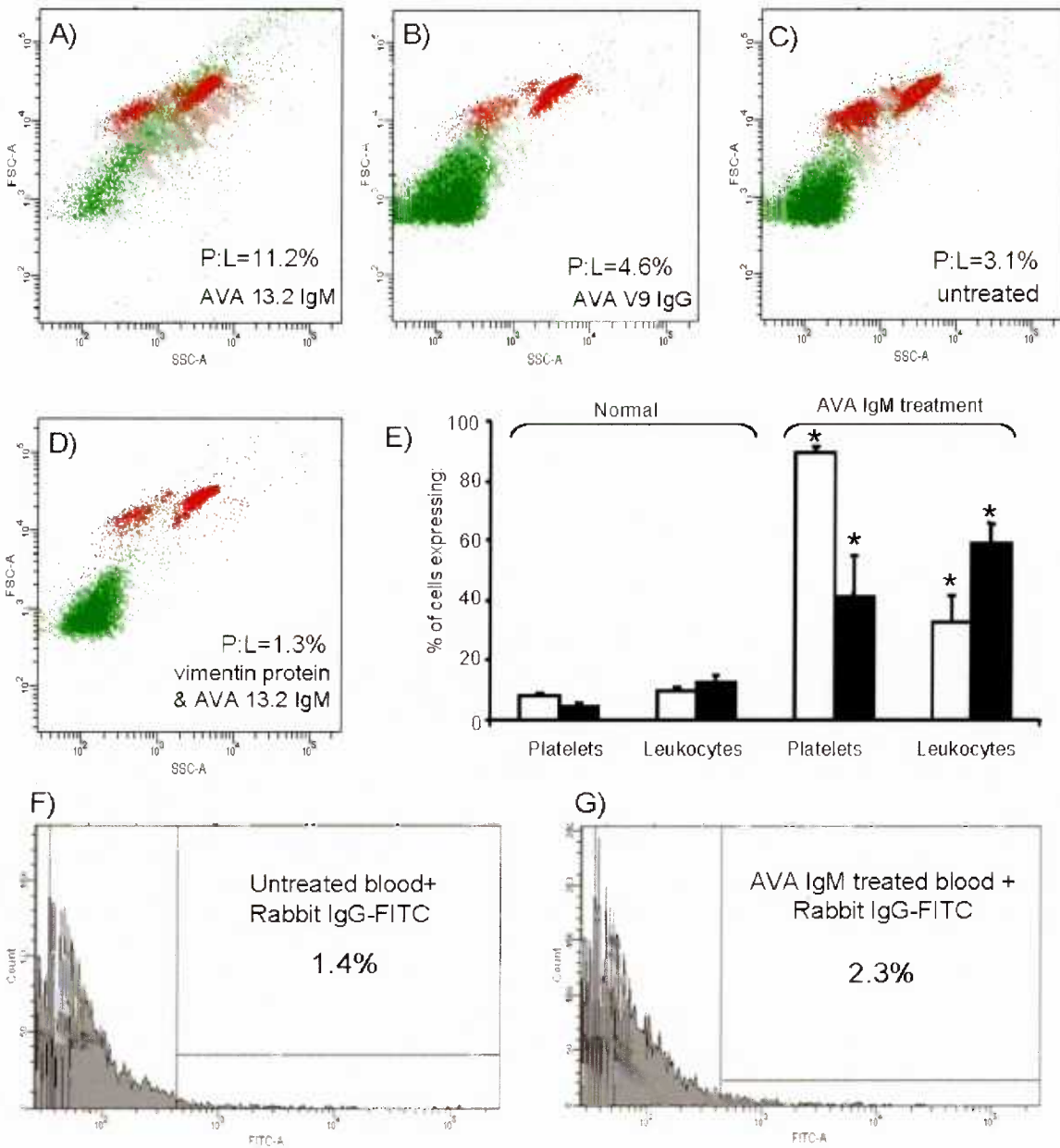
Figure 5.1. AVA monoclonals induce platelet:leukocyte conjugate formation and surface expression of C3d and fibrinogen. Figures 5.1A-D are forward/side scatter plots of blood under different treatments incubated for 30 mins. The green population represents platelets; the red represents nucleated leukocytes. Incubation with 13.2 IgM (A) resulted in platelet depletion and P:L conjugate formation, whereas incubation with V9 IgG (B) gave similar results to untreated (C) blood. P:L conjugate formation induced by 13.2 IgM was inhibited by recombinant vimentin protein+13.2 IgM (D). Figure 5.1E summarizes data on the percentage of platelets and leukocytes expressing fibrinogen (white bars) and C3d (black bars), before and after AVA IgM treatment. Representative of 5 experiments. *denotes (compared to no treatment, p<0.05; t-test, 2-tailed) compared to untreated.
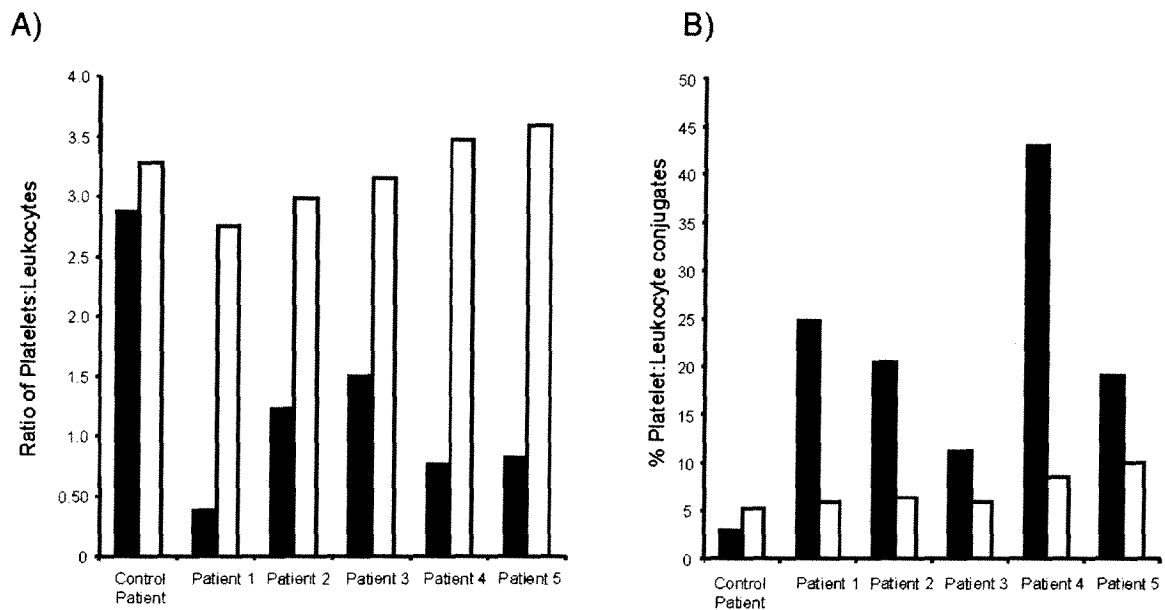
Figure 5.2. Patient sera with anti-vimentin autoantibodies (AVA's) induce platelet activation and formation of platelet:leukocyte conjugates. Normal blood was treated with patient sera containing high titre AVA (filled bars), control serum (labelled control patient), or the same patient sera depleted of AVA using agarose coated beads (unfilled bars) for 30 mins. In A), the extent of platelet activation was characterized by the ratio of CD41-positive cells to Hoechst-positive cells. In B), formation of platelet:leukocyte conjugates was characterized by the percentage of cells co-expressing Hoechst+CD41 over the total number of Hoechst-positive cells.

treated patient serum known to contain high titres of antibodies to HLA (human leukocyte antigens) with vimentin coated agarose beads, this had no effect on the HLA antibody titre (not shown). These results demonstrate that the AVA's in patients' sera can also induce formation of P:L conjugates.

5.3.2. Effect of other IgM antibodies on whole blood

In view of the fact that the AVA V9 IgG had no effect on platelets and that the majority of transplant patients produce IgM and not IgG AVA (9), the remainder of the study focused on IgM antibodies. We next determined whether the effect of AVA was comparable to the effects seen with IgM antibodies to another cell surface ligand such as the Major Histocompatibility Complex (MHC) antigen subtypes, HLA-A2 and HLA-A3. All leukocytes express MHC antigens. Hence, AVA 13.2-IgM was tested against two other IgM mAbs specific for HLA-A2 and HLA-A3 and blood used for these experiments were from individuals who were HLA-A2 positive and HLA-A3 negative. Treatment of whole blood with AVA 13.2-IgM and HAL-A2 IgM resulted in significant P:L conjugate formation (Fig 5.3A,B), compared to untreated blood (Fig 5.3D). The HLA-A3 antibody had no effect on blood from the HLA-A2 positive individual (Fig 5.3C). Upon flow cytometric analysis (Fig 5.3E), the percentage of P:L conjugates were higher in whole blood treated with AVA13.2-IgM (17.2±2.6%) and HLA-A2 IgM (64.3±2.7%) compared to treatment with HLA-A3 IgM (4.8±0.5%) and endogenous levels in untreated whole blood (5.9±0.5%). In order to investigate the phenotype of platelets attached to leukocytes,
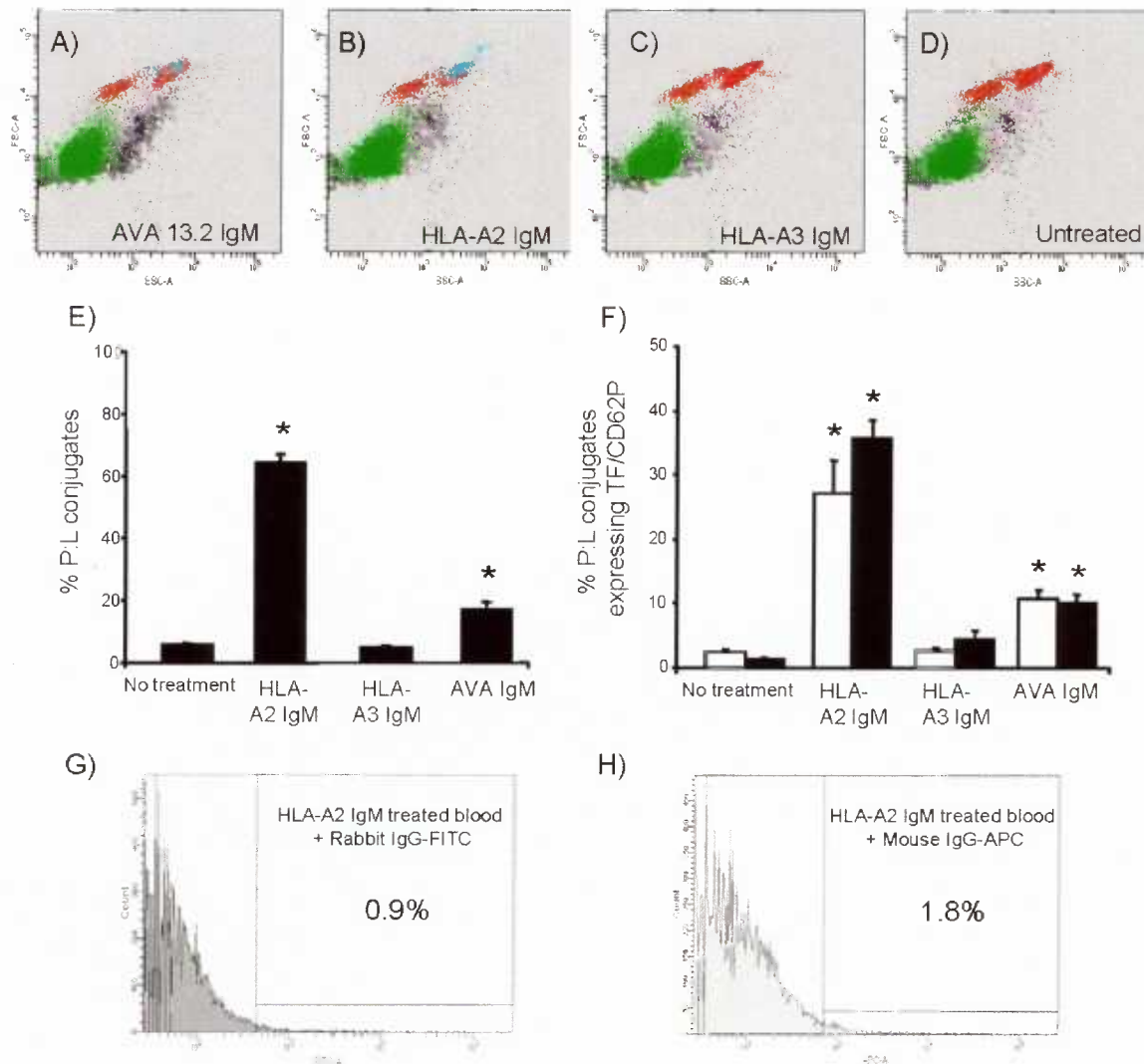
Figure 5.3. AVA- and HLA- IgM's induce platelet:leukocyte conjugates which express tissue factor and P-selectin. Whole blood was either treated with AVA 13.2 (A) A2 IgM (B) A3 IgM (C) or untreated (D). The effects of IgM treatment on platelets and leukocytes were expressed as forward/side scatter plots in Panels A-D (the blue area indicates P:L conjugates, the red population indicates nucleated cells, the green population indicates platelets, and the black population represents activated platelets that did not bind the CD41 antibody). Panel E summarizes the extent of platelet:leukocyte conjugate formation in all four groups. Panel F summarizes the extent of tissue factor(+)ve (white bars) and P-selectin(+)ve (black bars) platelet:leukocyte conjugates in all four groups. Both E and F summarize experiments performed four times. *denotes (compared to no treatment, $p < 0.05$; t-test) compared to untreated.

expression of P-selectin and tissue factor was examined on platelets within P;L conjugates. After HLA-A2 IgM treatment, 27.2±5.1% and 35.6±2.9% of platelets within P:L conjugates were tissue factor and P-selectin positive (Fig 5.3F). Following AVA 13.2 IgM treatment, 10.8±1.3% and 10.1±1.2% of platelets within P;L conjugates were also tissue factor and P-selectin positive respectively (Fig 5.3F). In contrast, untreated whole blood and HLA-A3 IgM treated whole blood, which contained few P:L conjugates had very few platelets that were also positive for tissue factor or P-selectin (<5%). Addition of HLA-A2 or 13.2 IgM antibody to whole blood did not cause non-specific binding of FITC rabbit IgG or APC-mouse IgG respectively (Fig 5.3G&H for HLA-A2 IgM), data not shown for 13.2 IgM AVA.

5.3.3. Effect of AVA IgM and anti-HLA-A2 IgM on purified platelets

In order to compare the effects of IgM antibodies on platelets in the absence of leukocytes, platelet rich plasma (PRP) was used. In Fig 5.4, panels A-D show forward/side scatter plots from a single experiment to illustrate formation of platelet microparticles after addition of AVA and anti-HLA IgM antibodies to PRP. Platelet microparticles (PMP) are released by activated platelets and are characterized as exhibiting significant CD41-PE signal with a forward scatter less than a 1.0 μm bead particle. Platelets were unaffected by AVA 13.2- and HLA-A3 IgM treatments but addition of HLA-A2 IgM induced platelet microparticle formation. In Fig 5.4E, the results of 4 experiments are summarized. Analysis of normal platelet-rich plasma yielded 11.0±1.1% PMP, indicating that ~11% of CD41-PE positive particles in the sample were of microparticle size and morphology. When this plasma was treated with AVA 13.2 IgM, the %PMP at 4.8±0.8% was lower than the %PMP observed in PRP. Treatment with HLA-A2 IgM resulted in 40.0±7.5% PMP, presumably a result of
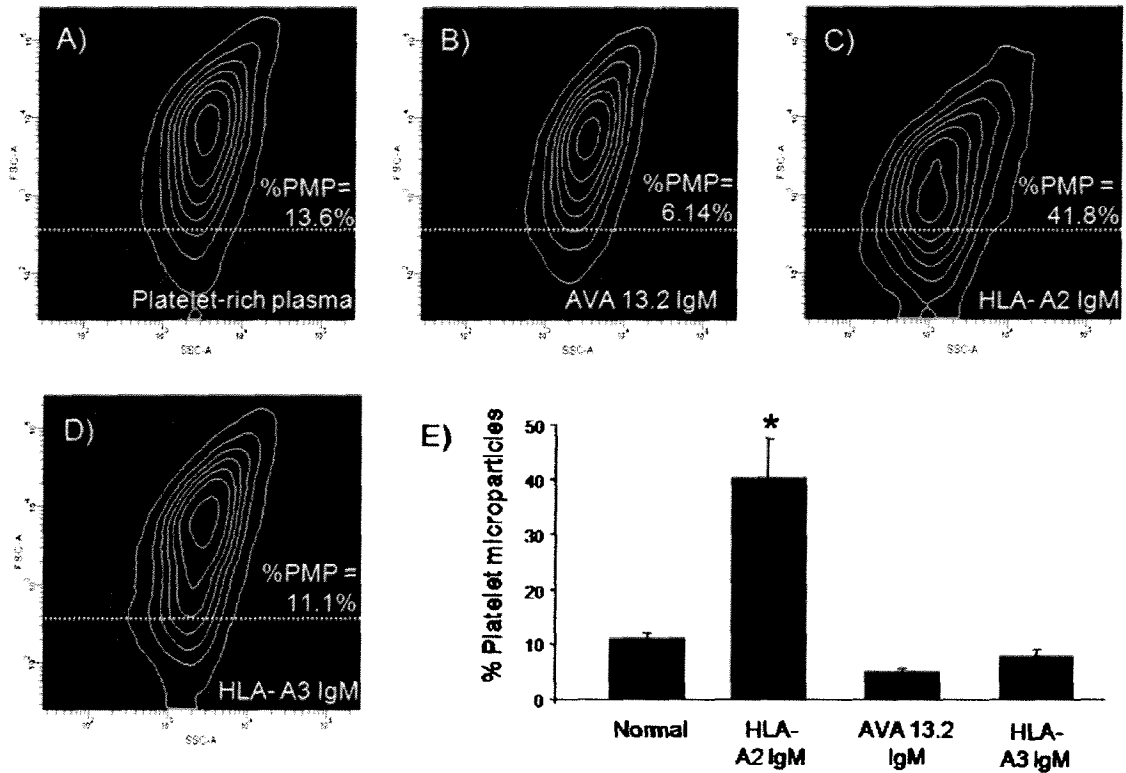
Figure 5.4. AVA-IgM does not directly induce platelet activation. Panels A-D are forward/side scatter plots in a density contour format. Results of platelet activation are expressed as "% PMP"; in which # of CD41-positive particles with a diameter below 1.0μm, over the total number of CD41-positive events. Results of %PMP after treatment of PRP with 13.2 IgM(B), A2 (C) and A3 IgM(C) compared to untreated (A) for 30 mins are summarized in (E). Representative of 4 experiments. * denotes (p<0.05; t-test) compared to normal treatment.

complement-mediated lysis by the HLA-A2 IgM (23). Treatment of PRP with the A3-IgM resulted in 7.9±1.3%, a level similar to untreated PRP. These observations strongly suggest that unlike A2-IgM, the 13.2 IgM has a negligible effect on resting platelets which are negative for cell surface vimentin, but constitutively express MHC class I antigens. Overall, the results suggest that the platelet depletion observed in the whole blood and not in PRP by AVA-IgM were caused by an initial interaction of AVA-IgM with leukocytes with no platelets binding to them; subsequently leading to platelet activation and vimentin surface expression on platelets.

5.3.4. Effect of anti-vimentin antibodies (AVA) on purified neutrophils

To determine which leukocytes in whole blood bind the various mAb IgM antibodies, anti-mouse IgM-FITC secondary antibody was used to track localization of HLA-A2 IgM, HLA A3 IgM and AVA 13.2 IgM antibodies which had been added to whole blood (Fig 5.5A-D). HLA-A2 IgM was found to bind to all leukocytes (Fig 5.5A). In contrast, the HLA-A3 IgM was not found to specifically bind to any cell population (Fig 5.5B). The 13.2-IgM antibody was shown to specifically bind to monocytes, neutrophils, and activated platelets (Fig 5.5C), as determined by the light scattering properties of these cells. Minimal binding of the secondary antibody alone was observed in untreated blood (Fig 5.5D). These results were confirmed by addition of AVA 13.2 IgM to washed buffy coat leukocytes, followed by FITC anti-mouse IgM (Fig 5.5E), in which it can be seen that approximately 15% of leukocytes binded to AVA 13.2 IgM. These vimentin-positive cells were predominantly of neutrophil identity as determined
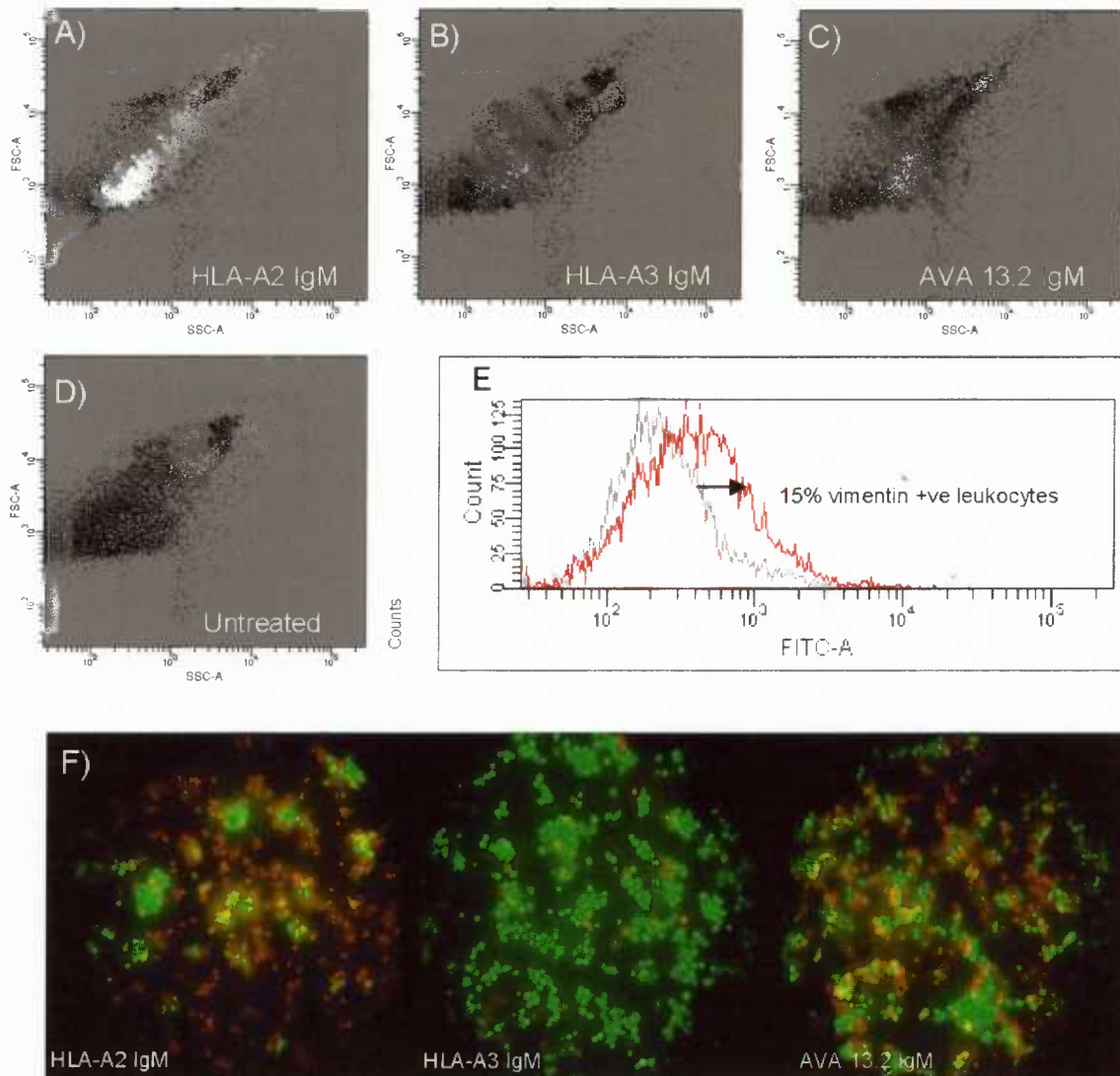
Figure 5.5. Localization of IgM to granulocytes and activated platelets and their cytotoxic effect on leukocytes. FITC goat anti-mouse IgM was added to whole blood to track A2 IgM (A), A3 IgM (B) and 13.2 IgM AVA (C) or untreated blood (D). The white population denotes cells with positive IgM binding. Representative of 3 experiments. Panel E presents flow cytometry of whole blood to which has the polyclonal sheep anti-vimentin antibody has been added to normal whole blood. A2 IgM, A3 IgM and 13.2 IgM were added to purified leukocytes and incubated with excess complement to induce antibody-mediated cell death (F). Viability was assessed by ethidium bromide/acridine orange labelling of treated cells. Representative of 3 experiments.

by their light scattering properties. Hence, a subpopulation of leukocytes expressing vimentin are the potential binding site for AVA-IgM antibodies.

In order to determine whether AVA were cytotoxic and could mediate complement dependent cell lysis, purified leukocytes from an HLA-A2 positive individual were incubated with AVA 13.2-IgM, HLA-A2 IgM or HLA-A3 IgM in the presence of exogenous rabbit complement (Fig 5.5F); not surprisingly, incubation with HLA-A2 IgM, resulted in >75% cell death and incubation with HLA-A3 IgM resulted in minimal cell death. Interestingly, the AVA 13.2-IgM induced substantial cell death (~50-75%) upon addition of excess exogenous complement. Patient sera containing high AVA titres (but negative for antibodies to HLA antigens) were also tested for complement dependent cytotoxicity; 18/21 sera were cytotoxic for leukocytes (killing 20-100% of cells), in contrast 12/54 sera without AVA showed leukocytotoxic activity (data not shown).

5.3.5. Supernatant of AVA-activated leukocytes induces platelet activation

To determine if AVA-bound granulocytes release mediators that subsequently activate platelets, leukocytes were purified and treated with AVA13.2-IgM, HLA-A2 IgM or HLA A3 IgM for 30 mins and the supernatant was transferred to purified platelets (PRP). Platelet activation was assessed by generation of platelet microparticles (PMP) at 30 mins. Supernatant from HLA-A3 IgM did not result in significant PMP formation (Fig 5.6B) compared to untreated control (Fig 5.6A). Supernatant from leukocytes treated with AVA 13.2-IgM resulted in substantial platelet microparticle formation (Fig 5.6C). Quantitative data from these experiments are presented in Fig 5.6E. The large amount of PMPs generated by transfer of supernatant from HLA-A2 IgM treated leukocytes is probably partially due to carry over of HLA-A2 IgM

antibody, which causes direct activation of HLA-A2 positive resting platelets (Fig 5.4C). Although the supernatant from AVA 13.2 IgM treated neutrophils contains both released inflammatory mediators and the AVA IgM, we demonstrated previously (Fig 5.4B,E) that the AVA IgM alone does not have an activating effect on platelets. Hence, the activation observed in Fig 5.6C indicates activation is due to the released inflammatory mediators and not the AVA 13.2 IgM.
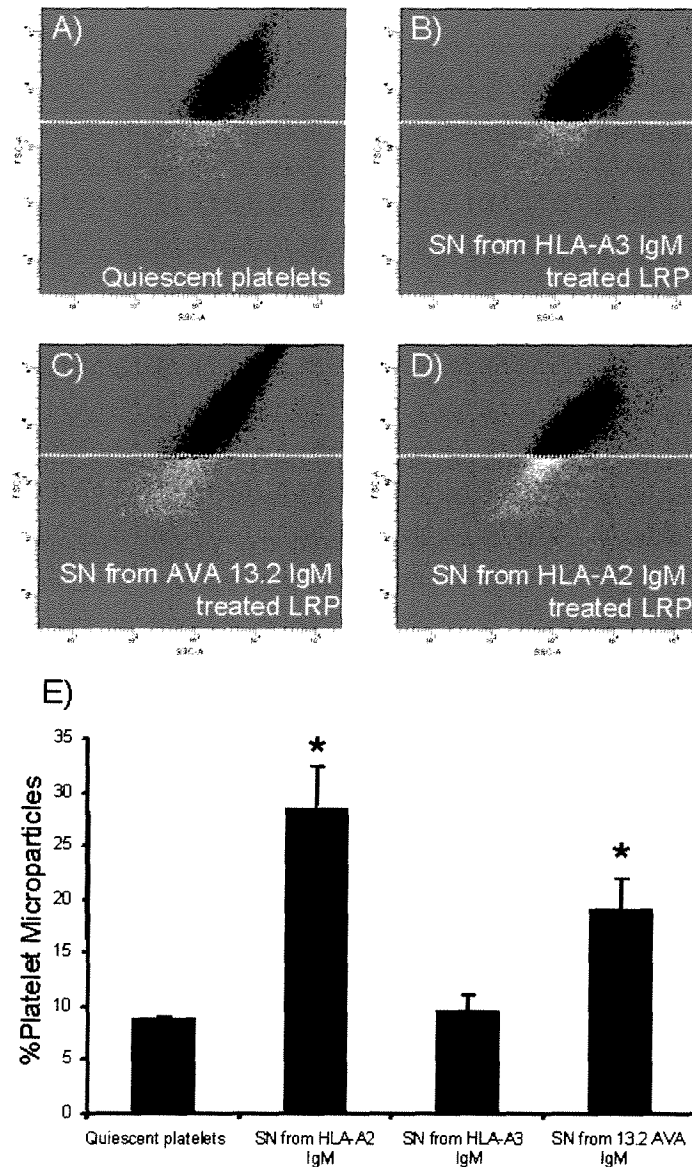
Figure 5.6. **Effect of supernatant (SN) from IgM treated leukocytes on platelet activation.** Results are expressed as an analysis of platelet particles according to size and only CD41+ particles are presented above. Data points in black are CD41-positive, and data points in white are CD41-positive cells with a forward scatter lower than a 1.0 μm diameter fluorescent counting bead, which are considered to be platelet microparticles. Panel A shows untreated platelets. In B), SN from A3-IgM treatment did not result in platelet microparticle formation greater than control (A). Treatment of PRP with SN from AVA-IgM resulted in platelet aggregation and PMP formation (C), while SN from A2-IgM resulted in the highest generation of platelet microparticles compared to all treatments. Quantitative data shown in E. Representative of 3 experiments. * denotes (p<0.05; t-test) compared to no treatment.

102

5.3.6. AVA IgM-bound leukocytes release PAF

The previous experiments demonstrated that AVA binding to neutrophils results in release of factor(s) that cause platelet activation and formation of PMP's, one of which may be Platelet-Activating Factor (PAF). To test this hypothesis, blood was briefly pretreated with CV-6209, an inhibitor of the PAF receptor (PAFR) at a final concentration of $1\mu M$ before being incubated with AVA13.2-IgM. Preliminary experiments had shown that 1uM CV-6209 is sufficient to produce 100% inhibition of thrombin mediated platelets activation (not shown). After 45 minutes of IgM incubation, normal blood treated with the AVA13.2-IgM demonstrated platelet depletion (Fig 7B), but when CV-6209 pre-treated blood was incubated with AVA 13.2-IgM, platelet counts were not depleted and were similar to levels found in untreated blood (Fig 7C,D). Interestingly, although PAF-inhibition prevented disappearance of whole platelets, it did not prevent them becoming covered in C3d (Fig 7E).
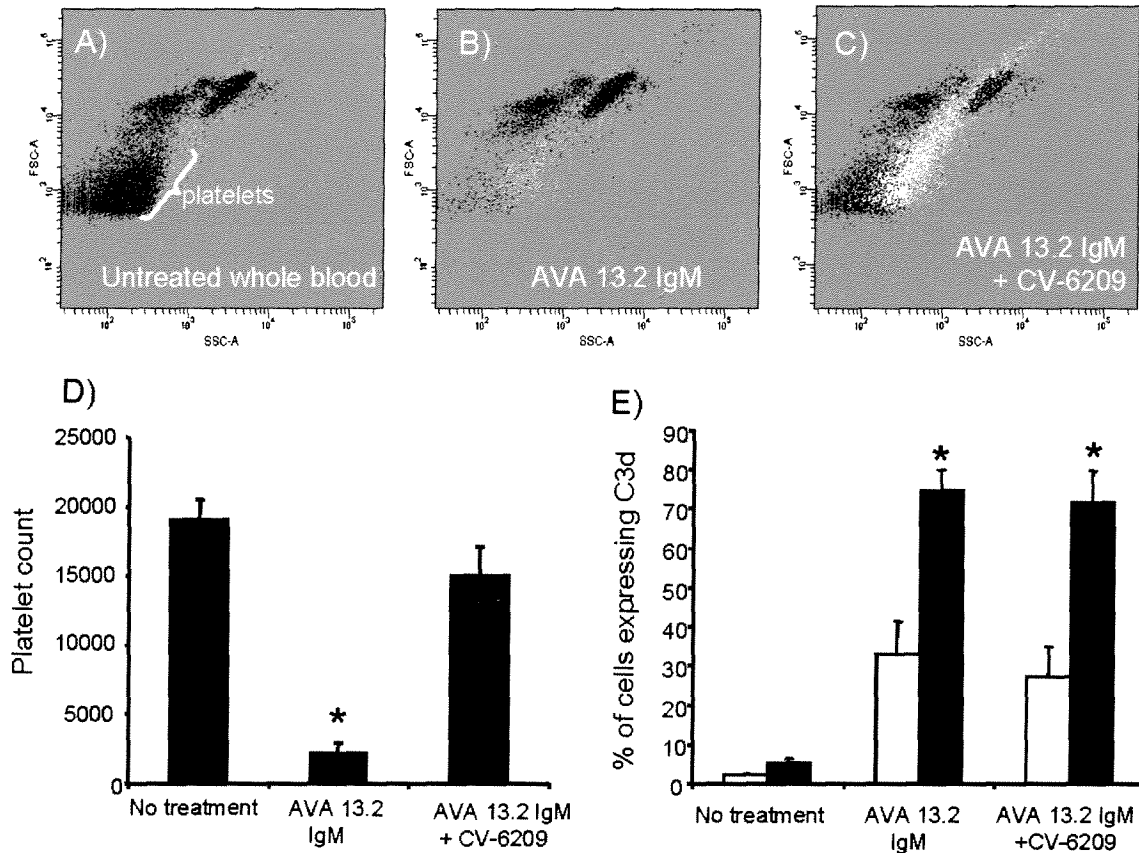
Figure 5.7. **PAF inhibition attenuates platelet activation and blood cell agglutination.** Whole blood was untreated (A), or incubated for 45 minutes with 13.2 IgM AVA in the absence (B) or presence (C) of the PAF receptor inhibitor CV-6209. Flow cytometry of treated blood was used to determine platelet depletion (summarized in D) and C3d expression (summarized in E, where white bars represent leukocytes and black bars represent platelets). The white coloured data points in scatterplots A-C represents platelets with C3d-positive signal, and the position of platelets is marked as a bracket in (A). Pretreatment of whole blood with CV-6209 attenuated platelet depletion, but an increase in C3d deposition on platelets was still observed (A vs. C). Platelet counts were determined by analyzing 5000 leukocyte events for each sample. Representative of 4 experiments. * denotes (p<0.05; t-test) compared to no treatment.

104

5.6. Discussion:

Anti-vimentin antibodies have been described in a number of diverse conditions including autoimmunity (1;2;24), chronic infections (25), and clinical rejection of solid organ allografts (5-9). It has been recently demonstrated that vimentin immunised mice undergo accelerated rejection of their cardiac allografts (26) but the mechanisms were not elucidated. This is the first study to demonstrate interactions between IgM anti-vimentin antibodies and leukocytes and suggest a mechanism for their pathogenicity. The study was initiated by the observation that activated platelets express cell surface vimentin (13) leading us to hypothesize that AVA would have an effect on platelet activation or thrombosis. Treatment of normal whole blood with the AVA13.2-IgM monoclonal resulted in platelet:leukocyte conjugate formation and depletion of platelet counts. This was accompanied by induction of P-selectin on platelets attached to leukocytes (Fig3F), and deposition of fibrinogen, C3d and tissue factor on platelets and leukocytes. P-selectin is known to be a crucial molecule in P:L conjugate formation (27). That these effects can be produce by patient's antibodies was demonstrated by use of serum from cardiac transplant recipients, which were selected on the basis of their high IgM AVA titre; when these serum samples were depleted of AVA's, the formation of platelet:leukocyte conjugates was prevented and platelet counts were unaffected.

To compare the effects of the AVA IgM to other antibodies known to bind to platelets, IgM molecules specific for HLA antigens were chosen. Antibodies to A2, but not A3 had an effect on blood from an A2 individual, confirming the importance of the antigen binding part of the IgM molecule and discounting the possibility that IgM antibodies could non-specifically activate platelets to form P:L conjugates. Experiments using purified platelets as opposed to whole blood described an important difference between A2-IgM and AVA-IgM, namely that

only anti-HLA antibodies bind to purified platelets and AVA IgM did not. This is not surprising, since it is known that only activated and not quiescence platelets express surface vimentin (13). Podor et al. also described vimentin expression on platelet microparticles (13); this would explain the decrease in %PMP observed when AVA 13.2 IgM was added to purified platelets (Figs 4A,B). We suggest that AVA IgM binds to the vimentin-positive PMPs in normal platelet-rich plasma, resulting in complement-mediated lysis and further degradation of platelet microparticles.

Using whole blood and a secondary antibody detecting 13.2-IgM, it was determined that AVA's bind to approximately 12 % of circulating neutrophils; this has been verified by Moisan et al who described a similar number of vimentin positive neutrophils in normal blood and demonstrated them to be spontaneously apoptosing neutrophils (28). We have not formally proven that the neutrophils that bind 13.2 IgM are undergoing apoptosis, but in view of the literature describing the presence of vimentin on apotosing cells of various types (10;12;29), this seems a probable explanation for the association between AVA and neutrophils. The possibility that AVA's bind to neutrophils that subsequently release factors to activate resting platelets was confirmed by using supernatant from AVA treated leukocytes and adding it to platelets and observing PMP formation. Thus, platelet activating factor (PAF) was implicated as a primary factor leading to platelet activation because it can be rapidly synthesized and released by activated neutrophils. In our studies leukocytes expressed tissue factor following AVA treatment of whole blood (Fig 3F); this is also likely to have originated from activation of neutrophils by AVA (30;31); however, unlike PAF which has direct platelet agonist effects Tissue Factor does not directly activate platelets (32). PAF binds to Platelet-Activating Factor Receptor (PARF) present on platelets and leukocytes (33). Upon PAF binding, calcium channels are opened,

initiating activation of the platelet.   In our experiments, although the platelet count was normal

with the inhibitor, platelets were still expressing C3d; this is probably because the PAF inhibitor

did not affect release of activating factors from the neutrophils, but inhibited opening of the

calcium channels necessary for cell lysis. It is unlikely that PAF is the only mediator released by

AVA-activated granulocytes. In summary, we hypothesize that AVA induce platelet activation

and PMP formation via four stages; 1) activation of neutrophils and release of platelet activating

factors, expression of tissue factor 2) induction of P-selectin, vimentin and tissue factor on

platelets 3) binding of fibrinogen to activated platelets (via GPII$_b$III$_a$) and formation of P:L

conjugates and 4) binding of AVA to activated platelets and generation of PMP's. The latter

process is likely to be mediated by complement as demonstrated by the presence of C3d on

platelets and ability of AVA to fix complement and cause leukocyte lysis *in vitro* (Fig 5C).

Previous studies have shown sensitivity of platelets to complement mediated lysis (23;34). We

have not yet formally demonstrated the complement dependence of this process using

complement inhibitors.

The formation of platelet:leukocyte conjugates by AVA is an observation that sheds light

on possible hemostatic mechanisms leading to GVD development in allografts. It may also be

important for atherosclerotic disease progression in autoimmune diseases such as SLE, which are

characterised by AVA. When platelet:leukocyte conjugates are formed, the effectiveness of

these leukocytes to roll and tether to activated endothelium is substantially increased (35;36).

The release of tissue factor or its expression on activated granulocytes may also potentiate T-cell

activation (37) alongside its pro-coagulation effects.

This study has described effects of IgM AVA on leukocytes which are antigen dependent.

In 1984, Hansson et al. demonstrated Fc dependent binding of non-specific IgG to vimentin

exposed on the surface of damaged endothelial cells (38); in the current study the failure of V9 to bind to senescent neutrophils. The fact that A3-IgM and A2-IgM behave in a different way to 13.2-IgM and the fact that vimentin coated agarose beads deplete only AVA from patients serum (and not IgG HLA antibodies) argues against vimentin acting as a general Fc receptor for circulating immunoglobulin. Whether IgG AVA interact with leukocytes in a similar manner warrants further investigation.

It is interesting to speculate that the effects of AVA's described here, *in vitro*, may be partly responsible for the neutropenia and thrombocytopenia typically present in lupus patients. Indeed the effects of AVA on vimentin positive senescent neutrophils, may be analogous to the effect of anti-neutrophil cytoplasmic autoantibodies which are associated with specific forms of systemic vasculitis (39). In the latter case, it is known that cytokine treatment exposes these autoantigens proteinase-3 and myeloperoxidase on the neutrophil surface, although the *in vivo* stimulus of such exposure is not known. In conclusion, the mechanism we describe here may reflect a novel mechanism of how autoantibodies lead to thrombosis and atherosclerosis.

5.7   References for Chapter V

1. Vossenaar, E. R., Despres, N., Lapointe, E., van der, H. A., Lora, M., Senshu, T., van Venrooij, W. J., Menard, H. A. (2004) Rheumatoid arthritis specific anti-Sa antibodies target citrullinated vimentin. *Arthritis Res.Ther.* **6**, R142-R150.

2. Thebault, S., Gilbert, D., Hubert, M., Drouot, L., Machour, N., Lange, C., Charlionet, R., Tron, F. (2002) Orderly pattern of development of the autoantibody response in (New Zealand White x BXSB)F1 lupus mice: characterization of target antigens and antigen spreading by two-dimensional gel electrophoresis and mass spectrometry. *J.Immunol.* **169**, 4046-4053.

3. Senecal, J. L., Rothfield, N. F., Oliver, J. M. (1982) Immunoglobulin M autoantibody to vimentin intermediate filaments. *J Clin.Invest* **69**, 716-721.

4. Li, Q. Z., Xie, C., Wu, T., Mackay, M., Aranow, C., Putterman, C., Mohan, C. (2005) Identification of autoantibody clusters that best predict lupus disease activity using glomerular proteome arrays. *J Clin.Invest* **115**, 3428-3439.

5. Azimzadeh, A. M., Pfeiffer, S., Wu, G. S., Schroder, C., Zhou, H., Zorn, G. L., III, Kehry, M., Miller, G. G., Rose, M. L., Pierson, R. N., III (2005) Humoral immunity to vimentin is associated with cardiac allograft injury in nonhuman primates. *Am.J Transplant.* **5**, 2349-2359.

6. Carter, V., Shenton, B. K., Jaques, B., Turner, D., Talbot, D., Gupta, A., Chapman, C. E., Matthews, C. J., Cavanagh, G. (2005) Vimentin antibodies: a non-HLA antibody as a potential risk factor in renal transplantation. *Transplant.Proc.* **37**, 654-657.

7. Danskine, A. J., Smith, J. D., Stanford, R. E., Newell, H., Rose, M. L. (2002) Correlation of anti-vimentin antibodies with acute and chronic rejection following cardiac transplantation. *Hum.Immunol.* **63**, S30-S31.

8. Jonker, M., Danskine, A., Haanstra, K., Wubben, J., Kondova, I., Kuhn, E. M., Rose, M. (2005) The autoimmune response to vimentin after renal transplantation in nonhuman primates is immunosuppression dependent. *Transplantation* **80**, 385-393.

9. Jurcevic, S., Ainsworth, M. E., Pomerance, A., Smith, J. D., Robinson, D. R., Dunn, M. J., Yacoub, M. H., Rose, M. L. (2001) Antivimentin antibodies are an independent predictor of transplant-associated coronary artery disease after cardiac transplantation. *Transplantation* **71**, 886-892.

10. Nakanishi, K., Maruyama, M., Shibata, T., Morishima, N. (2001) Identification of a caspase-9 substrate and detection of its cleavage in programmed cell death during mouse development. *J Biol.Chem.* **276**, 41237-41244.

11. Rose, M. L. (2004) De novo production of antibodies after heart or lung transplantation should be regarded as an early warning system. *J Heart Lung Transplant* **23**, 385-395.

12. Rosen, A., Casciola-Rosen, L. A. (1999) Autoantigen as substrates for apoptopic proteases:implications for the pathogenesis of systemic autoimmune diseases. *Cell Death Diff* 6, 6-12.

13. Podor, T. J., Singh, D., Chindemi, P., Foulon, D. M., McKelvie, R., Weitz, J. I., Austin, R., Boudreau, G., Davies, R. (2002) Vimentin exposed on activated platelets and platelet microparticles localizes vitronectin and plasminogen activator inhibitor complexes on their surface. *J.Biol.Chem.* 277, 7529-7539.

14. Morishima, N. (1999) Changes in nuclear morphology during apoptosis correlate with vimentin cleavage by different caspases located either upstream or downstream of Bcl-2 action. *Genes Cells* 4, 401-414.

15. Frostegard, J. (2005) SLE, atherosclerosis and cardiovascular disease. *J Intern.Med.* 257, 485-495.

16. D'Andrea, D. M., Coupaye-Gerard, B., Kleyman, T. R., Foster, M. H., Madaio, M. P. (1996) Lupus autoantibodies interact directly with distinct glomerular and vascular cell surface antigens. *Kidney Int.* 49, 1214-1221.

17. Chapman, J. R., O'Connell, P. J., Nankivell, B. J. (2005) Chronic renal allograft dysfunction. *J Am.Soc.Nephrol.* 16, 3015-3026.

18. Ramzy, D., Rao, V., Brahm, J., Miriuka, S., Delgado, D., Ross, H. J. (2005) Cardiac allograft vasculopathy: a review. *Can.J Surg.* 48, 319-327.

19. Labarrere, C. A., Nelson, D. R., Faulk, W. P. (1998) Myocardial fibrin deposits in the first month after transplantation predict subsequent coronary artery disease and graft failure in cardiac allograft recipients. *Am.J.Med.* 105, 207-213.

20. Labarrere, C. A., Pitts, D., Nelson, D. R., Faulk, W. P. (1995) Vascular tissue plasminogen activator and the development of coronary artery disease in heart-transplant recipients. *N.Engl.J.Med.* 333, 1111-1116.

21. Minami, K., Murata, K., Lee, C. Y., Fox-Talbot, K., Wasowska, B. A., Pescovitz, M. D., Baldwin, W. M., III (2006) C4d deposition and clearance in cardiac transplants correlates with alloantibody levels and rejection in rats. *Am.J Transplant.* 6, 923-932.

22. Newell, H., Smith, J. D., Rogers, P., Birks, E., Danskine, A. J., Fawson, R. E., Rose, M. L. (2006) Sensitization following LVAD implantation using leucodepleted blood is not due to HLA antibodies. *Am.J Transplant.* 6, 1712-1717.

23. Sims, P. J., Faioni, E. M., Wiedmer, T., Shattil, S. J. (1988) Complement proteins C5b-9 cause release of membrane vesicles from the platelet surface that are enriched in the membrane receptor for coagulation factor Va and express prothrombinase activity. *J Biol.Chem.* 263, 18205-18212.

24. Sato, Y., Matsumori, A., Sasayama, S. (1994) Autoantibodies against vimentin in a murine model of myocarditis. *Autoimmunity* **18**, 145-148.

25. Yang, Y., Fujita, J., Bandoh, S., Ohtsuki, Y., Yamadori, I., Yoshinouchi, T., Ishida, T. (2002) Detection of antivimentin antibody in sera of patients with idiopathic pulmonary fibrosis and non-specific interstitial pneumonia. *Clin.Exp.Immunol* **128**, 169-174.

26. Mahesh, B., Leong, H. S., McCormack, A., Sarathchandra, P., Holder, A., Rose, M. L. (2007) Autoantibodies to vimentin cause accelerated rejection of cardiac allografts. *Am.J Pathol.* **170**, 1415-1427.

27. Larsen, E., Celi, A., Gilbert, G. E., Furie, B. C., Erban, J. K., Bonfanti, R., Wagner, D. D., Furie, B. (1989) PADGEM protein: a receptor that mediates the interaction of activated platelets with neutrophils and monocytes. *Cell* **59**, 305-312.

28. Moisan, E., Girard, D. (2006) Cell surface expression of intermediate filament proteins vimentin and lamin B1 in human neutrophil spontaneous apoptosis. *J Leukoc.Biol.* **79**, 489-498.

29. Boilard, E., Bourgoin, S. G., Bernatchez, C., Surette, M. E. (2003) Identification of an autoantigen on the surface of apoptotic human T cells as a new protein interacting with inflammatory group IIA phospholipase A2. *Blood* **102**, 2901-2909.

30. Maugeri, N., Brambilla, M., Camera, M., Carbone, A., Tremoli, E., Donati, M. B., de, G. G., Cerletti, C. (2006) Human polymorphonuclear leukocytes produce and express functional tissue factor upon stimulation. *J Thromb.Haemost.* **4**, 1323-1330.

31. Nakamura, S., Imamura, T., Okamoto, K. (2004) Tissue factor in neutrophils: yes. *J Thromb.Haemost.* **2**, 214-217.

32. Orfeo, T., Butenas, S., Brummel-Ziedins, K. E., Mann, K. G. (2005) The tissue factor requirement in blood coagulation. *J Biol.Chem.* **280**, 42887-42896.

33. Centemeri, C., Colli, S., Tosarello, D., Ciceri, P., Nicosia, S. (1999) Heterogeneous platelet-activating factor (PAF) receptors and calcium increase in platelets and macrophages. *Biochem.Pharmacol.* **57**, 263-271.

34. Sims, P. J., Rollins, S. A., Wiedmer, T. (1989) Regulatory control of complement on blood platelets. Modulation of platelet procoagulant responses by a membrane inhibitor of the C5b-9 complex. *J Biol.Chem.* **264**, 19228-19235.

35. Ludwig, R. J., Schultz, J. E., Boehncke, W. H., Podda, M., Tandi, C., Krombach, F., Baatz, H., Kaufmann, R., von Andrian, U. H., Zollner, T. M. (2004) Activated, not resting, platelets increase leukocyte rolling in murine skin utilizing a distinct set of adhesion molecules. *J Invest Dermatol.* **122**, 830-836.

36. Esposito, C. J., Popescu, W. M., Rinder, H. M., Schwartz, J. J., Smith, B. R., Rinder, C. S. (2003) Increased leukocyte-platelet adhesion in patients with graft occlusion after peripheral vascular surgery. *Thromb.Haemost.* **90**, 1128-1134.

37. Shrivastava, S., McVey, J. H., Dorling, A. (2007) The interface between coagulation and immunity. *Am.J Transplant.* **7**, 499-506.

38. Hansson, G. K., Starkebaum, G. A., Benditt, E. P., Schwartz, S. M. (1984) Fc-mediated binding of IgG to vimentin-type intermediate filaments in vascular endothelial cells. *Proc.Natl.Acad.Sci.U.S.A* **81**, 3103-3107.

39. Pankhurst, T., Savage, C. O. (2006) Pathogenic role of anti-neutrophil cytoplasmic antibodies in vasculitis. *Curr.Opin.Pharmacol.* **6**, 190-196.

CHAPTER VI: CONCLUSIONS AND FUTURE DIRECTIONS

6.1 Overall themes of dissertation

In this dissertation, I present data on the dissection of the intracellular and extracellular fates of a ternary complex composed of vimentin, vitronectin and PAI-1. First, I constructed a fluorescent form of PAI-1 to track the intracellular localization of the anti-fibrinolytic component of the ternary complex within cells such as megakaryocytes (MEG-01 cell line) and endothelial cells (Eahy926 cell line). I later determined that the majority of synthesized PAI-1 did not bind to the surface of megakaryocytes post-thrombin activation but did bind to the surface of activated endothelial cells. Previous to these observations, we demonstrated that PAI-1 synthesized by endothelial cells was organized into storage granules that also contained vWF and P-selectin. This was a novel observation, as previous work had shown that PAI-1 was not compartmentalized to a storage granule, but was instead loosely dispersed within the cytoplasm of transfected endothelial cells and megakaryocytes. It was previously determined that PAI-1 was bound to the surface of activated cells such as platelets and platelet microparticles by first binding to vitronectin (VN) in PAI-1:VN complexes, the VN mediating its localization to exposed vimentin on the cell surface. Hence, it became important to understand the mechanism of vimentin exposure on activated endothelial cells and platelets.

A morphological analysis ensued whereby a novel technique was devised to visualize surfaces of platelets and platelet microparticles at a high resolution (nanometer level) to identify vimentin and multimers of vitronectin as sites of ternary complex assembly. Using a combination of FACS and atomic force microscopy, only PMP's expressing CD41a and a combination of PAI-1, VN and vimentin were isolated and individually imaged. AFM morphological analysis revealed platelet microparticles with a diameter range from 350-800 nm,

and surface morphology differed between PMP's isolated from expired platelet concentrates or from AMI-patient plasma. PMP's from expired platelet due to Platelet Storage Lesion (PSL) concentrates demonstrated continuous, smooth surfaces with sparse protein distribution whereas PMP's from patient-AMI plasma demonstrated a highly irregular and decorated surface characterized by protein distribution. The surface morphology of PMP's generated by PSL reflects their *in vitro* origin and instrinsic mechanism of activation whereas PMP's in patient-AMI plasma are generated *in vivo* and thus more susceptible to association with other plasma proteins such as acute phase proteins, coagulation proteins such as fibrin and Factor VII, as well as interactions with apoptotic or necrosed cells and their releaseates. In contrast, PMP's formed *in vitro* by platelet storage lesion present with far less surface irregularities, likely due to the lack of possible binding partners released in an activated *in vivo* setting. Another key observation was membrane flap-like appendages that extended from the base of vimentin positive PMP's of which some contained intermediate filament structures as verified by AFM. The height dimension of these membrane flaps corresponded to previous AFM measurements of phospholipid bilayer membrane of ~5 nm.

We have also uncovered a mechanism of how vimentin can induce vitronectin activation as determined from the cell-free experiments with purified VN and VIM133 peptide and AFM. The purified VN imaged by AFM demonstrated a height of 3 nm, presumably the native and inactive conform of VN. However, addition of VIM133 peptide which contains extensive regions of basic amino acid residues, caused the formation of VN-vimentin multimers with a maximum observed height of 1.6 nm, a noticeable lack of 3 nm VN monomer structures. These observations also hold true for conditions in which molar ration of VN:vimentin was 3:2 or 6:1. In Figure 6.1, we propose a mechanism of how VN activation may occur via the unraveling of

the VN molecule when the basic resides of VIM133 ionically interact with the 340-380 aa region of VN that contains acidic residues, thus revealing the basic resides contained in 50-100 aa on VN. This unravelling and subsequent exposure of basic resides can induce further destabilization of intramolecular ionic bonds in another VN molecule, inducing co-operative binding between VN to induce VN multimerization.
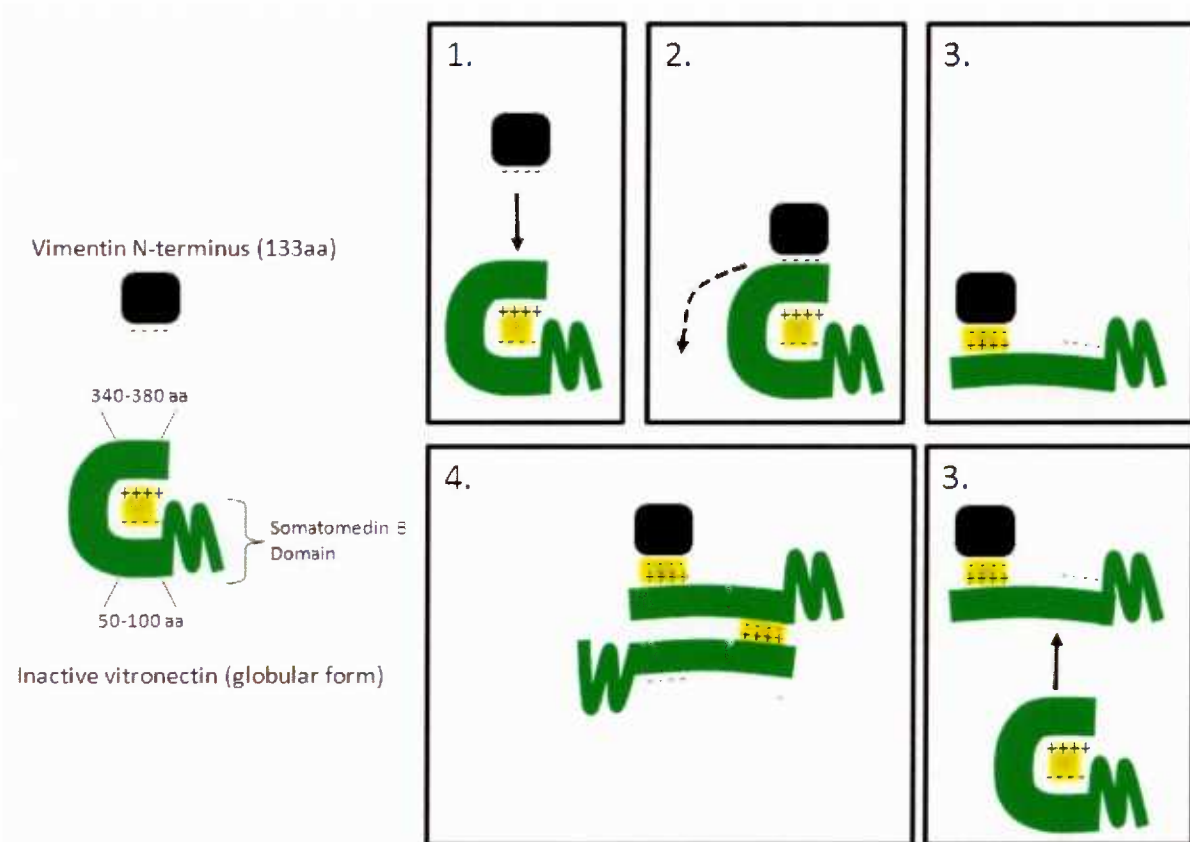
Figure 6.1. Proposed mechanism of vimentin-induced vitronectin multimerization.
Vitronectin contains a region of basic amino acids (50-100 aa) and a region of acidic amino acids (340-380 aa) that interacts in an ionic binding interaction that contributes to folding and its globular tertiary structure. When the region of basic amino acids on vimentin interacts with the acidic region on VN, it may induce a major conformational change such that the VN molecule "unravels" and in doing so, reveals the endogenous basic amino acid region to other inactive VN, subsequently inducing further "unravelling" on another inactive VN, thus propagating VN-VN interactions to the extent of VN multimerization.

From the observations made in Chapters III and IV, I propose a model that supports our initial hypothesis of how the ternary complex is assembled on activated platelets and platelet microparticles in Figure 6.2. Essentially, the model describes how the ternary complex is formed at the sites of microparticle release whereby vimentin cytoskeleton of platelet pseudopods that release PMP's become externalized at the pseudopod-PMP breakage junction. At these psuedopod-PMP junctions, this exposed vimentin may be readily susceptible to a range of protein interactions such as VN multimerization and incorporation PAI-1-VN complexes, which may originate from pre-existing plasma sources or from exocytosis during platelet activation.

Vimentin is typically not exposed to plasma because of its properties as a cytoskeleton protein; my proposed mechanism of vimentin exposure provides a hypothesized manner of vimentin presentation that may be relevant in discussions involving vimentin autoantibody generation during organ transplant vasculopathy. Moreover, the effects of these anti-vimentin antibodies (AVA's) were not understood, and whether or not they exert any pathogenic effect in the context of organ transplant vasculopathy. We were able to determine that AVA's in normal whole blood specifically bind to a subpopulation of senescent granulocytes expressing vimentin on their surface. As shown in Figure 6.2, when AVA's bind to this subpopulation of senescent granulocytes, they induce complement-mediated cell lysis leading to cell death and during this process, the release of platelet agonists such as tissue factor and platelet-activating factor (PAF) may occur. The release of these platelet agonists lead to platelet activation, platelet:leukocyte conjugate formation and PMP formation. Lastly, these observations are in agreement with other published reports describing elevated levels of markers of platelet activation in the literature and the contribution of activated platelets to atherogenesis in transplant vasculopathy [1, 2].

6.2. Strengths and limitations of thesis research

6.2.1. Chapter III

The primary aim of this dissertation was to understand the role of vimentin in hemostasis and antibody-mediated complement fixation and how vimentin is exposed on the surface of cells. The means in understanding how vimentin is exposed on the surface of cells, did not yield to the typical conventions or techniques of biomedical research. One of the main findings of this dissertation is that the majority of synthesized PAI-1 is not bound to the surface of the activated megakaryocyte, a cell model analogous to its much smaller associate, the platelet. These observations were made by constructing a chimeric form of PAI-1, fusing a fluorescent red protein, dsRed, to the C-terminus of the PAI-1 cDNA sequence. Although not an extraordinary process, extensive validation was performed to ensure its suitability as an intracellular marker of PAI-1. This process of validation is comparable to work performed on other GFP/dsRed fusion chimeras such as tPA-GFP [1, 2], granzyme B-GFP [3], keratins K8-GFP K11-GFP [3], vimentin-GFP [4], thrombopoietin receptor Mpl-dsRed [5]. This is considered a strength of this dissertation, a validation that enabled investigation of PAI-1 trafficking and compartmentalization in megakaryocytes and endothelial cells, observations that are an important contribution to vascular biology, hemostasis and ECM metabolism.

One of the key limitations in chapter III of this dissertation was the lack of PAI-1-dsRed quantification on the surface of activated megakaryocytes, which proved to be difficult during flow cytometric analysis. Both thrombin- and calcium-ionophore- activated megakaryocytes proved to be unamenable to flow cytometry due to a subpopulation of large cellular aggregates obstructing fluidics; aggregation possibly due to thrombin and cell adhesion. Our inability to perform flow cytometric analysis did not allow for PAI-1-dsRed signal comparison at pre- and

post-activation states of megakaryocytic and microparticle fractions. However, judging by the general lack of PAI-1-dsRed on the surface of thrombin-activated megakaryocytes as visualized by videomicroscopy (Figure 3.8.), the proportion of surface-bound PAI-1-dsRed is minimal. However, more work needs to be done to determine why ternary complex is expressed on activated endothelium as determined in Figure 3.6. Major determinants in ternary complex formation may depend on two major criteria: 1) cell surface area available for microparticle release and; 2) cortical vimentin cytoskeleton network underneath the cell membrane. Endothelial cells may hold a greater capacity in ternary complex assembly because of their larger surface area and the density of underlying vimentin cytoskeleton network compared to platelets and megakaryocytes [6-8].

6.2.2. Chapter IV

Another key strength of this dissertation is the use of AFM to visualize individual platelet microparticles (PMP's). Prior to this work, imaging of PMP's was limited to transmission electron microscopy but with no ability to specifically image PMP's expressing just ternary complex. These images provided insight as to how vimentin may be exposed on the surface of activated cells, which can lead to extracellular ternary complex assembly. The combination of FACS-mediated isolation of ternary complex-positive PMP's for AFM imaging is a novel technique that can be extended to visualizing protein distribution on the surface of larger cells such as endothelial cells, cardiomyocytes, and leukocytes.

My proposed model (Figure 4.6) describing the mechanism of vimentin cell surface expression also provides insights relating to the origin of vimentin autoantibody production. I believe allograft implantation induces immune responses that immediately target graft
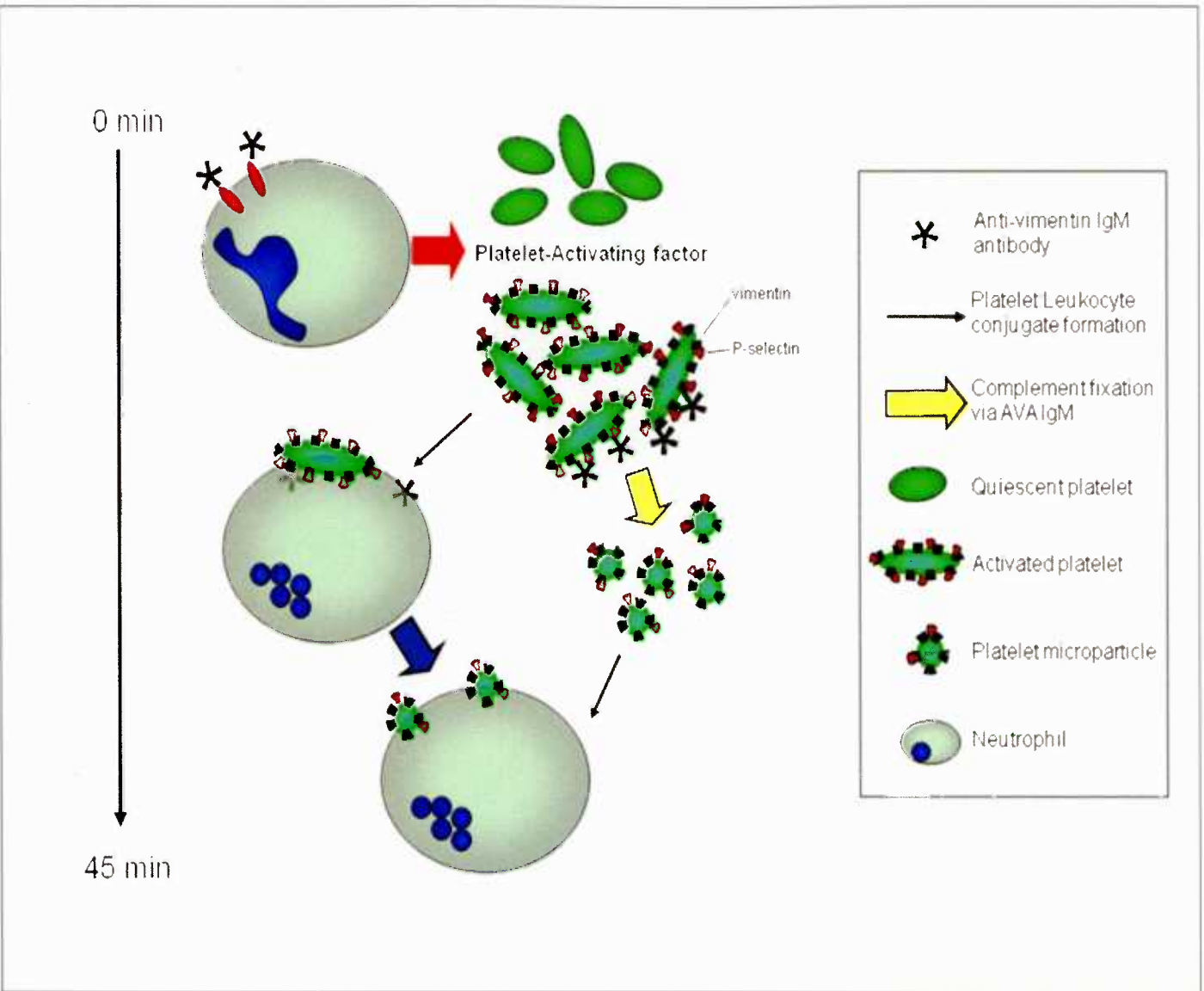
endothelium, inducing the production of endothelial microparticles [9, 10]. The formation of these endothelial microparticles may result in vimentin expression on both the microparticle and endothelial cell and upon processing by antigen processing cells, potentially leading to an auto-immune response against vimentin. We have also determined the binding site of these vimentin autoantibodies in normal whole blood and determined how they can induce blood cell activation (Figure 6.1). The model of vimentin surface expression by microparticle release requires further investigation, for example, imaging of vimentin-positive platelets with cryo-electron microscopy. However, I propose a model in Chapter IV in which AFM images of platelet microparticles (PMP) provide insight as to how vimentin is formed, albeit interpretations based on artifactual membrane appendages attached to the base of the PMP.

There is another important limitation to be considered in Chapter IV regarding atomic force microscopy of activated platelets. Although only CD41+ve platelets with high vitronectin signal were sorted for AFM imaging, it was difficult to translate surface topography with our *in vitro* observations on purified vitronectin and vimentin multimers. Furthermore, the fields of the supposed vitronectin-vimentin multimers also contain antibodies specific for vitronectin and vimentin, causing interpretation to be even more speculative. Despite these potential artefacts, it is possible that the areas of high topographic activity are fields of multimerized protein containing vitronectin and vimentin. Overall, this chapter showcases the potential of atomic force microscopy in providing insights with the ultrastructure of protein-protein complexes, and submicron ultrastructure of biological samples such as microparticles.

6.2.3. Chapter V

Another strength of this dissertation is the comprehensive evaluation of anti-vimentin antibodies (AVA's) and their pathogenic effects on whole blood, a role previously unknown and

thought to be benign in effect. By using an *in vitro* effect but using both commercially available and patient-derived AVA's, I was able to determine the mechanism of AVA-induced blood cell activation. Similar reports describing the cytotoxic effects of other autoantibodies such as anti-neutrophil cytotoxic antibodies (ANCA) have established pathological effects of auto-antibodies while others such as anti-dsDNA antibodies and their effects remain unclear. Although their presence remains associative in relationship to the actual pathogenesis of vasculitis in kidneys; they are postulated to activate and induce neutrophils to release their proteolytic contents, thus causing inflammation of the vessel wall [11, 12]. Chapter V described a mechanism of how AVA can induce blood cell activation by determining the binding site of AVA in normal whole blood – neutrophils.

The limitations associated with this chapter are primarily application-related and stem from the fact that this work was performed *in vitro*. Some of the key experiments we designed had utilized mouse whole blood of a vimentin -/- genotype. We initially hypothesized that AVA would not have any effect on vimentin-/- blood when compared to AVA on normal blood. Surprisingly, AVA did not exert any effect in terms of activation on both normal and vimentin-/- whole blood (data not shown). Similar comparisons with isolated leukocytes and AVA cytotoxicity tests also generated inconclusive results, bringing into doubt a cross-species relevance of AVA and pathogenesis. Definitive studies based on AVA specificity for vimentin on activated murine platelets and leukocytes must be performed, both from washed and plasma sources. As well, it is conceivable that other murine plasma proteins bind to exposed vimentin, sterically hindering AVA binding to surface exposed vimentin on platelets and leukocytes. However, it has been determined by our laboratory that immunization of mouse models with human vimentin does not lead to murine AVA production and brings to light a cross-species

difference in vimentin homologues, a 446/453 amino acid residue similarity between *Mus musculus* and *Homo sapiens*. Hence, all future *in vitro* tests should use enough murine specific AVA in order to adequately compare the observed *in vitro* effects in normal human blood and murine blood.

6.3. Evaluation of current knowledge and proposals for future directions

PAI-1 exerts its pleiotrophic effects in both plasma and on extracellular membrane surfaces, but the mechanism of its localization to cell surfaces is still unclear despite continued progress. One major mechanism of PAI-1 extracellular presentation is related to its interactions with a classical receptor, uPAR (urokinase-type plasminogen activator receptor). In detail, PAI-1 binds to uPA (urokinase-type plasminogen activator) that is already associated with the cell surface receptor, uPAR, which coordinates both intracellular signals and extracellular proteolysis for cellular motility. In this classical receptor-based mechanism, PAI-1 binds directly to uPA, thus inhibiting uPA and preventing the formation of plasmin[13]. At this site, VN can also bind to uPAR via its somatomedin B domain, although it is not definitively understood whether VN can mediate PAI-1 binding to the VN-uPAR complex. It is also unclear whether or not a uPA vacancy is required for VN complex formation with the uPAR receptor [14, 15] in order for VN to recruit PAI-1 localization to the uPAR receptor.

There is also a non-classical receptor mechanism of PAI-1 localization in which Podor et al. revealed the ability of VN to mediate PAI-1 localization to activated cell surfaces by binding to exposed vimentin cytoskeleton on activated platelets and platelet microparticles[16]. This non-classical receptor based mechanism partially explains PAI-1 expression on activated cells such as platelets, thus implicating PAI-1's anti-thrombolytic effects within thrombi. However,

the acceptance of this mechanism became dependent on the understanding of how vimentin is extracellularly presented. The proposed model in Figure 6.1 provides a plausible model for 1) vimentin surface expression leading to 2) PAI-1:vitronectin:vimentin ternary complex assembly on cells such as platelets and endothelial cells. Future studies must determine the proportion of PAI-1 bound to either the uPAR or vimentin receptor; studies that can utilize the PAI-1-dsRed intracellular probe. This is the ultimate objective of the PAI-1-dsRed probe, to permit the understanding of the extracellular fate of PAI-1 and the mechanism of its localization: whether by the exposure of vimentin or by a receptor-based mechanism such as uPAR. I believe that the extracellular fate of PAI-1 will differ between cell types offering another dimension of the pleiotrophic effects PAI-1 exerts in the areas of cell motility, cell adhesion and fibrinolysis.

The PAI-1-dsRed probe also catalyzed the understanding of PAI-1 trafficking within endothelial cells, which will bring forth new ventures in controlling this factor via modulation of PAI-1 secretion, hence regulating pathways such as hemostasis, fibrosis and vascular patency. This intracellular marker will also rejuvenate studies once centered on intracellular trafficking of PAI-1 in platelets and endothelial cells as well as extracellular imaging studies on hemostasis via intravital imaging by photochemical induced thrombosis animal models. This probe will permit real-time evaluation of pro-thrombotic factors and their spatial distribution during thrombus formation in these intravital imaging experiments. In disease models of pulmonary fibrosis, the generation of lentiviral vectors or murine models with endothelium expressing only PAI-1-dsRed can provide further understanding of the endothelium's role in disease progression in this disease.

Atomic force microscopy of PMP's has proved to be an exciting contribution in the field of microparticle biology, shedding light on the morphology of PMP's. Once referred to as

"platelet dust" [17] and primarily assessed by flow cytometry, we have provided the first definitive images of PMP's providing major insight to their origin, structure and potential as "miniature envoys", expressing other important proteins, e.g. tissue factor [18]. Moreover, their small size (<1.0μm in diameter) renders their level of interactions to an almost soluble phase and it would be of interest to evaluate the functionality of CD41 integrin to determine its capability to bind to fibrin/fibrinogen. The ability of PMP's to bind to fibrin/fibrinogen will determine their ability to be incorporated into thrombi and whether they can contribute to clot strength in a manner analogous to activated platelets in a thrombus. If not, then their ability to express PAI-1 may only be realized at a soluble level and not within a cell surface/cell adhesion/cell motility environment.

Investigations regarding the requirement of vimentin for ternary complex formation on the surface of platelets and endothelial cells can be readily determined by pre-treating platelets or cultured endothelial cells with inhibitors such as cytochalasin D [19]. These inhibitors cause the vimentin intermediate filament cytoskeleton to collapse and reorganize tightly around the nucleus, dissolving the original cortical distribution of the intermediate cytoskeleton. When these pre-treated platelets or endothelial cells are treated with agonists such as thrombin or TNF-α, the surface expression of ternary complex (PAI-1:VN:VIM) can be evaluated as microparticles are released from pseudopods formed via activation. This is one example in which pharmacological vimentin inhibition may provide an avenue of downregulated surface expression of PAI-1.

This vimentin inhibition or general cytoskeleton inhibition via cytochalasin D or other inhibitors may provide avenues of insight as we continue to build on the knowledge gained from vimentin exposure from activated endothelium and endothelial microparticles. A collapse of

vimentin cortical cytoskeleton and actin cytoskeleton by these inhibitors in graft endothelium will decrease microparticle formation [20] and may prove beneficial by preventing the release of graft endothelial microparticles available for antigenic processing. However, grafts would require this treatment prior to implantation to prevent cytoskeleton disruption in the host blood cells. Aims toward reducing the processing of graft microparticles may result in the decreased formation of non-MHC antibodies, or autoantibodies. Although there are no current strategies to prevent the formation of antibodies targeting the MHC molecules of organ grafts, cytoskeletal reorganization by pharmacological inhibitors may be a means to limit the formation and impact of non-MHC antibodies, which are thought to arise from the destruction of graft cells caused by the host immune system. This experimental methodology would also prove to be beneficial in preventing the assembly of ternary complex on the surface of endothelium, and decreasing the amount of PAI-1 bound to the activated cell surface. Whether the origin of PAI-1 is platelet or endothelial derived, the absence of a vimentin anchor for the ternary complex would ultimately decrease the incorporation of PAI-1 into atherosclerotic lesions, thus decreasing future thrombotic complications [21-23].

6.4. Three most significant contributions

6.4.1 Mechanism of microparticle release from activated blood cells and endothelium

Microparticles are sub-micron sized ($< 1.0\mu m$) vesicles that are released from the surface of activated cells such as platelets, leukocytes and endothelial cells. I set forth a mechanism of microparticle release and how PAI-1 may be bound to the surface of these activated cells and on the surface of microparticles. This mechanism is important because it explains in part how a

variety of proteins such as PAI-1 can be bound to the surface of activated cells without a classical receptor, ie. integrins.

6.4.2. The role of neutrophils in thrombus stabilization and structural integrity.

I have performed microscopic and biophysical assessments on thrombi collected via aspiration of intracoronary culprit lesions from infarct patients. I have determined that neutrophils are specifically bound to thrombus fibrin via CD11b on their surface. This binding interaction contributes to ~15% of clot strength and can be inhibited via inhibitory antibodies against the CD11b integrin. I have also shown that neutrophils may be partially responsible for thrombolytic resistance because azurophilic granule release can result in the biochemical modification of fibrin, rendering it unrecognizable by other proteins or fibrin-specific antibodies.

6.4.3. Formation of platelet:leukocyte conjugates in transplant vasculopathy.

Anti-vimentin antibodies (AVA) are a prognostic indicator of cardiovascular disease in cardiac transplant recipients but their mechanism of action in the pathogenesis in chronic organ rejection was unclear. I determined that anti-vimentin antibodies specifically bind to a population of senescent leukocytes, primarily of neutrophil and monocyte cell type. When AVA's bind to these leukocytes, platelet-activating factor was secreted which in turn, activated platelets. This activation of platelets subsequently led to the formation of platelet:leukocyte conjugates. When these platelet:leukocyte conjugates are present in the circulation of these patients, it is postulated that there may be increased infiltration of leukocytes and platelets into the graft vasculature. This increased infiltration may exacerbate graft function, resulting in cardiovascular disease and validating use of AVA titres as a prognostic indicator of graft life.

6.5. References for Chapter VI:

1. Jovin IS, Taborski U, Szalay Z, Friedel A, Segieth I, Jovin A, Heidinger K, Schreiner K, Frass O, Klovekorn WP, Muller-Berghaus G. Trapidil decreases the aggregation of platelets from heart transplant recipients ex vivo. *Transplant Proc* 2006; 38:1523-5.

2. Fateh-Moghadam S, Bocksch W, Ruf A, Dickfeld T, Schartl M, Pogatsa-Murray G, Hetzer R, Fleck E, Gawaz M. Changes in surface expression of platelet membrane glycoproteins and progression of heart transplant vasculopathy. *Circulation* 2000; 102:890-7.

3. Yoon KH, Yoon M, Moir RD, Khuon S, Flitney FW, Goldman RD. Insights into the dynamic properties of keratin intermediate filaments in living epithelial cells. *J Cell Biol* 2001; 153:503-16.

4. Yoon M, Moir RD, Prahlad V, Goldman RD. Motile properties of vimentin intermediate filament networks in living cells. *J Cell Biol* 1998; 143:147-57.

5. Zhang YP, Tang YS, Chen XS, Xu P. Regulation of cell differentiation by hNUDC via a Mpl-dependent mechanism in NIH 3T3 cells. *Exp Cell Res* 2007; 313:3210-21.

6. Dellagi K, Vainchenker W, Vinci G, Paulin D, Brouet JC. Alteration of vimentin intermediate filament expression during differentiation of human hemopoietic cells. *Embo J* 1983; 2:1509-14.

7. Dellagi K, Tabilio A, Portier MM, Vainchenker W, Castaigne S, Guichard J, Breton-Gorius J, Brouet JC. Expression of vimentin intermediate filament cytoskeleton in acute nonlymphoblastic leukemias. *Blood* 1985; 65:1444-52.

8. Tablin F, Taube D. Platelet intermediate filaments: detection of a vimentinlike protein in human and bovine platelets. *Cell Motil Cytoskeleton* 1987; 8:61-7.

9. Garcia S, Chirinos J, Jimenez J, Del Carpio Munoz F, Canoniero M, Jy W, Horstman L, Ahn Y. Phenotypic assessment of endothelial microparticles in patients with heart failure and after heart transplantation: switch from cell activation to apoptosis. *J Heart Lung Transplant* 2005; 24:2184-9.

10. Meehan SM, Limsrichamrern S, Manaligod JR, Junsanto T, Josephson MA, Thistlethwaite JR, Haas M. Platelets and capillary injury in acute humoral rejection of renal allografts. *Hum Pathol* 2003; 34:533-40.

11. Falk RJ, Terrell RS, Charles LA, Jennette JC. Anti-neutrophil cytoplasmic autoantibodies induce neutrophils to degranulate and produce oxygen radicals in vitro. *Proc Natl Acad Sci U S A* 1990; 87:4115-9.

12. Reumaux D, Duthilleul P, Roos D. Pathogenesis of diseases associated with antineutrophil cytoplasm autoantibodies. *Hum Immunol* 2004; 65:1-12.

13. Chazaud B, Bonavaud S, Plonquet A, Pouchelet M, Gherardi RK, Barlovatz-Meimon G. Involvement of the [uPAR:uPA:PAI-1:LRP] complex in human myogenic cell motility. *Exp Cell Res* 2000; 258:237-44.

14. Madsen CD, Ferraris GM, Andolfo A, Cunningham O, Sidenius N. uPAR-induced cell adhesion and migration: vitronectin provides the key. *J Cell Biol* 2007; 177:927-39.

15. Waltz DA, Natkin LR, Fujita RM, Wei Y, Chapman HA. Plasmin and plasminogen activator inhibitor type 1 promote cellular motility by regulating the interaction between the urokinase receptor and vitronectin. *J Clin Invest* 1997; 100:58-67.

16. Podor TJ, Singh D, Chindemi P, Foulon DM, McKelvie R, Weitz JI, Austin R, Boudreau G, Davies R. Vimentin exposed on activated platelets and platelet microparticles localizes vitronectin and plasminogen activator inhibitor complexes on their surface. *J Biol Chem* 2002; 277:7529-39.

17. Wolf P. The nature and significance of platelet products in human plasma. *Br J Haematol* 1967; 13:269-88.

18. Ahn YS. Cell-derived microparticles: 'Miniature envoys with many faces'. *J Thromb Haemost* 2005; 3:884-7.

19. Pryzwansky KB, Merricks EP. Chemotactic peptide-induced changes of intermediate filament organization in neutrophils during granule secretion: role of cyclic guanosine monophosphate. *Mol Biol Cell* 1998; 9:2933-47.

20. Yano Y, Kambayashi J, Shiba E, Sakon M, Oiki E, Fukuda K, Kawasaki T, Mori T. The role of protein phosphorylation and cytoskeletal reorganization in microparticle formation from the platelet plasma membrane. *Biochem J* 1994; 299 (Pt 1):303-8.

21. Landmesser U, Hornig B, Drexler H. Endothelial function: a critical determinant in atherosclerosis? *Circulation* 2004; 109:II27-33.

22. Schafer K, Muller K, Hecke A, Mounier E, Goebel J, Loskutoff DJ, Konstantinides S. Enhanced thrombosis in atherosclerosis-prone mice is associated with increased arterial expression of plasminogen activator inhibitor-1. *Arterioscler Thromb Vasc Biol* 2003; 23:2097-103.

23. Sobel BE, Taatjes DJ, Schneider DJ. Intramural plasminogen activator inhibitor type-1 and coronary atherosclerosis. *Arterioscler Thromb Vasc Biol* 2003; 23:1979-89.

APPENDIX I: List of Publications, abstracts, and presentations

A. Peer-Reviewed Publications

Leong HS, Mahesh BM, Day JR, Smith JD, McCormack AD, Podor TJ, Rose ML..Vimentin Auto-Antibodies Induce Platelet Activation and Formation of Platelet-Leukocyte Conjugates via Platelet-Activating Factor. J Leuk Biol Nov 1 2007 (Epub)

Mahesh B, **Leong HS**, McCormack A, Sarathchandra P, Holder A, Rose ML.. Autoantibodies to vimentin cause accelerated rejection of cardiac allografts. Am J Pathol. 2007 Apr;170(4):1415-27.

Walinski HP, Gyorffy SF, **Leong HS**, Slaughter GR, Dawood F, Pate GE, Liu PP, Parker TG, Podor TJ.. Exercise increases tissue-type plasminogen activator expression in rat cardiomyocytes. Thromb Haemost. 2006 Dec;96(6):859-61.

Cheung C, Luo H, Yanagawa B, **Leong HS**, Samarasekera D, Lai JC, Suarez A, Zhang J, McManus BM.. Matrix metalloproteinases and tissue inhibitors of metalloproteinases in coxsackievirus-induced myocarditis. Cardiovasc Pathol. 2006 Mar-Apr;15(2):63-74.

B. Reviews and Chapters

Heine, H., **Leong, H.S.**, Rossi, F., McManus, B.M., Podor, T.J.. Conditional Gene Expression in Myocardium: an Overview. Molecular Cardiology: Methods and Protocols.

C. Manuscripts Submitted and In Preparation

Leong HS, Bateman RM, Walinski HP, Podor TJ. Targeting of recombinant PAI-1-dsRed and vitronectin to storage granules in endothelial and megakaryocyte cell lines. J Thromb Hemo (submitted)

Leong HS, Bateman RM, Whalen B, Meredith A, VanEeden S, Walinski HP, Podor TJ.. Distribution of PAI-1:vitronectin:vimentin ternary complexes on activated platelets and platelet microparticles by atomic force microscopy. Blood (in preparation)

Spiro J, **Leong HS**, Ghimire G, Dalby M, Kharbanda R, Mitchell A.. An Unusual Cause of ST-Segment Elevation Myocardial Infarction; a case report. Nat Clin Pract Cardiovasc Med (submitted)

D. Oral Presentations

Leong HS, Mahesh BM, Day JR, Smith JD, McCormack AD, Podor TJ, Rose ML.. Vimentin Antibodies Induce Formation of Platelet-Leukocyte Conjugates and Blood Agglutination via

Platelet-Activating Factor. <u>Oral presentation</u>. San Francisco, USA. April 25-29, 2007. International Society for Heart and Lung Transplantation.

Leong HS, Mahesh BM, Day JR, Smith JD, McCormack AD, Podor TJ, Rose ML. Vimentin Antibodies Induce Formation of Platelet-Leukocyte Conjugates and Blood Agglutination via Platelet-Activating Factor. <u>Oral presentation</u>. Manchester, UK. March 28-30, 2007. British Transplant Society Annual Congress.

E. Abstracts

Leong HS, Ghimire G, Spiro JR, Kharbanda R, Mitchell AG, Mason MJ, Ilsley C, Podor TJ, Rose ML, Dalby MC.. Characterization of human in vivo intracoronary thrombi from acute myocardial infarction suggests a role for CD11b. Orlando, USA. November 9-14, 2007. American Heart Association Basic Science Sessions.

Ghimire G, **Leong HS**, Spiro JR, Kharbanda R, Rose ML, Dalby MC.. Increased numbers of activated T-cells from coronary artery aspirate in patients with acute myocardial infarction undergoing primary angioplasty. Orlando, USA. November 9-14, 2007. American Heart Association Basic Science Sessions.

Mahesh B, **Leong HS**, McCormack A, Holder A, Sarathchandra P, Smith J, Rose ML.. Antivimentin Antibodies Cause Acute and Chronic Damage In MHC-Matched Allografts. San Francisco, USA. April 25-29, 2007. International Society for Heart and Lung Transplantation.

Mahesh B, Leong HS, McCormack A, Holder A, Sarathchandra P, Smith J, Rose ML.. Antivimentin Antibodies Cause Acute and Chronic Damage In MHC-Matched Allografts. Manchester, UK. March 28-30, 2007. British Transplant Society Annual Congress.

Leong HS, McManus BM, Podor TJ.. Increases in Activated Platelet Microparticles Expressing Surface PAI-1 Vitronectin- and Vimentin-Ternary Complexes in Mice Allograft Recipients. Madrid, Spain. April 3-9, 2006. International Society for Heart and Lung Transplantation.

Leong, HS, Bateman, RM, van Eeden, S, Jiao, YK, Walinski, H, Podor, TJ
Imaging of Highly Organized Vitronectin-Vimentin Polymeric Complexes that Express on the Surface of Activated Platelets and Platelet Microparticles using Atomic Force Microscopy. Sydney, NSW, Australia, August 6-12, 2005. International Society of Thrombosis and Haemostasis.

Leong, HS, Bateman, RM, Walinski, H, Podor, TJ
Chimeric PAI-1-dsRed Fusion Protein Characterization in MEG-01 Megakaryocytic Cells: Model for PAI-1 Trafficking from α-Granules to Cell Surfaces. Sydney, NSW, Australia, August 6-12, 2005. International Society of Thrombosis and Haemostasis.

Bateman, RM, Leong, H, Walley KR, Podor TJ
The Effect of Thrombin Concentration on Fibrin Clot Structure Imaged by

Multiphoton Microscopy and Quantified by Fractal Analysis. Sydney, NSW, Australia, August 6-12, 2005. International Society of Thrombosis and Haemostasis.

Bateman, R.M., Leong, H., Podor, T., Hodgson, K.C., Kareco, T., Walley, K.R.. The Effect of Thrombin Concentration on Fibrin Clot Structure Imaged by Multiphoton Microscopy and Quantified by Fractal Analysis. Honolulu, Hawaii, July 31-Aug 4, Microscopy and Microanalysis, 2005.

Bateman, R.M., Hodgson, K.C., Leong, H.S., Podor, T., Walley K.R.. Intravital and Ex vivo Microvascular Imaging using Dual Fluorescence Multiphoton Microscopy. Jena, Germany, Mar 18-23, Focus on Microscopy, 2005.

Walinski, H., Lowe, R., Bohunek, L., Pate, G., Leong, H., Hamburger, J., McManus, B.M., Podor, T.. Vitronectin deficient mice exhibit reduced cardiac remodeling and wound healing following acute myocardial infarction. San Diego, CA. April 2-6, FASEB 2005.

Leong, H.S., Walinski, H., Westoby, M.A., Podor, T.J.. Characterization of PAI-1-dsRed Chimeric Protein Expression by Cultured Megakaryocyte and Endothelial Cells. Toronto, ON, June 1-5, International Vascular Biology Meeting 2004.

Leong, H.S., Walinski, H., Westoby, M.A., Podor, T.J.. Characterization of PAI-1-dsRed Chimeric Protein Expression by Cultured Megakaryocyte and Endothelial Cells. Winnepeg, MB, May 6-9. CIHR Young Investigators Forum 2004.

F. Awards

Personnel funding:
Canadian Blood Services PhD traineeship (2006-2008)
Michael Smith Foundation PhD traineeship (2006-2008)
Royal Brompton & Harefield Hospital Honorary Fellowship (2007)
British Heart Foundation Travel Fellowship (2006)
Heart and Stroke Foundation Focus on Stroke PhD Traineeship (not accepted)
CIHR/CBS travel awards (2005&2006)
CIHR/Dept of Surgery PhD Traineeship for Transplantation (2005-2006)
CIHR/CBS PhD Traineeship for Transfusion Science (2005-2006)

Operating grants:
CIHR International Opportunities Planning Grant ($24,800 for 1 year)
CRC Royal Brompton and Harefield Clinical Sciences Pilot Graft (£50,000 for 1 year)
British Heart Foundation International Collaborations Grant (£3,000 for 3 months)